MECHANISTIC ASPECTS OF LIGNIN DEGRADATION.
ROLE OF RADICALS AND RADICAL IONS

Claudia Fabbri

Dottorato di Ricerca in Scienze Chimiche (XVII Ciclo)

Dipartimento di Chimica
Università degli Studi di Roma "La Sapienza"

Coordinatore: Prof. Pasquale De Sanctis
                       Dipartimento di Chimica
                       Università degli Studi di Roma "La Sapienza"

Supervisore: Prof. Osvaldo Lanzalunga
                       Dipartimento di Chimica
                       Università degli Studi di Roma "La Sapienza"

Docenti Esaminatori: Prof. Lucio Pellicani
                       Dipartimento di Chimica
                       Università degli Studi di Roma "La Sapienza"

                       Prof. Maurizio D'Auria
                       Dipartimento di Chimica
                       Università della Basilicata

                       Prof. Raffaele Saladino
                       Dipartimento di Agrobiologia ed Agrochimica
                       Università della Tuscia

INDEX

PART III

The Role of Ketyl Radicals in Photoyellowing of Lignin Containing Pulps and Paper

<u>SUMMARY</u>   107

GENERAL INTRODUCTION

1. The Lignin Polymer

Wood is a porous material consisting of a matrix of fiber wall and air space. The wood fiber wall has three major constituents: cellulose, hemicellulose and lignin. In Figure 1 the detailed macroscopic composition of a wood fibre is reported. The fiber wall is constituted by various layers: the primary wall (P), the secondary wall, and the middle lamella (ML). The secondary wall is further subdivided into three sublayers (S_1, S_2, and S_3).[1,2]
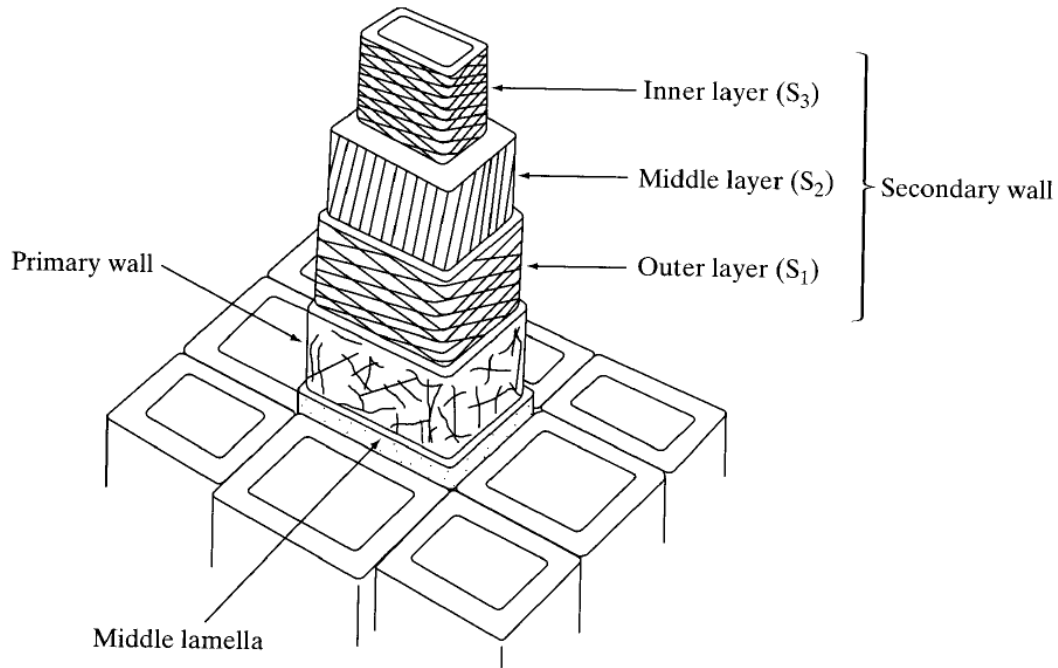
Figure 1. Diagrammatic representation of a wood fiber.

The concentration of lignin in the middle lamella is extremely high, however it is the secondary wall that contains about 70 % of the overall lignin present in wood due to its large volume.[1]

Lignin is the most abundant aromatic biopolymer on Earth.[1,3] Lignification is associated with the development of vascular systems in plants and provides resistance to biodegradation and environmental stresses.[1] This macromolecule, in fact, mixed with hemicelluloses within the cellulosic fibre wall, gives strength and rigidity to trees and plants.[1,4]

Lignin is formed starting from three phenylpropanoid precursors synthesised from L-phenylalanine: p-coumaryl alcohol, coniferyl alcohol and synapyl alcohol (Figure 2).[1] The lignins of softwood, hardwoods and grasses differ with regard to their content of guaiacyl, syringyl and 4-hydroxyphenyl units. Softwood lignins are predominantly polymers of coniferyl alcohol, hardwood lignins are composed of coniferyl and syringyl units in various proportions, while lignin obtained from grasses contains all the three units.[5]
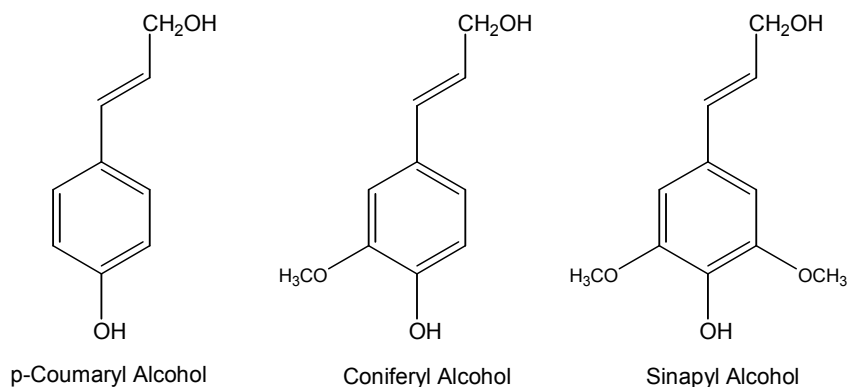
Figure 2. Phenyl propanoid precursors of lignin.

The dehydrogenative polymerisation of lignin monomers in plants is promoted by the peroxidase-H_2O_2 system. This system effects the removal of the phenolic hydrogen atom from the precursors leading to phenoxyl radicals, which by non enzymatic (random) radical-radical coupling produce a three dimensional amorphous polymer lacking regular, ordered repeating units (Figure 3).[5]
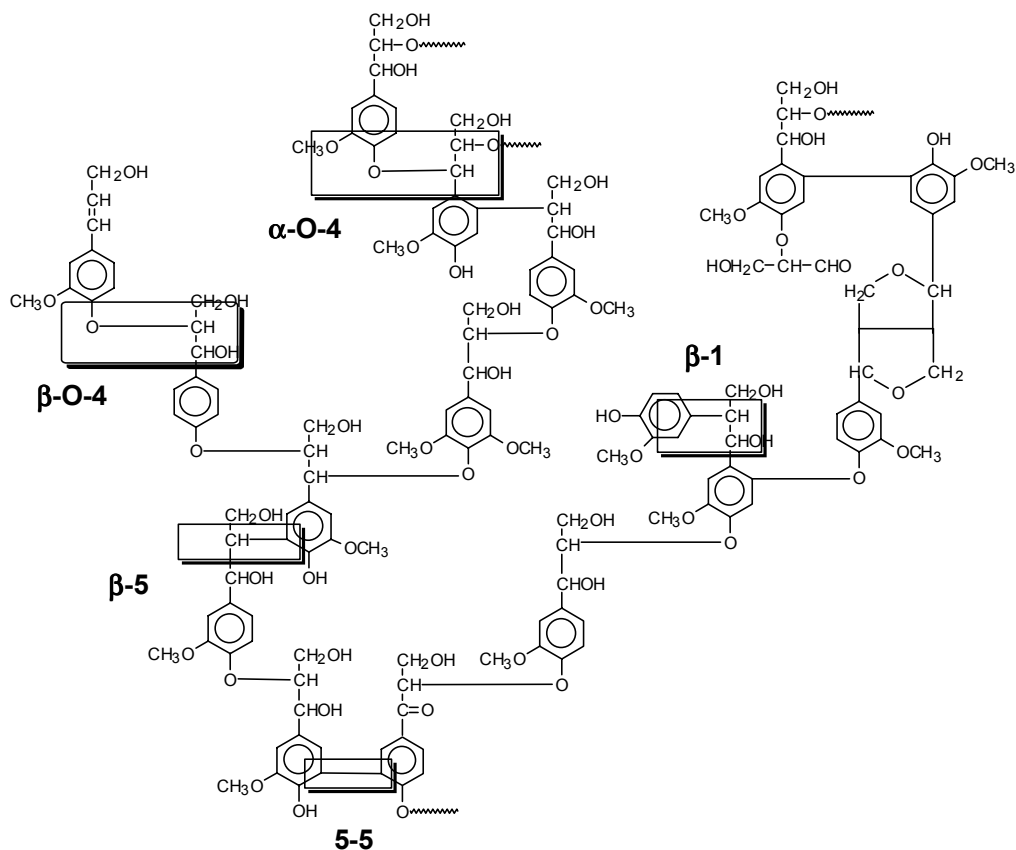
Figure 3. Schematic representation of the structure of lignin.

Among the different bonds formed in the random radical-radical coupling the β-O-4[§] (arylglycerol β-aryl ether) inter-unit linkage is the most abundant and accounts for about 50% of the phenylpropane units. Other important linkages and their relative abundances are: β-5

[§] β– refers to the C_β carbon atom of the phenylpropane unit, -O- indicates the oxygen atom of the C_β and -4 refers to the carbon atom in the aromatic ring with C-1 carrying the propyl side-chain.

(phenylcoumaran, 9-12%), 5-5' (biphenyl, 9-11%), α-O-4 (arylglycerol α-aryl ether, 5-8%) and β-1 (diarylpropane, 5-8%).[6]

Lignin is closely associated to cellulose and hemicellulose in plant cell wall. These carbohydrates are linked to lignin by covalent bonds, such as ether linkages involving L-arabinose side chain or xylose units. Arabinose, galactose and 4-O-methyl-glucuronic acid have been suggested to be the connecting link of the backbone of hemicellulose to lignin (Figure 4).[2]
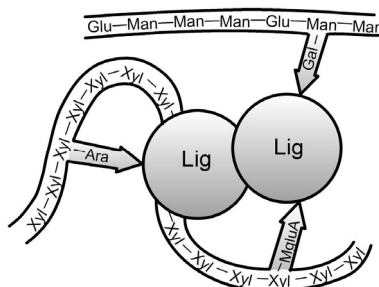
Figure 4. Schematic representation of connections between hemicellulose and lignin.

2. Degradation of Lignin and its Relevance in the Pulp and Paper Industry

The oxidative degradation of lignin is a process of fundamental importance not only because it can convert lignin into low molecular weight aromatic compounds, thus making this polymer a renewable source for the industrial preparation of a number of chemicals,[7] but also because the selective degradation of lignin and its removal from the carbohydrate component of wood is a key step in the pulp and paper industry.[8] The quality of paper is inversely proportional to the content of the residual lignin which affects both the physical properties, such as strength and flexibility, and the chemical stability.[9] In the manufacture of paper, individual wood cells, or fibers, are separated from one to another in a pulping process and then bleached.[9] Pulp is the fibrous mass that results when a pulping process ruptures the bonds in the wood structure that hold the woody cell together (Figure 5).[10]
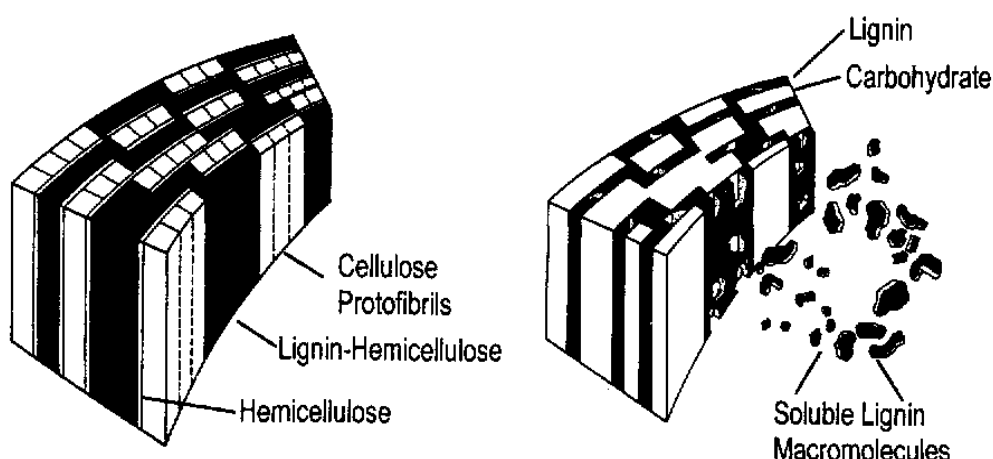
Figure 5. A section of the fiber wall structure in the chemical pulp-bleaching.

Pulping processes are generally divided into two broad classes, mechanical and chemical. These processes produce substantially different fiber characteristics, thus, the choice of the process depends on the end application of the pulp and the raw material. In many

papermaking operations, a combination of mechanical and chemical treatments is used to obtain the desired paper characteristics.[2]

2.1 Mechanical Pulping

This process involves the conversion of raw wood into papermaking pulp by use of mechanical means only.[5] Nowadays one of the major process is a thermo-mechanical pulping process in which the wood is steamed under pressure to obtain a stronger pulp with a higher percentage of long fibers.[5]

Mechanical pulping has the advantage of converting up to 95% of the dry weight of wood into pulp but requires a large amount of energy.[10] Much of the lignin is leaved in the fibers and the paper produced is of low quality with a great tendency to turn yellow with time. The paper obtained by mechanical pulping is suitable only for products with a short life span such as newsprint.[5]

2.2 Chemical Pulping

In chemical pulping the fibers in wood are separated by dissolving away the lignin component, leaving behind a fiber that retains most of its cellulose and hemicellulose.[10] Kraft process represents 91% of chemical pulping and 75% of all pulping treatments.[10] It consists in cooking wood chips at high temperature (ca. 170ºC) in an aqueous liquor consisting in sodium hydroxide and sulphide. This process removes roughly 80-90% of the original lignin by nucleophilic cleavage with the concomitant fragmentation and solubilisation of the polymer.[9] The remaining lignin is called residual kraft lignin and is structurally distinct from native lignin.[9] Some highly conjugated structures are generated and impart a dark brown colour to the kraft pulp.[9] Unbleached pulps are generally used for packaging products.[10] However for high quality manufacture such as white printing and writing paper the pulp must be bleached to chemically remove residual kraft lignin.

Chemical pulping is a low yield process (about 40-50%). Chlorine and compounds of chlorine have been the most widely used bleaching agents for chemical pulps causing environmental pressure for the use of chlorine free bleaching system.[8]

2.3 Biopulping

In nature wood and other ligninocellulosic materials are degraded by a variety of fungi and bacteria, which, in general, have an unselective mode of operation because they attack both carbohydrates and lignin.[2] White-rot fungi are among the best degraders of lignin, they owe their name to the specific bleaching process that occurs during degradation of wood.[11-13] The ability of the white-rot group to efficiently remove lignin from wood makes them suitable for industrial application where lignin needs to be removed.[2] Biopulping, the pre-treatment of wood chips with lignin degrading fungi, has received great attention in recent years.[14] Application of biopulping as a pre-treatment of mechanical pulping should reduce electrical energy consumption, improve paper quality and reduce the environmental impact.[14] A screening program was developed to select fast-growing species of fungi that could selectively remove lignin from wood among the hundreds of white-rot fungi.[14] The main difficulty in biopulping applications is due to processes scale up and many studies are carried out to develop the scientific and engineering knowledge needed for the commercial utilisation of fungi in pulping.[14]

2.4 Delignifying Enzymes

Both the size and the inaccessibility of the lignin polymer indicate that the initial step in lignin biodegradation cannot be an intracellular process.[15] White-rot fungi produce an array of extracellular oxidative delignifying enzymes, the best characterised of which are lignin peroxidase (LiP), manganese peroxidase (MnP) and laccase.[14] MnP acts exclusively as a phenol oxidase on phenolic substrates using the redox couple Mn^{2+} / Mn^{3+}. Mn(II) ions are

oxidised to Mn(III) ions which form a complex with a proper chelating agent and oxidise in turn phenolic substrates to phenoxyl radicals.[2] Laccase is a true phenol oxidase and oxidises phenols and phenolic lignin substructures with formation of radicals and concomitant reduction of oxygen to water.[16] LiP oxidises its substrate by two consecutive one-electron oxidation steps. Because of its high redox potential, LiP can oxidise not only phenolic compounds to phenoxyl radicals but also nonphenolic compounds to the corresponding radical cations.[2] Other enzymes of importance in lignin biodegradation are the H_2O_2-producing ones,[2] in fact the extracellular peroxidases need H_2O_2 for activity.[4]

3. Aim of This Thesis

In my thesis I analysed in detail three important aspects of lignin degradation which are characterised by the involvement of radicals or radical ions as reactive intermediates.

Due to the practical problems posed by the use of the lignin macromolecule, these studies were carried out with simple monomeric, dimeric or trimeric models (with these terms it is generally indicated the number of phenylpropane units present in the model) containing isolated structural motifs of the polymer.[17-19]

In the first part I investigated the lignin peroxidase-catalysed oxidation of nonphenolic trimeric lignin model compounds. By this study it was possible to obtain information on the type of bonds which are broken in the radical cations formed as reaction intermediates and on how the structure of the radical cation may influence the relative rate of cleavage of these bonds.

In the second part I investigated the oxidation of a series of α-alkyl substituted benzyl alcohols (as lignin model compounds) catalysed by iron tetraaryl porphyrins. These biomimetic catalysts are synthetic systems structurally related to the prosthetic group of heme proteins such as peroxidases. Product studies were carried out with the aim of shedding more light on the mechanism of the biomimetic oxidation of lignin model compounds.

Finally I studied some aspects concerning the colour reversion (photoyellowing) of lignin containing pulps and paper. The role of the ketyl radicals in this process was examined to assess their relative contribution to the formation of chromophores responsible of photoyellowing. Both time-resolved and products studies were carried out by means of photo and radiation-chemical techniques.

References

1. D. S. Argyropoulos, S. B. Menachem, *Lignin* in: K. –E. L. Eriksson (Ed.), Biotechnology in the Pulp and Paper Industry (Vol.57 in Advances in Biochemical Engineering Biotechnology), Springer Verlag, Berlin Heidelberg, **1997,** pp. 127-158.
2. R. C. Kuhad, A. Singh, K. -E. Eriksson, *Microorganism and Enzymes Involved in the Degradation of Plant Fiber Cell Walls* in: K. –E. L. Eriksson (Ed.), Biotechnology in the Pulp and Paper Industry, (Vol.57 in Advances in Biochemical Engineering Biotechnology), Springer Verlag, Berlin Heidelberg, **1997,** pp. 47-125.
3. D. W. Goheen, C. H. Hoyt, *Lignin,* in: M. Grayson (Ed.), Encyclopedia of Chemical Technology, Wiley Interscience, **1981,** *14,* 294-312.
4. E. de Jong, J. A. Field, J. A. M. de Bont, *FEMS Microbiol. Rev.,***1994,** *13,* 153-188.
5. O. Lanzalunga, M. Bietti*, J. Photochem. Photobiol B*, **2000,** *56,* 85-108.
6. K. V. Sarkanen, *Lignins: Occurence, Formation, Structure and Reactions,* K. V. Sarkanen, C. H. Ludwig (Eds.), Wiley-Interscience, New York, **1971,** pp. 95-195.
7. H. -R. Biørsvik, F. Minisci, *Organic Process Research & Development* **1999,** *3,* 330.
8. J. C. Roberts, *The Chemistry of Paper*, The Royal Society of Chemistry, Cambridge, UK, **1996.**
9. I. A. Weinstock, R. H. Atalla, R. S. Reiner, M. A. Moen, K. E. Hammel, C. J. Houtman, C. L. Hill, M. K. Harrup, *J. Mol. Cat.A: Chemistry,* **1997,** *116,* 59-84.
10. D. Briggs, *Forest Product Measurements and Conversion Factors,* The College of Forest Resources, University of Washington (Ed.), United States of America, **1994,** Chapter 8.
11. T. K. Kirk, R. L. Farrell, *Annu. Rev. Microbiol.,* **1987,** *41,* 465-505.
12. G. F. Leatham, *Appl. Microbiol. Biotechnol.,* **1986,** *24,* 51.
13. I. D. Reid, M. G. Paice, *FEMS Microb. Rev.,* **1994,** *13,* 369-376.
14. M. Akhtar, R. A. Blanchette, T. K. Kirk, *Fungal Delignification and Biomechanical Pulping of Wood* in: -E. L. Eriksson (Ed.), Biotechnology in the Pulp and Paper Industry (Vol.57 in Advances in Biochemical Engineering Biotechnology), Springer Verlag, Berlin Heidelberg, **1997,** pp. 159-195.
15. H. E. Shoemaker, *Recl. Trav. Chim. Pays-Bas.* **1990,** *109,* 255-272.
16. T. Higuchi, *Biosynthesis and Biodegradation of Plant Cell Polymers*, N. G. Lenis, M. G. Paice (Eds.), ACS Symp. 399, American Chemical Society, Washington, DC, **1989,** p. 482.
17. R. Ten Have, P. J. M. Teunissen, *Chem. Rev.,* **2001,** *101,* 3397.
18. T. K. Kirk, M. Tien, P. J. Kersten, M. D. Mozuch, B. Kalyanaraman, *Biochem. J.,* **1986,** *236,* 279.
19. T. Mester, K. Ambert-Balay, S. Ciofi-Baffoni, L. Banci, A. D. Jones, M. Tien, *J. Biol. Chem.,* **2001,** *25,* 22985.

PART I

Lignin Peroxidase-Catalysed Oxidation of Nonphenolic Trimeric Lignin Model Compounds

1. Introduction

White-rot fungi are the basidiomycetes responsible for the fastest and most extensive degradation of lignin.[1] One of the most important white-rot fungus is *Phanerochaete chrysosporium* which has been used extensively as a model organism to study the physiological requirements and enzymes involved in lignin biodegradation.[2,3] This microorganism metabolises the lignin during the stationary phase, the metabolism is accelerated in a static medium[4] (maximum contact between substrate and mycelium), poor in nitrogen and rich in glucose as a carbon source.[5-7]

Among the various enzymes produced by *Phanerochaete chrysosporium*, lignin peroxidase (LiP) plays a fundamental role for the ligninolitic activity.[3]

LiP, isolated for the first time in 1983,[8,9] is a glicoprotein containing an iron(III) protoporphyrin IX as prosthetic group (Figure 1).[10,11]
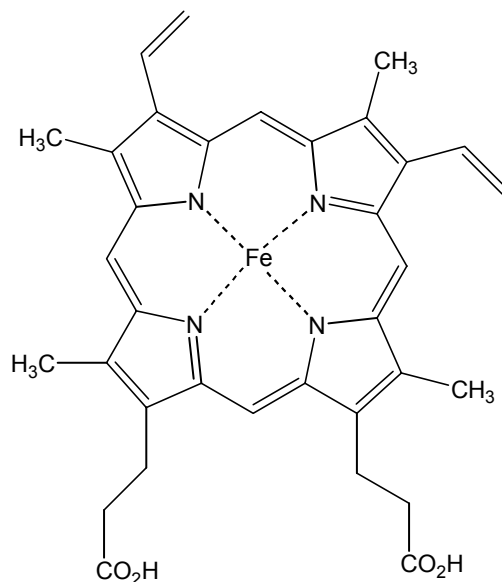
Figure 1. Iron protoporphyrin IX.

Initially LiP was thought to be a H_2O_2-dependent oxygenase, because it was observed incorporation of oxygen from O_2 in the oxidation products under aerobic conditions.[12-14] Afterwards it was clarified that this enzyme belongs to the family of peroxidases.[11-15] In fact it was observed, in the presence of $H_2^{18}O$ in anaerobic conditions, incorporation of ^{18}O in the oxidation products.[16] Although the primary structure of the active site is similar to those of other peroxidases,[17-21] LiP is unique in its ability to oxidise aromatic nonphenolic substrates with high redox potential (1.4 V vs. NHE)[22-25] and in its low optimum pH (ca.3) for the activity.[26-30]

Different isozymes of LiP are known, their molecular weights varies from 38.000 to 43.000 dalton.[31] The crystal structure of one of the most important isozyme (H8) shows the presence of two subunits each containing 343 aminoacidic residues, one heme molecule, two calcium ions, four disulphide bridges, 370 water molecules and carbohydrate molecules (Figure 2).[32,33]
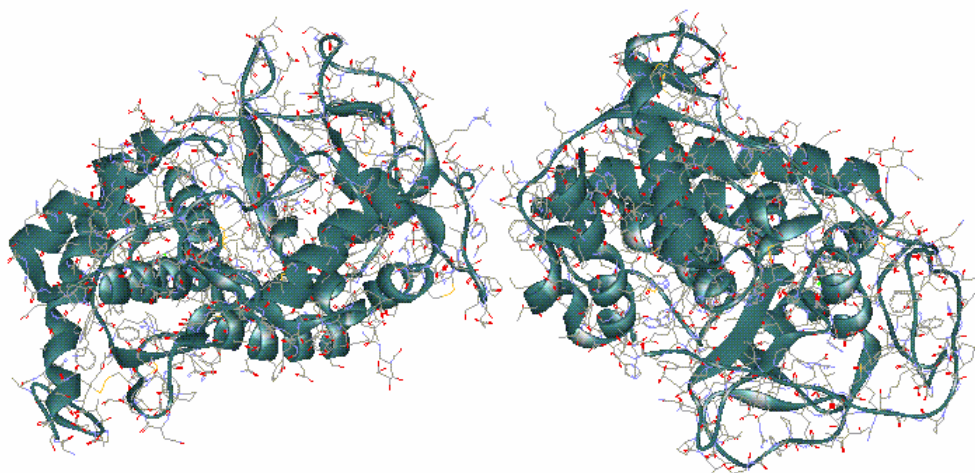
Figure 2. LiP crystallographic cell.

In the crystal structure of LiP H8 11 helicoidal segments were identified. The heme molecule is not planar but has a saddle-like shape with two pyrrolic rings turned towards the proximal helix and the other two towards the distal helix.[34] Iron (III) is coordinated to a proximal histidine (His176) which is hydrogen-bonded to an aspartate residue (Asp238) and parallel to a phenylalanine residue (Phe193). In the distal side, where H_2O_2 is binded, there is a pocket containing a histidine (His47) and arginine (Arg43) residues. These two residues, together with phenylalanine (Phe46) are the three key catalytic residues and form the peroxide-binding pocket (Figure 3). The heme propionates are hydrogen-bonded to alanine (Ala180) and aspartic acid (Asp183). The low optimum pH for the activity of LiP can be explained by the fact that at pH > 3 there is a breaking of the propionate hydrogen bonds which destabilises the heme.[33]
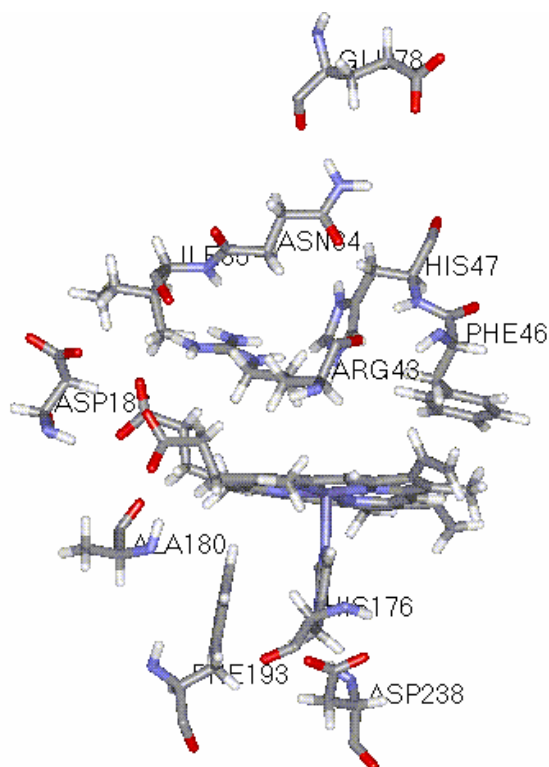
Figure 3. Schematic representation of LiP catalytic site.

Calcium ions probably play a fundamental role in the maintenance of the integrity of the enzyme active site since they coordinate groups attached to the helices that form the active site.[35] The proximal calcium ion might be responsible of the iron-histidine distance which could influence the redox potential.[36] The carbohydrate chains are concentrated at the top of the protein and seem to protect the protein against proteolitic attack.[33]

Electronic spin resonance (EPR) and resonance Raman (RR) studies indicate that at 2°C the heme group is six-coordinate, with a water molecule as sixth ligand.[10] On the opposite at 25°C resonance Raman spectra show a five-coordinate geometry for the heme.[11] Probably the two form are in equilibrium: in fact at 17°C two species were found, one six-coordinated and the other five-coordinated. Thus, at 25°C one site in axial position is available to bind an oxygen atom.[37]

The catalytic cycle of LiP is similar to that of horseradish peroxidase (HRP). The reaction of the native enzyme [PorFe(III)] with H_2O_2 leads to the formation of LiP Compound I (LiP I), an iron(IV)-oxo porphyrin radical cation [Por$^{+\bullet}$Fe(IV)=O], which is two oxidising equivalents above the resting state (Scheme 1, path **a**).[38,39] LiP I is the active oxidant able to abstract one electron from substrates with redox potential less then 1.4 V, leading to [PorFe(IV)=O], LiP Compound II (LiP II), and the radical cation of the substrate (Scheme 1, path **b**).[8] One electron oxidation of the substrate by LiP II (Scheme 1, path **c**) regenerates the native enzyme. In the presence of an excess of H_2O_2, Compound II is further oxidised to [Por-Fe(III)-$O_2^{\bullet-}$], LiP Compound III (LiP III), a species with limited catalytic activity (Scheme 1, path **d**).[15,40]
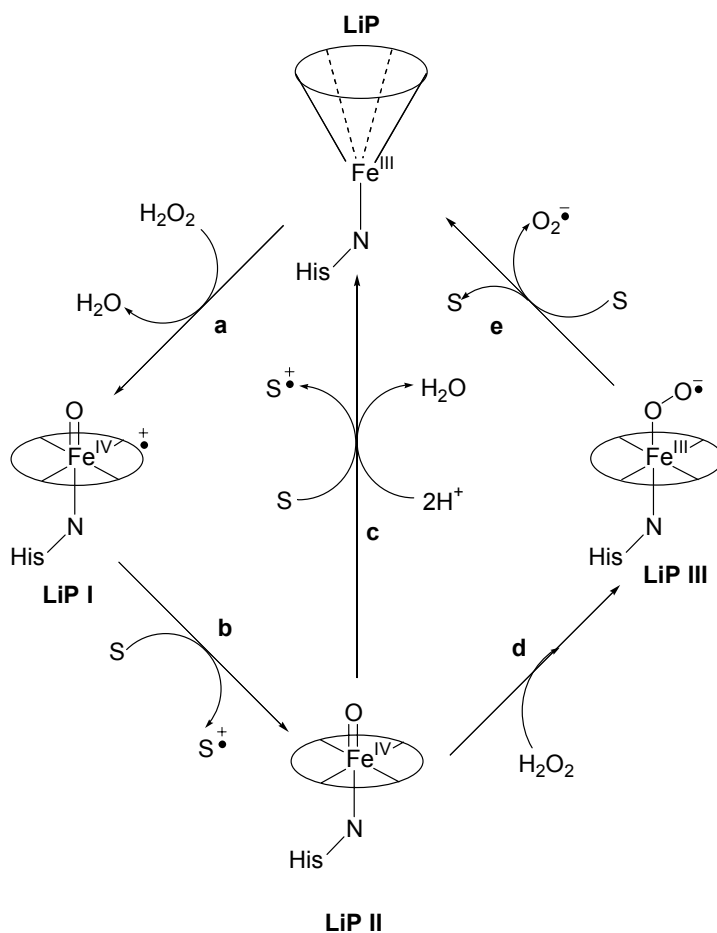
Scheme 1. Catalytic cycle of LiP.

Since LiP is not inactivated under physiological conditions in the presence of an excess of H_2O_2, some mechanism must exist to stabilise this enzyme. It was suggested that some secondary aryl alcohols, metabolites of basidiomycetes, and in particular veratryl alcohol (3.4-dimethoxybenzyl alcohol), exert a stabilising effect.[41] This assessment is also confirmed by the fact that Compound III in the presence of veratryl alcohol rapidly decomposes to yield ferric enzyme (Scheme 1, path **e**).[42]

The analysis of the crystal structure of LiP indicates that the heme is not in direct contact with the bulk solvent: one of the heme meso positions is turned towards the end of a cleft connecting the distal side pocket to the surface. This cleft is conserved in heme peroxidases but varies considerably in size[33], in LiP it seems to be extremely small in consistence with the fact that the heme position is not attacked by aryl hydrazine as in HRP[43] and chloroperoxidase.[44] The presence of bulky residues in the access channel of LiP prevents the direct interaction of large substrates with the heme. In such a case electron transfer processes are likely to occur since they can operate at long distances.

The first step in lignin peroxidase catalysed oxidation of lignin should be the oxidation of the macromolecule by LiPI with formation of a radical cation in which the positive charge is localised on one aromatic ring. The electron transfer can occur by direct interaction of lignin with the enzyme, however, it is significantly accelerated by the presence of veratryl alcohol (VA), which should act as a one-electron redox mediator transferring oxidising equivalents from the enzyme to the large, insoluble, and hydrophobic lignin polymer. The oxidation of VA would involve the transfer of one electron to LiPI, leading to the formation of $VA^{+\bullet}$ which would then exchange one electron with one of the aromatic rings of the macromolecule, thus initiating its degradation (Scheme 2, path **a**).[15,45-49] The aromatic radical cation formed in the polymer can undergo several processes depending on the structure of the phenylpropane unit. In α-OH β-O-4 structures, which are the most abundant in lignin, the main process involves the cleavage of a bond in a β position with respect to the aromatic ring bearing the positive charge.[50] Either C-H or C_α-C_β cleavage can occur. The former process leads to the formation of a α-hydroxyl benzyl radical (Scheme 2, path **b**), which is further oxidised to an aromatic carbonyl group (Scheme 2, path **c**) thus resulting in an enrichment of the α-carbonyl structures in the lignin polymer. The C_α-C_β cleavage leads instead to the breaking of the polymer chain and to the formation of two fragments with lower molecular weights, one is an aromatic aldehyde and another is a carbon centred radical (Scheme 2, path **d**).
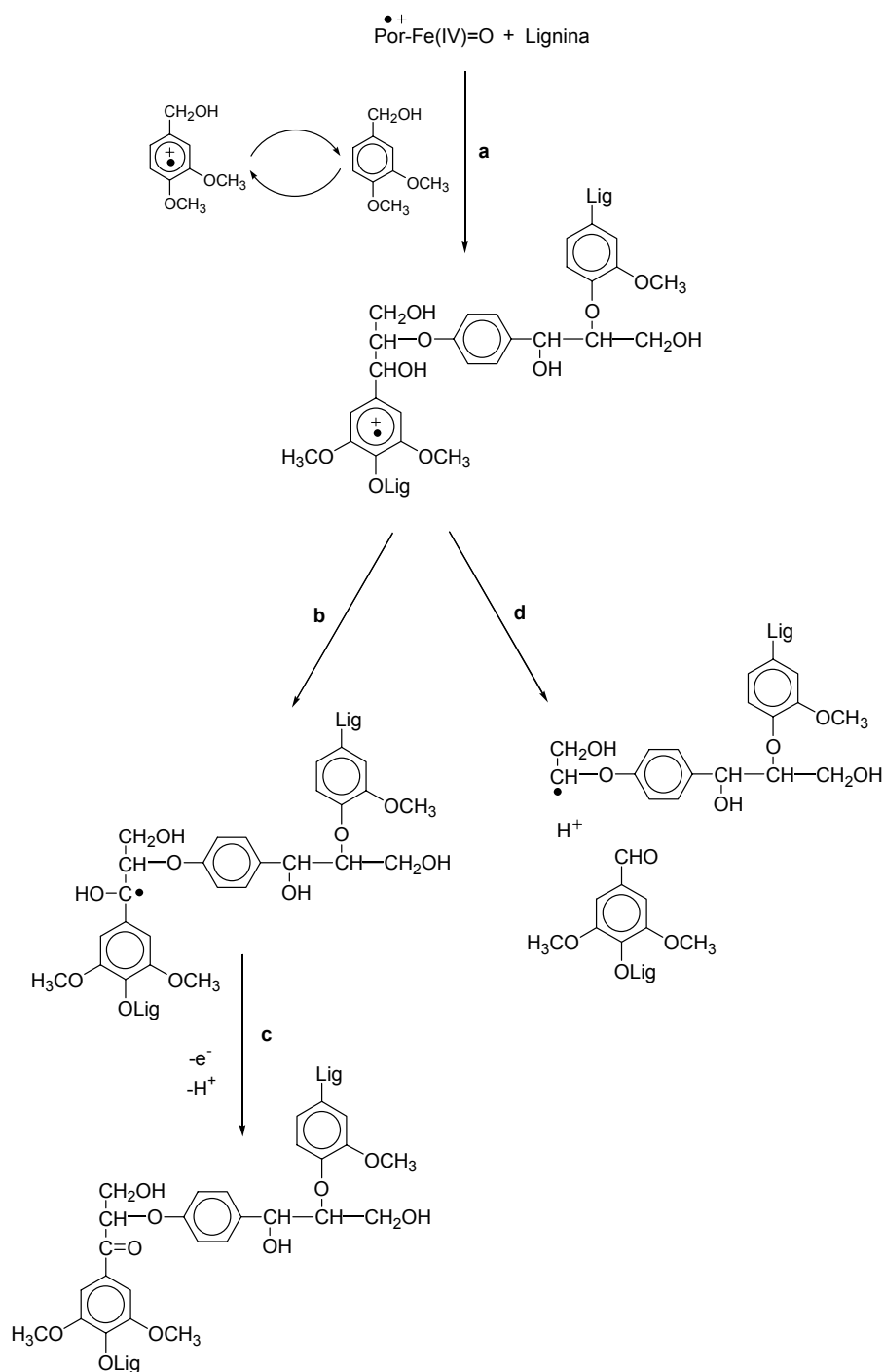
Scheme 2. Oxidation of lignin LiP-catalysed mediated by VA.

Due to the complexity of the lignin polymer which makes difficult the identification and characterisation of the oxidation products, many mechanistic studies of the LiP-catalysed oxidation have been carried out using lignin models compounds (LMCs) containing the isolated structural motifs of lignin. Even though interesting information has been collected from these studies, the structural factors, which may play a role in determining the particular type of bond that undergoes the cleavage, have not been fully understood. One of the reasons is that the models used contain two or more aromatic rings similarly activated towards electron transfer, making practically impossible to know the localisation of the positive charge. As an example the most studied lignin model compound is adlerol [1-(3,4-dimethoxyphenyl)-2-(2'-methoxyphenoxy)-1,3-propandiol] (Figure 4).[51]
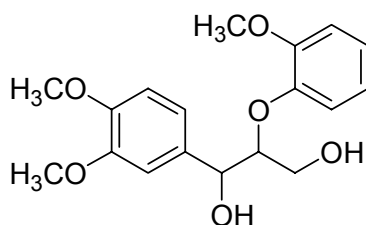
Figure 4. Adlerol.

This dimeric model compound contains two aromatic rings with a similar redox potential. Thus, in the monoelectronic oxidation catalysed by LiP both the aromatic rings may form the corresponding radical cations.

In order to obtain unambiguous information on the bonds which are broken and on how the structure of the radical cation may influence the relative rate of cleavage of these bonds, overcoming the problem of similarly activated aromatic rings, I synthesised the two non-phenolic trimeric lignin model compounds **1** and **2** both containing two β-O-4 linkages (Figure 5).

1 and **2** present a substitution pattern such that upon one-electron oxidation they should form the radical cations $1^{+\bullet}$ and $2^{+\bullet}$ in which the positive charge is reasonably expected to be predominantly localised in the dialkoxylated ring A.[52]
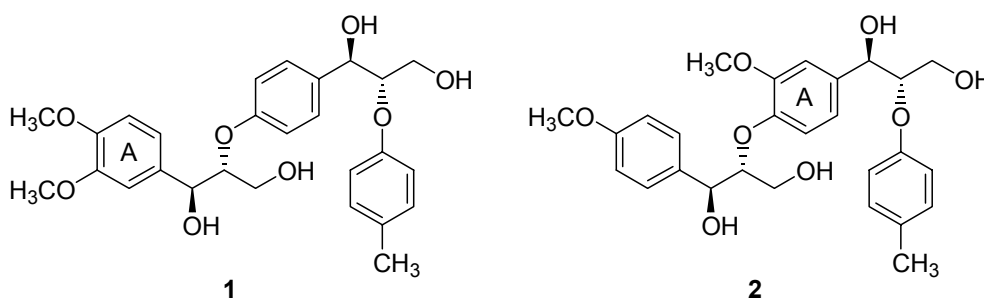
Figure 5. Non-phenolic trimeric lignin model compounds **1** and **2.**

In order to confirm this hypothesis and to obtain information on the structure of $1^{+\bullet}$ and $2^{+\bullet}$ I carried out pulse radiolysis experiments. In this technique a short pulse (on the nanoseconds to microseconds timescale) of high-energy electrons (in the order of MeV) induces ionisation and excitation of the solvent molecules, usually water. Dilute aqueous solutions of the compounds are used so that the energy is exclusively spent in the production of reactive species derived from the solvent water, namely the hydrated electron, the hydroxyl radical $^\bullet OH$ and the hydrogen atom $H^\bullet$. These species react with organic compounds leading to reduction, oxidation, hydrogen or hydroxy addition or abstraction. Electron transfer can also be affected by using e_{aq} or $^\bullet OH$ to generate one-electron acceptors species such as Tl^+ and $SO_4^{-\bullet}$. Detection of the intermediates that grow in and decay can be done on the basis of their optical absorption.[55]

For a better interpretation of the results of the LiP-catalysed oxidation of **1** and **2** by H_2O_2, the same substrates **1** and **2** were reacted with the genuine one-electron oxidant $K_5[Co(III)W_{12}O_{40}]$, from now on simply indicated as Co(III)W.[56,57] In this eteropolyanion complex the cobalt ion is deeply buried within a shell of WO_6 octahedra (Figure 6) and is completely shielded from contact with external species thus making it a good oxidant for outer-sphere electron transfer processes. Moreover, its extremely low ability to form solvates

via hydrogen bonding minimises the usual strong inhibition of electron transfer through hydration shells.
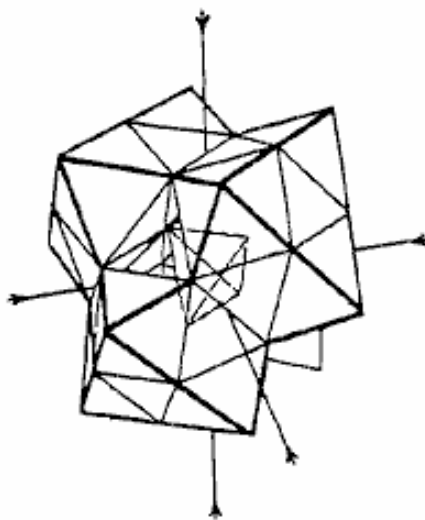
Figure 6. Structure of the 12-tungstocobalt(III)ate ion.

On the same topic, I considered worthwhile to investigate to what degree the size of the non-phenolic model compounds may influence the rate of the LiP-catalysed oxidation.[58] This information is of fundamental importance in order to assess that the oxidation of the lignin polymer can occur directly or it needs to be mediated by small molecules like VA. To this purpose I determined the kinetic enzymatic constants K_M and k_{cat} for the monomeric LMC 3,4-dimethoxybenzyl alcohol (VA, **3**), for the dimeric LMC 1-(3,4-dimethoxyphenyl)-2-phenoxy-1-ethanol **4** (Figure 7) and for the trimeric LMC **2**. As in the product analysis studies, the results have been compared with the kinetic data obtained in the oxidation of the same substrates with the chemical oxidant Co(III)W.

4
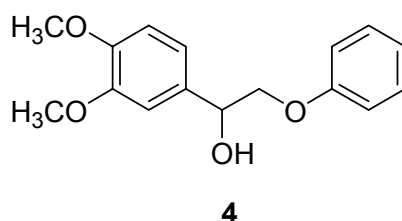
Figure 7. The dimeric lignin model compound **4.**

2. Results

2.1 Pulse Radiolysis Study
The radical cations **1$^{+\bullet}$** and **2$^{+\bullet}$**, were generated from **1** and **2**, respectively, by pulse radiolysis using Tl^{2+} as the oxidant.[60] Tl^{2+} was produced by irradiating N$_2$O saturated aqueous solutions (pH 3.5) of Tl$_2$SO$_4$ (5 mM) (eqs 1-4):

$$H_2O \xrightarrow{\hspace{1.5cm}} H^+, \ ^\bullet OH, \ e^-_{aq} \qquad (1)$$

$$e^-_{aq} + N_2O + H_2O \longrightarrow N_2 + \ ^\bullet OH + \ ^- OH \qquad (2)$$

$$^\bullet OH + Tl^+ + H^+ \longrightarrow Tl^{2+} + H_2O \qquad (3)$$

$$Tl^{2+} + ArCH(OH)R \longrightarrow Tl^+ + Ar\overset{\centerdot\centerdot}{C}H(OH)R \qquad (4)$$
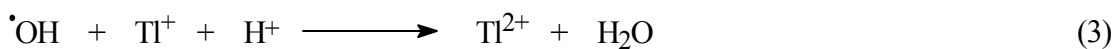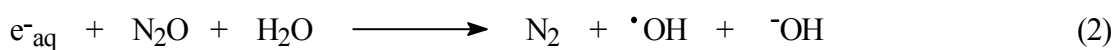
The function of N_2O is to scavenge e^-_{aq}, leading to the formation of an additional hydroxyl radical (eq 2), with $k = 9.1 \times 10^9 \ M^{-1}s^{-1}$.[63] Tl^{2+} is then produced by oxidation of Tl^+ by $^\bullet OH$ (eq 3) with $k = 1.2 \times 10^{10} \ M^{-1}s^{-1}$.[62] Tl^{2+} reacts with alkoxyaromatics by one-electron transfer to give the corresponding radical cations (eq 4) with $k \approx 5 \times 10^8 \ M^{-1}s^{-1}$.[64] The absorption spectra obtained from **1** and **2** recorded 100 µs after the pulse are displayed in Figures 8 and 9, respectively. Both these spectra present absorption bands at 310 nm and 420 nm, that is in a region typical for aromatic radical cations and can be safely assigned to **1$^{+\bullet}$** (Figure 8) and **2$^{+\bullet}$** (Figure 9).
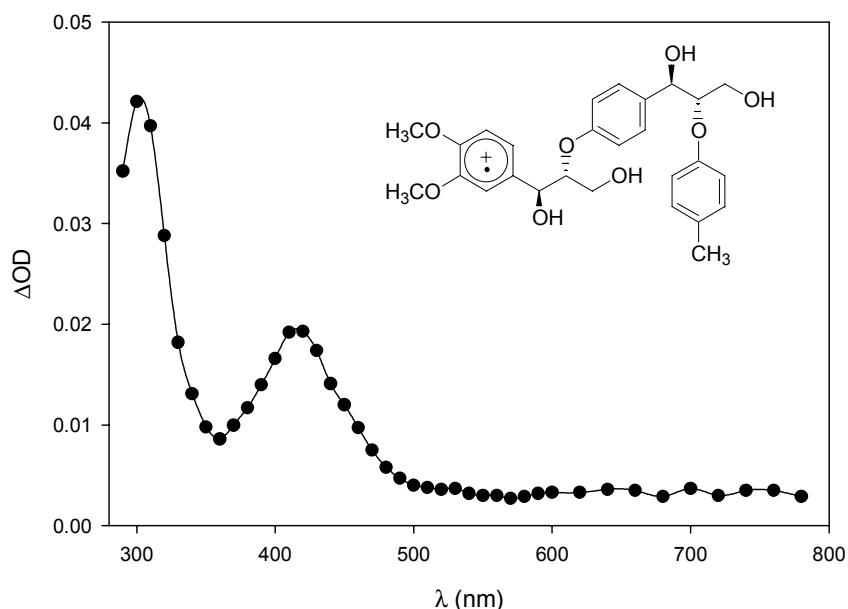
Figure 8. Absorption spectrum of **1$^{+\bullet}$** observed on reaction of Tl^{2+} with **1** (0.1 mM) at T = 25 °C, recorded after pulse radiolysis of an N_2O-saturated aqueous solution (pH = 3.5), containing 0.5 mM Tl_2SO_4, 200 µs after the 500 ns, 10-MeV electron pulse.
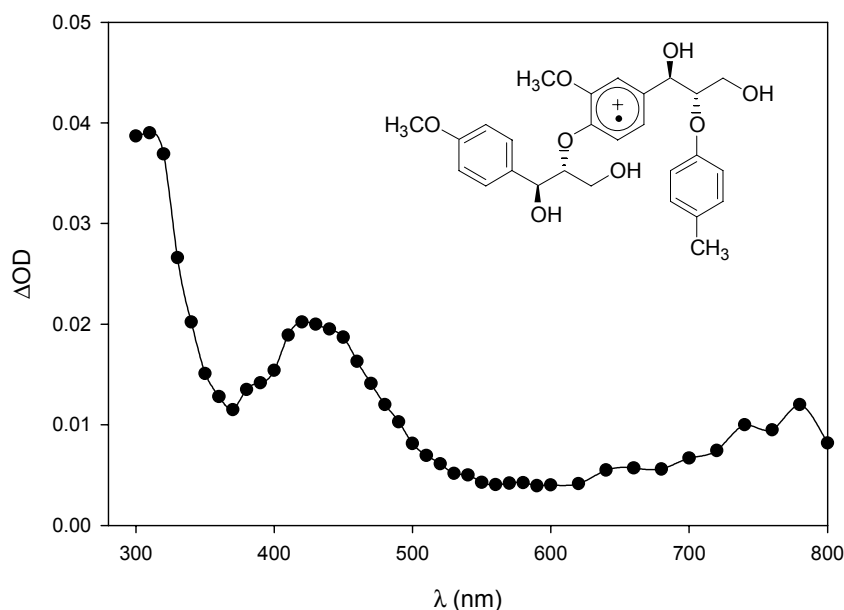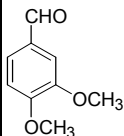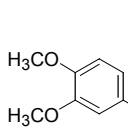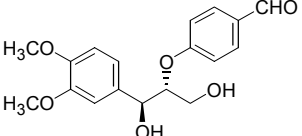
Figure 9. Absorption spectrum of **2**[+•] observed on reaction of Tl^{2+} with **2** (0.1 mM) at T = 25 °C, recorded after pulse radiolysis of an N_2O-saturated aqueous solution (pH = 3.5), containing 0.5 mM Tl_2SO_4, 200 μs after the 500 ns, 10-MeV electron pulse.

2.2 Enzymatic and Chemical Oxidation of **1** *and* **2**

Oxidations of **1** or **2** with H_2O_2 promoted by LiP were carried out in 50 mM aqueous sodium tartrate buffer, pH 3.5, with 6 % of acetonitrile added as cosolvent at 25°C and under an argon atmosphere. H_2O_2, equimolar with the substrate, was added gradually over 90 min using a syringe pump.

Oxidations of **1** or **2** promoted by Co(III)W were carried out using a 2:1 oxidant/substrate molar ratio in 50 mM aqueous sodium tartrate buffer, pH 3.5, with 6 % of acetonitrile added as cosolvent under an argon atmosphere at 60 °C for 48 h. After addition of an internal standard the reaction products were analysed by HPLC, HPLC-MS and ^{1}H NMR. The results are in Table 1 for the oxidations of the lignin model **1** and in Table 2 for the oxidation of the lignin model **2**.

Table 1. Products and yields in the LiP / H_2O_2 and Co(III)W promoted oxidation of the lignin model **1**.
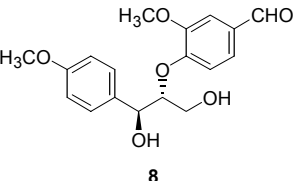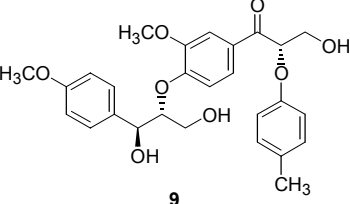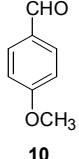
Oxidizing System	Products (Yields %)[a]			**1** (%)[a]
	5	**6**	**7**	
LiP/H_2O_2	9	4	11	68
Co(III)W	8	6	11	72

[a] Recovered starting material and yields of products are referred to the initial amount of the substrate. The average error is ± 10%.

15

The enzymatic oxidation of **1** promoted by the LiP/H$_2$O$_2$ system leads mainly to the formation of 3,4-dimethoxybenzaldehyde **5**, the trimeric ketone **6** and the dimeric aldehyde **7** (Table 1). The structure of these products was determined by comparison with authentic specimens (**5** and **7**) or by NMR and MS analysis (**6**). The same products, in similar proportions, were obtained in the oxidation of **1** promoted by Co(III)W in the same medium. The mass balance (with respect to the products containing the dimethoxylated ring) is satisfactory accounting for more than 90% of the starting material.

The oxidation of **2** promoted by the LiP/H$_2$O$_2$ system leads mainly to the formation of the dimeric aldehyde **8**, the trimeric ketone **9** and 4-methoxybenzaldehyde **10** (Table 2). The structure of these products was determined by comparison with authentic specimens.

Table 2. Products and yields in the LiP / H$_2$O$_2$ and Co(III)W promoted oxidation of the lignin model **2**.

Oxidizing System	Products (Yields %)[a]			2 (%)[a]
	8	**9**	**10**	
LiP/H$_2$O$_2$	7	2	18	71
Co(III)W	9	3	3	72

[a] Recovered starting material and yields of products are referred to the initial amount of the substrate. The average error is ± 10%.

The same products, but in different relative amounts, were also observed in the oxidation of **2** induced by Co(III)W in the same medium. Also in this case a good material balance (with respect to the products containing the monomethoxylated ring) was obtained, being 98% in the enzymatic reaction and 87% in the oxidation by Co(III)W.

2.3 Steady-State Kinetics

The Michaelis-Menten constants, k$_{cat}$ and K$_M$ were determined for the LiP catalysed oxidation of the trimeric model **2**, the dimeric model 1-(3,4-dimethoxyphenyl)-2-phenoxy-1-ethanol **4** and 3,4-dimethoxybenzyl alcohol **3**. The kinetics were carried out in tartrate buffer 50 mM at pH 3.5 and 25 °C. For each measure 50 μL of a solution of LiP 4.6 μM in tartrate buffer 50 mM at pH 4 were added to the buffer followed by the solution of substrates in acetonitrile (final concentration 10%). The reaction started by addition of 50 μL of a solution 0.012 M of H$_2$O$_2$. The results are reported in Table 3 together with the kinetic data concerning the oxidation of the same models with Co(III)W. The kinetics with Co(III)W were performed in AcOH/H$_2$O (70/30) solution, thoroughly purged with argon, containing 3 μmol of the substrate and 0.6 mmol of AcOK. The reaction was started by rapid addition of 0.1 ml of a Co(III)W solution (6 mM) in AcOH/H$_2$O (70/30).

Table 3. Kinetic parameters of the oxidation of **3**, **4** and **2** promoted by LiP / H$_2$O$_2$ and by Co(III)W

Substrate	Co(III)W	LiP / H$_2$O$_2$		
	k (M^{-1} s^{-1})	k$_{cat}$ (s^{-1})	K$_M$ (mM)	k$_{cat}$/K$_M$ (s^{-1}mM^{-1})
3	0.80	1.85	0.27	6.85
4	0.76	0.38	0.28	1.35
2	0.99	0.13	0.44	0.29

3. Discussion

In the Tl$^+$ induced oxidation of **1** and **2** the assignment of the absorption spectra recorded after the pulse, to the radical cations **1**$^{+\bullet}$ and **2**$^{+\bullet}$ is supported by the fact that these spectra closely resemble the spectrum of 3,4-dimethoxybenzyl alcohol radical cation (bands at 310 nm and 420 nm)[54] while they are significantly different from the spectrum of 4-methoxybenzyl alcohol radical cation which displays two main absorption bands at 290 and 450 nm.[65] Thus, in line with predictions, this result indicates that in both **1**$^{+\bullet}$ and **2**$^{+\bullet}$ the positive charge is localised on the dialkoxylated ring. This conclusion is also supported by the observation of a very slow decay of the absorption bands of **1**$^{+\bullet}$ and **2**$^{+\bullet}$ (too slow to be followed in the 1 ms time-scale of the experiment) as expected for a dimethoxy substituted aromatic radical cation.[54] Another interesting observation is that the spectrum of **2**$^{+\bullet}$ exhibits a broad band in the near infrared (NIR) region of the spectrum ($\lambda > 700$ nm). This band can be assigned to an intramolecular charge resonance (CR) interaction between a neutral donor ring and the charged acceptor ring in analogy with what previously observed for the diarylmethanol radical cations.[66] Since the NIR band is absent in **1**$^{+\bullet}$, it would appear that only in **2**$^{+\bullet}$, where the positive charge is located in the central aromatic ring, the geometry of the system fulfils the requirement of a co-facial arrangement between donor and acceptor rings necessary for efficient charge transfer and optimum electronic coupling.[67,68]

The results of the enzymatic and chemical oxidation indicates that the same products are formed in the reactions of both **1** and **2** with the LiP/H$_2$O$_2$ and Co(III)W systems thus suggesting that the enzymatic and chemical oxidation proceed by the same mechanism. Since it is well ascertained that the oxidations promoted by Co(III)W take place by an electron transfer mechanism, this observation fully confirms that also the oxidation of **1** and **2** promoted by LiP are one electron transfer processes, the radical cation being the key intermediate *en route* to the observed products.
Thus, in the oxidation of **1**, 3,4-dimethoxybenzaldehyde (**5**) should be formed, together with the carbon centred radical **11**, by C$_\alpha$-C$_\beta$ bond cleavage in **1**$^{+\bullet}$ (Scheme 3, path **a**), whereas C$_\alpha$-H bond cleavage in the same radical cation leads to the trimeric ketone **6** (Scheme 3, paths **b**, **d**).
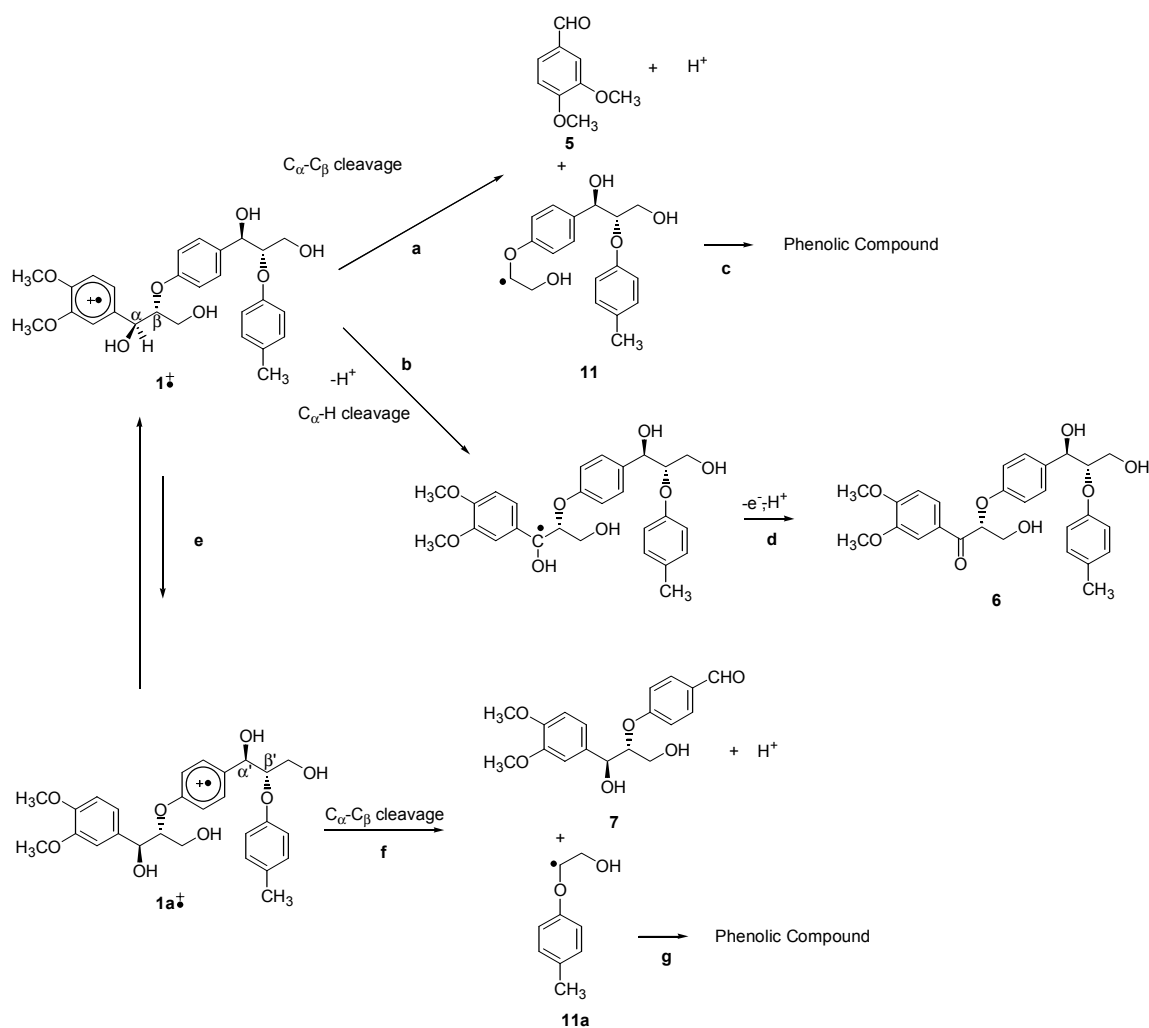
Scheme 3. Formation of the aldehydes **5** and **7** and of the ketone **6**.

The formation of the dimeric aldehyde **7**, the major reaction product, is more difficult to rationalise since a direct pathway leading from **1**[+•] to **7**, would involve the breaking of a bond which is very far apart from the positively charged ring. Thus, I suggest that an additional pathway for **1**[+•] is an intramolecular electron transfer to give the radical cation **1a**[+•] where the charge is now localised in the central ring of the model (path **e** in Scheme 3). Cleavage of the C-C bond β to this ring (the $C_{\alpha'}$-$C_{\beta'}$ bond) in **1a**[+•] can lead to **7**. Certainly, **1a**[+•] is much less stable than **1**[+•], but the thermodynamically uphill electron transfer is an unimolecular process and could be driven by the C-C bond cleavage reaction in **1a**[+•] which is expected to be much faster in the monoalkoxylated aromatic radical cation than in **1**[+•], as also clearly shown by the half lifetime data reported above.[54,65] In addition, since products coming from both **1**[+•] and **1a**[+•] are observed, whereas the UV-visible spectrum (Figure 8) presents only absorptions due to **1**[+•], it is possible to estimate for the **1**[+•] → **1a**[+•] intramolecular electron transfer a rate comparable with the decay rate of **1**[+•] (20-30 s^{-1}, estimated from the pulse radiolysis experiments). Now, on the basis of the Marcus equation, such a rate is consistent with an electron transfer process endoergic by 13 kcal mol^{-1} (the estimated free energy difference between the two radical cations) by assuming a quite reasonable value of 25 kcal mol^{-1} for the intrinsic barrier λ.

If the hypothesis of the intramolecular electron transfer is correct, it would result that C-C bond cleavage is the exclusive fragmentation process in **1a**[+•] while in **1**[+•] there is competition between C-C and C-H bond cleavages. This is not surprising since it is well known that

competition between C-C and C-H β bond cleavage is observed in the oxidation of dimethoxylated lignin model dimers[51,69] whereas monomethoxylated models undergo only C-C bond cleavage.[65]

It is also important to note that the C-C bond cleavage either from $1^{+\bullet}$ or $1a^{+\bullet}$ is also expected to lead to the carbon centred radicals **11** and **11a** respectively, and to the products derived there from. No such products were however observed. A possible explanation is that oxidation and hydrolysis of **11** and **11a** may lead to phenolic compounds (paths **c**, **g** in Scheme 3) which are then overoxidised to water soluble and/or polymeric species under the reaction conditions.[70] Fortunately, the lack of recovery of the products deriving from **11** and **11a** does not impair the mechanistic conclusions concerning the rupture modes in $1^{+\bullet}$. In view of the excellent mass balances noted before, there is no doubt that compounds **5**, **6** and **7** account for the main fragmentation routes available to $1^{+\bullet}$.

Coming to the products from **2**, the aldehyde **8** and the ketone **9** derive from $2^{+\bullet}$ by C_α-C_β and C_α-H bond cleavage processes, respectively, as shown in Scheme 4 (paths **a** and **b**), analogously to what proposed for the corresponding reactions in $1^{+\bullet}$. In this case too, however, there is a product, namely 4-methoxybenzaldehyde (**10**), which is by far the major product, whose formation from $2^{+\bullet}$ is more difficult to rationalise.
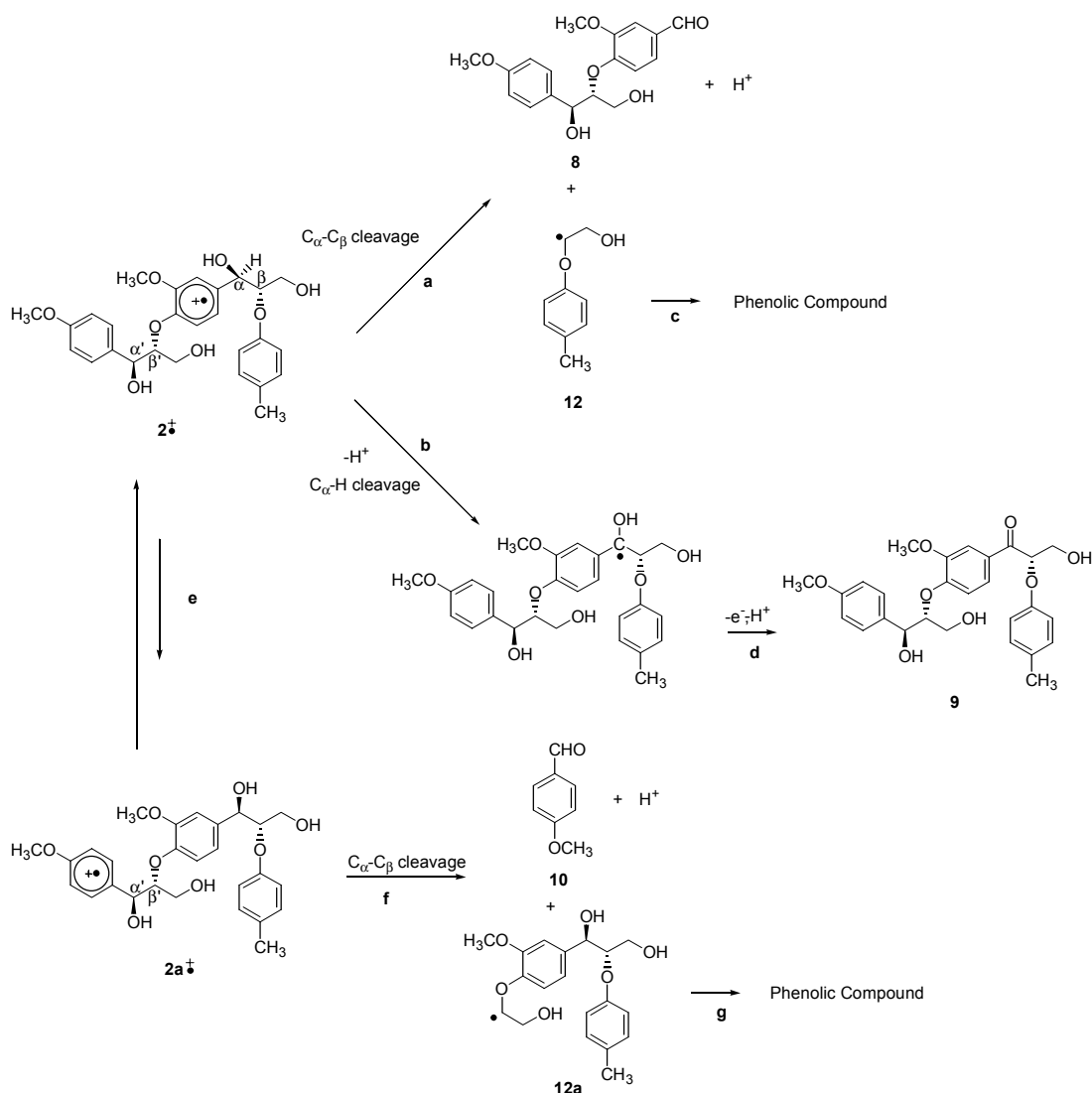
Scheme 4. Formation of the aldehydes **8** and **10** and of the ketone **9**.

19

Accordingly, the possibility that **10** derives from the cleavage of the $C_{\alpha'}\text{-}C_{\beta'}$ bond in $2^{+\bullet}$, is unlikely since this is a γ-bond with respect to the positively charged ring and this kind of cleavage has never been observed in an aromatic radical cation. Thus, also $2^{+\bullet}$ can undergo an intramolecular electron transfer to give the radical cation $2a^{+\bullet}$, a monoalkoxylated radical cation (Scheme 3, path **e**), which then undergoes the fast cleavage of the $C_{\alpha'}\text{-}C_{\beta'}$ bond, a β-bond with respect to the positively charged ring. The feasibility of the $2^{+\bullet} \rightarrow 2a^{+\bullet}$ intramolecular electron transfer can be supported by the same reasoning presented before for the $1^{+\bullet} \rightarrow 1a^{+\bullet}$ corresponding reaction. In this case, another mechanism leading to **10** might be an intramolecular nucleophilic attack of the alcoholic OH group to the dialkoxylated aromatic ring bearing the positive charge in $2^{+\bullet}$ followed by ring opening of the cyclohexadienyl radical[69] leading to an alkoxy radical, which undergoes β-scission (Scheme 5). However this mechanism should also form an isomer of **2** (Scheme 5, path **d**), which has not been observed.
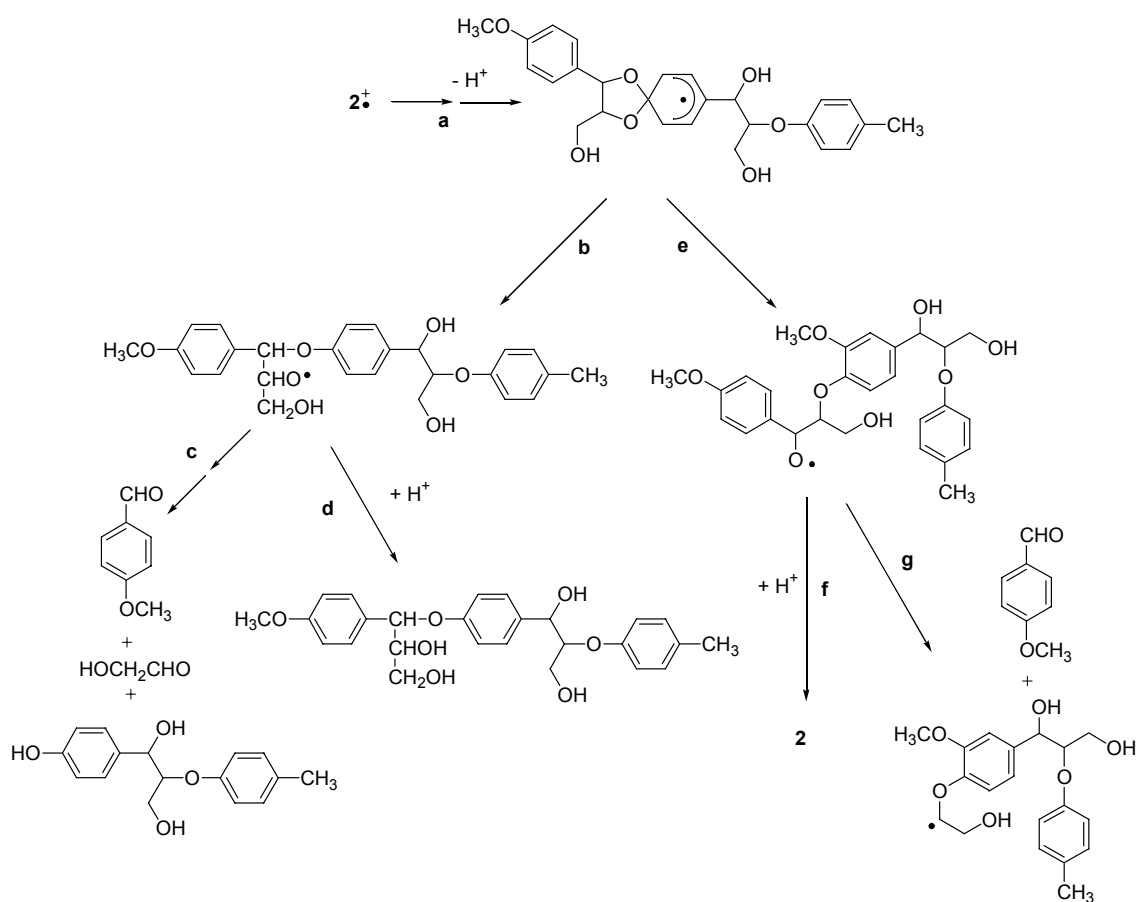
Scheme 5. Alternative pathway for formation of 4-methoxybenzaldehyde.

As already observed for **1**, also in the oxidation of **2** the products expected from the carbon radicals **12** and **12a** formed by C-C bond cleavage in $2^{+\bullet}$ and $2a^{+\bullet}$, respectively, were not observed. The same explanation presented before (formation of easily oxidisable phenolic products, paths **c**, **g** in Scheme 4) may also hold in this case. Anyway, in this case too, the excellent mass balance noted above makes me confident that the products **8**, **9** and **10** describe the main reaction pathways of **2**.

The observation that the LiP-catalysed oxidation of **1** and **2**, efficiently promotes the cleavage of a bond β to a monoalkoxylated ring is of great interest as it is well known that LiP is unable to catalyse the oxidation of monomethoxylated substrates.[71] For example, LiP cannot oxidise 4-methoxymandelic acid unless a mediator is present.[45,72] Thus, this observation clearly indicates that the initial interaction of the enzyme with **1** or **2** concerns the more

electron rich dialkoxylated ring from which the hole can be transferred to the less activated monoalkoxylated ring. In other words, the former ring acts as an intramolecular redox mediator.

More information about the interaction of the trimeric lignin models with the enzyme comes from the results of the kinetic experiments. It can be noted that the efficiency of the enzymatic catalysis, as expressed by k_{cat}, decreases by increasing the size of the substrate.[73] Thus, **3** is ca. 5 times more reactive than the dimer **4** which is ca. 3 times more reactive than the trimer **2**. In contrast, when tested against a chemical oxidant, namely Co(III)W, the three models exhibited practically the same reactivity as shown by the rate constants in Table 3. The observation that the efficiency of the enzymatic catalysis decreases by increasing the size of the substrate indicates that the reactivity trend observed with LiP is due to variations in the enzyme-substrate interaction related to the substrate structure. Even though **3**, **4** and **2** exhibit a similar affinity for the enzyme (K_M values), the way the substrate is oriented with respect to the enzyme might somewhat change with the size of the substrate itself, which might influence the efficiency of the long range ET. Apart from the possible interpretations of the kinetic parameters in Table 3, it is remarkable that the trimeric model still exhibits a substantial reactivity. This is an interesting result since LiP is reported to be the peroxidase with the most restricted access to the active site[33] and it seems therefore highly unlikely that a molecule as large as **2** may approach the heme-edge. Thus, the significant reactivity of **2** (and probably also of the dimer **4**) might support the recent hypothesis of another, much more accessible, interaction site in LiP, located on the external surface of the enzyme and namely in the proximity of the residue Trp 171.[74,75]

4. Conclusions

The results obtained provide significant indications about the fragmentation routes available to the intermediate radical cation in the LiP-induced oxidative degradation of trimeric model compounds **1** and **2**. The most important result is that with both the models, not only the cleavage of the C-C bond β with respect to the dialkoxylated ring (where the positive charge is initially localised) was observed but also the cleavage of the C-C bond β to a monoalkoxylated ring. In fact, the major products were those coming from the latter type of cleavage. This observation was explained by suggesting the occurrence, both in **1**$^{+\bullet}$ and **2**$^{+\bullet}$, of an intramolecular electron transfer thereby the hole is transferred from the dialkoxylated ring (which would act as an electron transfer internal mediator) to a monoalkoxylated ring. The driving force for this energetically uphill process may be provided by the very fast cleavage of the C-C bond β to the positively charged monoalkoxylated ring. Apart from the mechanistic interpretation, these results indicate that in the oxidative degradation of lignin C-C bonds can efficiently be broken which are not in a β position with respect to the ring where the positive charge is initially localised.

The steady state kinetic study has showed that the size of the model substrate influences the efficiency of the oxidation catalysed by LiP, the efficiency decreasing as the model becomes larger. In contrast, the three models exhibited a very similar reactivity towards Co(III)W, a chemical oxidant, suggesting a size-dependent interaction of the enzyme with the substrate that may influence the efficiency of the electron transfer. An additional observation is that with the trimeric model a substantial activity of the enzyme is still observed. Since the enzyme active site and the access channel appear almost inaccessible to the trimeric model, the above observation would support the recent suggestion of a substrate oxidation mediated by the LiP surface residue Trp 171.

5. Experimental Section

5.1 Instrumentation

^{1}H-NMR and ^{13}C-NMR spectra were recorded on a Bruker AC300P spectrometer in $CDCl_3$. GC-MS analyses were performed on a HP5890 GC (OV1 capillary column, 12 m x 0.2 mm) coupled with a HP5970 MSD. LC-MS analyses were performed on a Shimadzu LC10AD (column Supelcosil LC-18-DB, 25 cm x 4.6 mm) coupled with PE Sciex API 365 spectrometer (IS). HPLC analyses were carried out on a Hewlett Packard 1050 liquid chromatograph fitted with an UV-Vis detector and a column Supelcosil LC-18-DB (25 cm x 4.6 mm) The same instrument has been used for the separation of diastereomeric mixtures of precursors of substrates **1** and **2** using the column Supelcosil SPLC-18-DB (25 cm x 10 mm). UV-vis measurement was performed on a HP 8453 spectrophotometer. Pulse radiolysis experiments were performed by using a 10 MeV electron linear accelerator (Daresbury Laboratory, Warrington).

5.2 Materials

All the reagents and solvents were of the highest commercial quality available and used without further purification (unless otherwise specified). Milli-Q-filtered water was used for all solutions. The concentration of H_2O_2 was determined by titration with permanganate.[76] Co(III)W was prepared using the literature procedure[56] with some modifications.[57] Lignin peroxidase was prepared and purified as described in the literature.[77] The concentration of the enzyme solution was determined spectrophotometrically ($\varepsilon_{409nm} = 169$ mM^{-1} cm^{-1}).[78]

5.3 Substrates **1** and **2**

The trimeric lignin model compounds **1** and **2** have been synthesised following a procedure reported in the literature.[79] The detailed synthetic sequence is reported in Scheme 6.

The relative *anti* configuration of the stereocenters has been assigned on the basis of the preferential formation of the *anti* product in the condensation of the lithium enolate of **14a** or **14 b** with 3,4-dimethoxybenzaldehyde or 4-methoxybenzaldehyde (Scheme 1, step c) and in the condensation of the lithium enolate of compound **20** with the dimeric aldehydes **17a** or **17b** (Scheme 1, step g). The assignment of the relative *anti* configuration for the two stereocenters formed in step c of Scheme 1 has been also confirmed by ^{1}H and ^{13}C NMR analysis of the 1,3-diol acetonides **17a** and **17b**. In particular ^{13}C NMR spectrum of **17a** showed an axial methyl group at 19.1 ppm, an equatorial methyl group at 29.1 ppm and an acetal carbon at 99.6 ppm which suggest that the 1,3-dioxolane exist in a well defined chair conformation.[80] Then, the coupling constants of the two protons C(4)-H$_a$ and C(5)-H$_b$ ($J_{a,b}$ = 8.9 Hz) indicated a *trans* diequatorial relationship of the substituents.[80] Analogously ^{13}C NMR spectrum of **17b** showed an axial methyl group at 19.7 ppm, an equatorial methyl group at 28.5 ppm and an acetal carbon at 99.7 ppm. The coupling constants of the two protons C(4)-H$_a$ and C(5)-H$_b$ is $J_{a,b}$ = 9.5 Hz.

BrCH$_2$CO$_2$CH$_2$CH$_3$

K$_2$CO$_3$, acetone

a

HOCH$_2$CH$_2$OH

TsOH, C$_6$H$_6$

b

13a, X = H, 56%
13b, X = OCH$_3$, 94%

14a, X = H, 76%
14b, X = OCH$_3$, 81%

LDA, THF
-78°C

c

PPTS

acetone / H$_2$O

e

NaBH$_4$

THF / H$_2$O

d

7, X = H, Y = OCH$_3$, 96%
8, X = OCH$_3$, Y = H, 88%

16a, X = H, Y = OCH$_3$, 86%
16b, X = OCH$_3$, Y = H, 90%

15a, X = H, Y = OCH$_3$, 38%
15b, X = OCH$_3$, Y = H, 43%

TsOH
acetone

f

20

LDA, THF   -78°C

g

17a, X = H, Y = OCH$_3$, 55%
17b, X = OCH$_3$, Y = H, 53%

18a, X = H, Y = OCH$_3$, 64%
18b, X = OCH$_3$, Y = H, 73%

NaBH$_4$

THF / H$_2$O

h

PPTS

acetone / H$_2$O

i

1, X = H, Y = OCH$_3$, 75%
2, X = OCH$_3$, Y = H, 98%

19a, X = H, Y = OCH$_3$, 72%
19b, X = OCH$_3$, Y = H, 77%

Scheme 6. Synthesis of the lignin models compound **1** and **2**.

Ethyl (4-formylphenoxy)acetate (13a)

To a solution of 4-hydroxybenzaldehyde (10 g, 82 mmol) in dry acetone (120 mL) anydrous K$_2$CO$_3$ (17 g) was added, then ethyl α-bromoacetate (20.5 g, 0.12 mol, 10.9 mL) was added dropwise at room temperature. The mixture was heated at reflux for 3 h, then filtered and concentrated. The residue was dissolved in 50 mL of AcOEt, washed with NaOH 2 N and

with water. The organic layer was dried over anhydrous Na_2SO_4, filtered and concentrated to obtain 9.5 g, 45.7 mmol of a yellow liquid (yield 56%) sufficiently pure to be used in the following step.

^{1}H NMR (CDCl$_3$, 300 MHz) δ 1.30 (t, J = 7.1, 3H), 4.28 (q, J = 7.1, 2H), 4.71 (s, 2H), 6.98-7.05 (m, 2H), 7.81-7.89 (m, 2H), 9.90 (s, 1H).

GC-MS m/z (%) M$^+$ 208 (85), 207 (24), 135 (100), 121 (30), 107 (17), 106 (20), 105 (82), 79 (46), 78 (13), 77 (84), 76 (24), 65 (20), 63 (13), 59 (16), 51 (47).

Ethyl [4-(1,3-dioxolan-2-yl)phenoxy]acetate (14a)

Ethylene glycol (2 mL) and a catalytic amount of TsOH (0.05%) were added to a solution of **13a** (4.9 g, 23.7 mmol) in 75 mL of benzene. The solution was heated at reflux for 5 h in a Dean-Stark apparatus to distil off the azeotrope benzene-H_2O. The mixture was then washed with saturated aqueous NaHCO$_3$ and with H_2O, dried over anhydrous MgSO$_4$ and filtered. The solvent was evaporated to obtain 4.81 g, 17.9 mmol, yield 76% of a yellow oil sufficiently pure to be used in the following step.

^{1}H NMR (CDCl$_3$, 300 MHz) δ 1.29 (t, J = 7.2, 3H), 3.97-4.16 (m, 4H), 4.26 (q, J = 7.2, 2H), 4.62 (s, 2H), 5.75 (s, 1H), 6.91 (d, J = 8.5, 2H), 7.41 (d, J = 8.5, 2H).

GC-MS m/z (%) 252 (29), 251 (100), 207 (19), 180 (51), 179 (30), 165 (36), 164 (23), 149 (35), 135 (26), 121 (15), 107 (54), 105 (16), 91 (13), 79 (13), 77 (37), 73 (69), 65 (17), 51 (19).

(2R,3S),(2S,3R)-Ethyl 2-[4-(1,3-dioxolan-2-yl)phenoxy]-3-hydroxy-3-(3,4-dimethoxyphenyl)propionate (15a)

Compound **14a** (4.81 g, 17.9 mmol), dissolved in dry THF (20 mL), was added dropwise to a solution of LDA (12 mL of a 2 M solution in THF, eptane and ethylbenzene) in dry THF (15 mL) at -78°C. After 10 min at -78°C, a solution of 3,4-dimethoxybenzaldehyde (2.40 g, 17.9 mmol) in dry THF (20 mL) was added dropwise to this solution. After 50 min at -78°C the reaction was quenched with saturated aqueous NH$_4$Cl (30 mL) and extracted with AcOEt. The combined organic extracts were dried over Na$_2$SO$_4$, filtered and concentrated to give a viscous oil that contained the two diastereomers in 72:28 diastereomeric ratio (evaluated by NMR). Purification by flash chromatography on silica gel (eluent light petroleum:AcOEt 1:1) allowed the separation of the two diastereomers. 2.83 g, 6.77 mmol of the major diastereomer (2R,3S),(2S,3R)-ethyl 2-[4-(1,3-dioxolan-2-yl)phenoxy]-3-hydroxy-3-(3,4-dimethoxyphenyl)propionate **15a** were obtained (yield 38%).

^{1}H NMR (CDCl$_3$, 300 MHz) δ 1.14 (t, J = 7.1, 3H), 3.83 (s, 6H), 3.89-4.22 (m, 6H), 4.70 (d, J = 6.2, 1H) 5.09 (d, J = 6.2, 1H), 5.68 (s, 1H), 6.78-6.98 (m, 5H), 7.29-7.34 (m, 2H).

(1S,2R),(1R,2S)-2-[4-(1,3-Dioxolan-2-yl)phenoxy]-1-(3,4-dimethoxyphenyl)-1,3-propandiol (16a)

NaBH$_4$ (1.44 g, 38 mmol) was added at room temperature portionwise in 6h to a solution of **15a** (1.59 g, 3.80 mmol) in THF:H_2O 3:1 (40 mL). The first portion of NaBH$_4$ was added to the solvent mixture before **15a** to avoid deprotection of the aldehydic group. After 20 h at room temperature H_2O (30 mL) was added and the solution was extracted with Et$_2$O. The combined organic extracts were dried over Na$_2$SO$_4$, filtered and concentrated to give a white oil (1.23 g, 3.27 mmol, yield 86%) sufficiently pure to be used in the following step.

^{1}H NMR (CDCl$_3$, 300 MHz) δ 3.67-3.74 (m, 2H), 3.82 (s, 3H), 3.83 (s, 3H), 3.96-4.09 (m, 4H), 4.30-4.36 (m, 1H), 4.93 (d, J = 5.6, 1H), 5.69 (s, 1H), 6.76-6.98 (m, 5H), 7.28-7.38 (m, 2H).

(1S,2R),(1R,2S)-4-[1,3-Dihydroxypropan-1-(3,4-dimethoxyphenyl)-2-yloxy]benzaldehyde (7)

PPTS (0.18 g 0.72 mmol) was added at room temperature to a solution of **16a** (1.23 g, 3.27 mmol) in acetone:H_2O 4:1 (20 mL), then the mixture was heated at reflux for 5 h. Acetone was distilled off and saturated aqueous NaHCO$_3$ (20 mL) was added, the solution was then extracted with CH$_2$Cl$_2$. The combined organic extracts were washed with brine,

dried over Na_2SO_4, filtered and the solvent was evaporated to obtain a yellowish oil (1.04 g, 3.13 mmol, yield 96%) sufficiently pure to be used in the following step.

^{1}H NMR (CDCl$_3$, 300 MHz) δ 3.85 (s, 6H), 3.97 (d, J = 4.3, 2H), 4.56 (m, 1H), 5.02 (d, J = 5.8, 1H), 6.80-6.85 (m, 1H), 6.93-7.01 (m, 4H), 7.71-7.84 (m, 2H), 9.86 (s, 1H).

(4*S*,5*R*),(4*R*,5*S*)-4-[2,2-Dimethyl-1,3-dioxan-4-(3,4-dimethoxyphenyl)-5-yloxy]benzaldehyde (17a)

Anhydrous TsOH (32 mg, 0.19 mmol) was added to a solution of **7** (0.55 mg, 1.66 mmol) in dry acetone (23 mL). After 1 h molecular sieves 4 Å were added and the mixture was stirred for 17 h. The solution was filtered over celite and anhydrous Na_2CO_3 was added. The solvent was then evaporated and the residue dissolved in CH_2Cl_2 (10 mL), washed with saturated aqueous Na_2CO_3 (10 mL) and with water (10 mL), dried over Na_2SO_4, filtered and concentrated to give a mixture of **7** and **17a**. Compound **17a** was separated by flash chromatography on silica gel (eluent light petroleum:AcOEt 7:3) to give a yellow oil (343 mg, 0.92 mmol, yield 55%).

^{1}H NMR (CDCl$_3$, 300 MHz) δ 1.54 (s, 3H), 1.64 (s, 3H), 3.81 (s, 3H), 3.83 (s, 3H), 4.10-4.22 (m, 2H), 4.35-4.47 (m, 1H), 4.87 (d, J = 8.9, 1H), 6.70-6.82 (m, 3H), 6.97-7.01 (m, 2H), 7.67-7.72 (m, 2H), 9.81 (s, 1H).

^{13}C NMR δ 19.1, 29.1, 55.9, 56.0, 62.4, 72.9, 74.0, 99.6, 109.8, 110.7, 111.2, 115.7, 116.2, 119.3, 131.8, 148.9, 149.2, 163.3, 190.7.

Ethyl (4-methylphenoxy)acetate (20)

To a solution of 4-methylphenol (5 g, 46.2 mmol) in dry acetone (80 mL) anhydrous K_2CO_3 (9.6 g) was added, then ethyl α-bromoacetate (11.6 g, 69.2 mmol, 7.7 mL) was added dropwise at room temperature. The mixture was heated at reflux for 2 h, then filtered and concentrated. The residue was dissolved in 50 mL of Et_2O, washed with NaOH 2 N and with water. The organic layer was dried over anhydrous Na_2SO_4, filtered and concentrated to obtain 3.7 g, 19.1 mmol of an orange liquid (yield 41%) sufficiently pure to be used in the following step.

^{1}H NMR δ: 1.30 (t, J = 7.2, 3H), 2.29 (s, 3H), 4.27 (q, J = 7.2, 2H), 4.59 (s, 2H), 6.81 (d, J = 8.7, 2H), 7.09 (d, J = 8.7, 2H).

GC-MS m/z (%) M$^+$ 194 (73), 121 (95), 108 (11), 107 (22), 93 (23), 91 (100), 77 (21), 65 (29).

(2*R*,3*S*,4'*S*,5'*R*),(2*R*,3*S*,4'*R*,5'*S*),(2*S*,3*R*,4'*S*,5'*R*),(2*S*,3*R*,4'*R*,5'*S*)and(2*R*,3*R*,4'*S*,5'*R*),(2*R*,3*R*,4'*R*,5'*S*),(2*S*,3*S*,4'*S*,5'*R*)(2*S*,3*S*,4'*R*,5'*S*)-Ethyl 3-{4-[2',2'-dimethyl-1',3'-dioxan-4'-(3,4-dimethoxyphenyl)-5'-yloxy]phenyl}-3-hydroxy-2-(4-methylphenoxy)propionate (18a)

Compound **20** (178 mg, 0.92 mmol) dissolved in dry THF (3 mL), was added to a solution of LDA (0.56 mL of a 2 M solution in THF, eptane and ethylbenzene) in dry THF (4 mL). After 10 min at -78°C, a solution of compound **17a** (343 mg, 0.92 mmol) in dry THF (3 mL) was added dropwise. After 40 min at –78°C the reaction was quenched with saturated aqueous NH_4Cl and extracted with AcOEt. The combined organic extracts were dried over Na_2SO_4, filtered and the solvent was evaporated to give a crude oil which was purified by flash chromatography (gradient of elution light petroleum:AcOEt 4:1-2:1) to obtain a yellowish solid (328 mg, 0.58 mmol, yield 64%) as a mixture of diastereomers (diastereomeric ratio 68:32 as determined by HPLC).

Purification of 91 mg of the mixture by preparative HPLC (eluent MeOH-H$_2$O 8:2, column LC-18-DB) allowed the separation of the two couple of diastereomers (2*R*,3*S*,4'*R*,5'*S*),(1*R*,2*S*,4'*S*,5'*R*),(1*S*,2*R*,4'*R*,5'*S*), (1*S*,2*R*,4'*S*,5'*R*)-ethyl 3-{4-[2',2'-dimethyl-1',3'-dioxan-4'-(3,4-dimethoxyphenyl)-5'-yloxy]phenyl}-3-hydroxy-2-(4-methylphenoxy)propionate and (1*R*,2*R*,4'*R*,5'*S*),(1*R*,2*R*,4'*S*,5'*R*), (1*S*,2*S*,4'*R*,5'*S*),(1*S*,2*S*,4'*S*,5'*R*)-ethyl 3-{4-[2',2'-dimethyl-1',3'-dioxan-4'-(3,4-dimethoxyphenyl)-5'-yloxy]phenyl}-3-hydroxy-2-(4-methylphenoxy)propionate. 72 mg, 0.13 mmol of the major diastereomer were obtained and used in the next step.

18a: ^{1}H NMR (CDCl$_3$, 300 MHz) δ 1.09 (t, $J = 7.0$, 3H), 1.52 (s, 3H), 1.63 (s, 3H), 2.25 (s, 3H), 3.83 (s, 6H), 3.89-4.31 (m, 5H), 4.64 (d, $J = 5.9$, 1H), 4.84 (d, $J = 8.8$, 1H), 5.01-5.08 (m, 1H), 6.66-6.81 (m, 5H), 6.98-7.03 (m, 4H), 7.20-7.27 (m, 2H).

(1*R*,2*S*,4'*R*,5'*S*),(1*R*,2*S*,4'*S*,5'*R*),(1*S*,2*R*,4'*R*,5'*S*) and (1*S*,2*R*,4'*S*,5'*R*)-3-{4-[2',2'-Dimethyl-1',3'-dioxan-5'-yloxy-4'-(3,4-dimethoxyphenyl)]phenyl}-2-(4-methylphenoxy)-1,3-propanediol (19a)

NaBH$_4$ (15 mg, 0.40 mmol) was added at room temperature portionwise in 3 h to a solution of **18a** (72 mg, 0.13 mmol) in THF:H$_2$O 3:1 (2 mL). After 45 h at room temperature under stirring, H$_2$O was added and the solution was extracted with Et$_2$O. The combined organic extracts were dried over Na$_2$SO$_4$, filtered and the solvent was evaporated to give compound **19a** (49 mg, 93 µmol, yield 72%) sufficiently pure to be used in the following step.

^{1}H NMR (CDCl$_3$, 300 MHz) δ 1.53 (s, 3H), 1.63 (s, 3H), 2.26 (s, 3H), 3.68-3.94 (m, 2H), 3.83 (s, 6H), 3.89-4.29 (m, 4H), 4.83 (d, $J = 9.0$, 1H), 4.93 (d, $J = 5.1$, 1H), 6.61-6.83 (m, 5H), 6.97-7.04 (m, 4H), 7.15-7.21 (m, 2H).

(1*R*,2*S*,1'*R*,2'*S*),(1*R*,2*S*,1'*S*,2'*R*),(1*S*,2*R*,1'*R*,2'*S*),(1*S*,2*R*,1'*S*,2'*R*)-2-{4-[1',3'-Dihydroxypropyl-2'-(4-methylphenoxy)]-2-methoxyphenoxy}-1-(4-methoxyphenyl)-1,3-propanediol (19)

PPTS (12 mg, 47 mmol) was added to a solution of **19a** (49 mg, 93 µmol) in acetone:H$_2$O 3:2 (2 mL). The mixture was heated at reflux for 24 h, then acetone was distilled off, saturated aqueous NaHCO$_3$ was added and the solution was extracted with AcOEt. The combined organic extracts were washed with brine, dried over Na$_2$SO$_4$, filtered and the solvent was evaporated. The mixture was purified by preparative TLC (eluent light petroleum:AcOEt 1:2). **1** was obtained as a white solid (34 mg, 70 µmol, yield 75%).

^{1}H NMR δ: 2.25 (s, 3H), 3.84 (s, 6H), 3.73-3.94 (m, 4H), 4.23-4.38 (m, 2H), 4.96 (m, 2H), 6.74-6.93 (m, 7H), 7.00-7.04 (m, 2H), 7.23-7.27 (m, 2H).

^{13}C NMR δ 20.4, 55.9, 61.2, 61.4, 73.5, 73.8, 81.9, 82.1, 109.5, 111.0, 116.4, 116.6, 118.7, 127.6, 130.0, 131.3, 132.9, 133.8, 148.6, 148.9, 155.4, 157.3.

LC-MS: (M+Na$^+$) m/z 507.

Anal. Calcd for C$_{27}$H$_{32}$O$_8$·H$_2$O: C, 64.5; H, 6.8. Found C, 64.5; H, 6.7.[81]

Ethyl (4-formyl-2-methoxyphenoxy)acetate (13b)

To a solution of vanillin (10 g, 65.7 mmol) in dry acetone (110 mL) anhydrous K$_2$CO$_3$ (13.6 g) was added, then ethyl α-bromoacetate (16.44 g, 98.42 mmol, 10.91 mL) was added dropwise at room temperature. The mixture was heated at reflux for 3 h, then filtered and the solvent was evaporated. The residue was dissolved in 50 mL of AcOEt, washed with NaOH 2 N and with water. The organic layer was dried over anhydrous Na$_2$SO$_4$, filtered and concentrated to obtain 14.7 g, 61.9 mmol of a yellow oil (yield 94%), sufficiently pure to be used in the following step.

^{1}H NMR (CDCl$_3$, 300 MHz) δ 1.29 (t, $J = 7.1$, 3H), 3.95 (s, 3H), 4.27 (q, $J = 7.1$, 2H), 4.79 (s, 2H), 6.89 (dd, $J = 7.2$ and 1.6, 1H), 7.40-7.44 (dd, $J = 7.2$ and 1.6, 2H), 9.86 (s, 1H).

GC-MS m/z (%) M$^+$ 238 (100), 165 (53), 151 (45), 150 (38), 149 (17), 137 (27), 119 (31), 109 (15), 105 (29), 95 (32), 79 (26), 77 (64), 76 (15), 65 (20), 63 (23), 59 (32), 52 (16), 51 (36).

Ethyl [4-(1,3-dioxolan-2-yl)-2-methoxyphenoxy]acetate (14b)

Ethylene glycol (5.2 mL) and a catalytic amount of TsOH (0.05%) were added to a solution of **13b** (14.7 g, 61.9 mmol) in 180 mL of benzene. The solution was heated at reflux for 8 h in a Dean-Stark apparatus to distil off the azeotrope benzene-H$_2$O. The mixture was then washed with saturated aqueous NaHCO$_3$ and with H$_2$O, dried over anhydrous MgSO$_4$ and filtered. The solvent was evaporated to obtain 14.6 g, 50.4 mmol of a yellowish oil (yield 81%), sufficiently pure to be used in the following step.

^{1}H NMR (CDCl$_3$, 300 MHz) δ 1.28 (t, $J = 7.1$, 3H), 3.91 (s, 3H), 3.96-4.19 (m, 4H), 4.25 (q, $J = 7.1$, 2H), 4.69 (s, 2H), 5.75 (s, 1H), 6.81 (d, $J = 8.2$, 1H), 6.98 (d, $J = 1.8$, 1H), 7.03 (dd, $J = 8.2$ and 1.8, 1H).

GC-MS *m/z* (%) 282 (53), 281 (69), 210 (100), 209 (19), 137 (24), 123 (30), 122 (22), 95 (18), 92 (15), 79 (15), 77 (27), 76 (14), 73 (70), 65 (14), 63 (15), 59 (20), 51 (13).

(2*R*,3*S*),(2*S*,3*R*)-Ethyl 2-[4-(1,3-dioxolan-2-yl)-2-methoxyphenoxy]-3-hydroxy-3-(4-methoxyphenyl) propionate (15b)

Compound **14b** (14.6 g, 50.4 mmol), dissolved in dry THF (50 mL), was added dropwise to a solution of LDA (32.5 mL of a 2 M solution in THF, eptane and ethylbenzene) in dry THF (100 mL). After 20 min at −78°C, a solution of 4-methoxybenzaldehyde (6.85 g, 50.4 mmol) in dry THF (20 mL) was added dropwise to this solution. After 1 h at −78°C the reaction was quenched with saturated aqueous NH$_4$Cl (50 mL) and extracted with AcOEt. The combined organic extracts were dried over Na$_2$SO$_4$, filtered and concentrated to give a viscous oil that contained the two diastereomers in 76:24 diastereomeric ratio (determined by ^{1}H NMR). Purification by flash chromatography on silica gel (eluent light petroleum:AcOEt 1:1) allowed the separation of the two diastereomers. 9.0 g, 21.5 mmol of the major diastereomer (2*S*,3*R*),(2*R*,3*S*)-ethyl 2-[4-(1,3-dioxolan-2-yl)-2-methoxyphenoxy]-3-hydroxy-3-(4-methoxyphenyl) propionate **15b** were obtained (yield 43%).

^{1}H NMR (CDCl$_3$, 300 MHz) δ 1.14 (t, *J* = 6.8, 3H), 3.80 (s, 3H), 3.89 (s, 3H), 4.00-4.17 (m, 6H), 4.71 (d, *J* = 4.9, 1H), 5.15 (d, *J* = 4.9, 1H), 5.73 (s, 1H), 6.84-7.04 (m, 5H), 7.34-7.41 (m, 2H).

(1*S*,2*R*),(1*R*,2*S*)-2-[4-(1,3-Dioxolan-2-yl)-2-methoxyphenoxy]-1-(4-methoxyphenyl)-1,3-propandiol (16b)

NaBH$_4$ (1.2 g, 31.9 mmol) was added at room temperature portionwise in 6h to a solution of **15b** (1.25 g, 3.17 mmol) in THF:H$_2$O 3:1 (32 mL). The first portion of NaBH$_4$ was added to the solvent mixture before **15b** to avoid deprotection of the aldehydic group. After 16h at room temperature H$_2$O (20 mL) was added and the solution was extracted with Et$_2$O. The combined organic extracts were dried over Na$_2$SO$_4$, filtered and concentrated to give a yellowish oil (1.08 g, 2.87 mmol, yield 90%) sufficiently pure to be used in the following step.

^{1}H NMR (CDCl$_3$, 300 MHz) δ 3.70-3.78 (m, 2H), 3.80 (s, 3H), 3.91 (s, 3H), 4.00-4.18 (m, 5H), 4.99 (t, *J* = 4.9, 1H), 5.75 (s, 1H), 6.85-7.08 (m, 5H), 7.27-7.34 (m, 2H).

(1*S*,2*R*),(1*R*,2*S*)-4-[1,3-Dihydroxypropan-1-(4-methoxyphenyl)-2-yloxy]-3-methoxybenzaldehyde (8)

PPTS (0.14 mg, 0.56 mmol) was added at room temperature to a solution of **16b** (0.97 g, 2.58 mmol) in acetone:H$_2$O 4:1 (15 mL), then the mixture was heated at reflux for 4h. Acetone was distilled off and saturated aqueous NaHCO$_3$ (20 mL) was added, the solution was then extracted with Et$_2$O. The combined organic extracts were washed with brine, dried over Na$_2$SO$_4$, filtered and the solvent was evaporated to obtain a yellow solid (750 mg, 2.27 mmol, yield 88%) sufficiently pure to be used in the following step.

^{1}H NMR (CDCl$_3$, 300 MHz) δ 3.74-4.00 (m, 2H), 3.80 (s, 3H), 3.93 (s, 3H), 4.36-4.44 (m, 1H), 5.02 (d, *J* = 5.0, 1H), 6.85-7.05 (m, 3H), 7.31-7.41 (m, 4H), 9.86 (s, 1H).

(4*S*,5*R*),(4*R*,5*S*)-4-[2,2-Dimethyl-1,3-dioxan-4-(4-methoxyphenyl)-5-yloxy]-3-methoxybenzaldehyde (17b)

Anhydrous TsOH (36 mg, 0.19 mmol) was added to a solution of **8** (623 mg, 1.88 mmol) in dry acetone (24 mL). After 1 h molecular sieves 4 Å were added and the mixture was stirred for 2 h. The solution was then filtered over celite and anhydrous Na$_2$CO$_3$ was added. After the evaporation of the solvent the residue was dissolved in AcOEt, washed with water, dried over Na$_2$SO$_4$, filtered and concentrated to give a mixture of **8** and **17b**. Compound **17b** was separated by flash chromatography on silica gel (eluent light petroleum:AcOEt 7:3) to give a yellow oil (377 mg, 1.0 mmol, yield 53%).

^{1}H NMR (CDCl$_3$, 300 MHz) δ 1.52 (s, 3H), 1.64 (s, 3H), 3.75 (s, 3H), 3.86 (s, 3H), 3.96-4.22 (m, 2H), 4.29-4.40 (m, 1H), 4.95 (d, *J* = 9.5, 1H), 6.62 (d, *J* = 8.1, 1H), 6.78-6.86 (m, 2H), 7.21-7.32 (m, 2H), 7.36-7.43 (m, 2H), 9.77 (s, 1H).

^{13}C NMR δ 19.7, 28.5, 55.3, 56.0, 62.5, 74.1, 76.6, 99.7, 110.0, 113.8, 114.0, 114.8, 126.1, 128.4, 130.9, 150.6, 152.6, 159.6, 190.8.

(2R,3S,4'S,5'R),(2R,3S,4'R,5'S),(2S,3R,4'S,5'R),(2S,3R,4'R,5'S)and(2R,3R,4'S,5'R),(2R,3R,4'R,5'S),(2S,3S,4'S,5'R)(2S,3S,4'R,5'S)-Ethyl 3-{4-[2',2'-dimethyl-1',3'-dioxan-4'-(4-methoxyphenyl)-5'-yloxy]-3-methoxyphenyl}-3-hydroxy-2-(4-methylphenoxy)propionate (18b)

Compound **20** (1.48 g, 7.63 mmol), dissolved in dry THF (30 mL), was added to a solution of LDA (5 mL of a 2 M solution in THF, eptane and ethylbenzene) in dry THF (20 mL). After 15 min at -78°C, a solution of compound **17b** (2.84 g, 7.63 mmol) in dry THF (30 mL) was added dropwise. After 40 min at −78°C the reaction was quenched with saturated aqueous NH$_4$Cl and extracted with AcOEt. The combined organic extracts were dried over Na$_2$SO$_4$, filtered and the solvent was evaporated to give a crude oil which was purified by flash chromatography (gradient of elution light petroleum:AcOEt 4:1-1:1) to obtain a yellowish solid (3.0 g, 5.5 mmol, yield 73%) as a mixture of diastereomers.

^{1}H NMR (CDCl$_3$, 300 MHz) δ 1.12 (t, J = 7.2, 3H), 1.49 (s, 3H), 1.62 (s, 3H), 2.25 (s, 3H), 3.74 (s, 3H), 3.76 (s, 3H), 3.98-4.17 (m, 5H), 4.62 (d, J = 6.0, 1H), 4.90 (d, J = 8.9, 1H), 4.98-5.08 (m, 1H), 6.43 (d, J = 8.3, 1H), 6.68-7.06 (m, 8H), 7.39-7.43 (m, 2H).

(1R,2S,4'R,5'S),(1R,2S,4'S,5'R),(1S,2R,4'R,5'S),(1S,2R,4'S,5'R)-3-{4-[2',2'-Dimethyl-1',3'-dioxan-4'-(4-methoxyphenyl)-5'-yloxy]-3-methoxyphenyl}-2-(4-methylphenoxy)-1,3-propanediol (19b)

NaBH$_4$ (0.29 mg, 7.7 mmol) was added at room temperature portionwise in 3 h to a solution of **18b** (1.39 g, 2.6 mmol) in THF:H$_2$O 3:1 (20 mL). After 24 h at room temperature under stirring H$_2$O was added and the solution was extracted with Et$_2$O. The combined organic extracts were dried over Na$_2$SO$_4$, filtered and the solvent evaporated to give **19b** (1.04 g, 2.0 mmol, yield 77%) as a mixture of diastereomers (diastereomeric ratio 67:33 as determined by HPLC).

Purification of 55 mg by preparative HPLC (eluent MeOH-H$_2$O 7:3, column LC-18-DB) allowed the separation of two couple of diastereomers (1R,2S,4'R,5'S),(1R,2S,4'S,5'R),(1S,2R,4'R,5'S), (1S,2R,4'S,5'R)-3-{4-[2',2'-dimethyl-1',3'-dioxan-4'-(4-methoxyphenyl)-5'-yloxy]-3-methoxyphenyl}-2-(4-methylphenoxy)-1,3-propanediole and (1R,2R,4'R,5'S),(1R,2R,4'S,5'R), (1S,2S,4'R,5'S),(1S,2S,4'S,5'R)-3-{4-[2',2'-dimethyl-1',3'-dioxan-4'-(4-methoxyphenyl)-5'-yloxy]-3-methoxyphenyl}-2-(4-methylphenoxy)-1,3-propanediole. 21 mg, 40 μmol of the major diastereomers was obtained and used in the last step.

19b: ^{1}H NMR (CDCl$_3$, 300 MHz) δ 1.49 (s, 3H), 1.62 (s, 3H), 2.27 (s, 3H), 3.74-3.87 (m, 2H), 3.74 (s, 3H), 3.77 (s, 3H), 3.98-4.30 (m, 4H), 4.87-4.96 (m, 2H), 6.42 (d, J = 8.3, 1H), 6.67-6.85 (m, 6H), 7.03 (d, J = 8.7, 2H), 7.39 (d, J = 8.3, 2H).

(1R,2S,1'R,2'S),(1R,2S,1'S,2'R),(1S,2R,1'R,2'S),(1S,2R,1'S,2'R)-2-{4-[1',3'-Dihydroxypropyl-2'-(4-methylphenoxy)]-2-methoxyphenoxy}-1-(4-methoxyphenyl)-1,3-propanediole (2)

PPTS (5 mg, 20 μmol) was added to a solution of **19b** (21 mg, 40 μmol) in acetone:H$_2$O 3:2 (1 mL). The mixture was heated at reflux for 24 h, then acetone was distilled off. Saturated aqueous NaHCO$_3$ (1 mL) was then added and the solution was extracted with AcOEt. The combined organic extracts were washed with brine, dried over Na$_2$SO$_4$, filtered and the solvent was evaporated to give pure **2** (19.0 mg, 39.2 μmol, yield 98%).

^{1}H NMR (CDCl$_3$, 300 MHz) δ 2.25 (s, 3H), 3.79 (s, 3H), 3.82-3.98 (m, 4H), 3.82 (s, 3H), 4.06-4.17 (m, 1H), 4.27-4.34 (m, 1H), 4.93-5.01 (m, 2H), 6.73-7.04 (m, 9H), 7.26-7.30 (m, 2H).

^{13}C NMR δ 21.0, 55.2, 55.9, 60.7, 61.4, 72.6, 73.6, 82.1, 87.1, 110.3, 110.3, 113.8, 116.5, 119.3, 119.4, 120.5, 127.2, 128.2, 130.0, 131.3, 131.9, 136.5, 136.6, 146.3, 151.4, 155.4, 159.1.

LC-MS: (M+Na$^+$) m/z 507.

Anal. Calcd for $C_{27}H_{32}O_8 \cdot H_2O$: C, 64.5; H, 6.8. Found C, 64.3; H, 6.9.[81]

5.4 Products

4-Methoxybenzaldehyde and 3,4-dimethoxybenzaldehyde are commercially available. The dimeric aldehydes **7** and **8** have been synthesised as precursors of compounds **1** and **2**. The ketone **9** was synthesised starting from the precursor **19b** of compound **2** according to the following scheme:
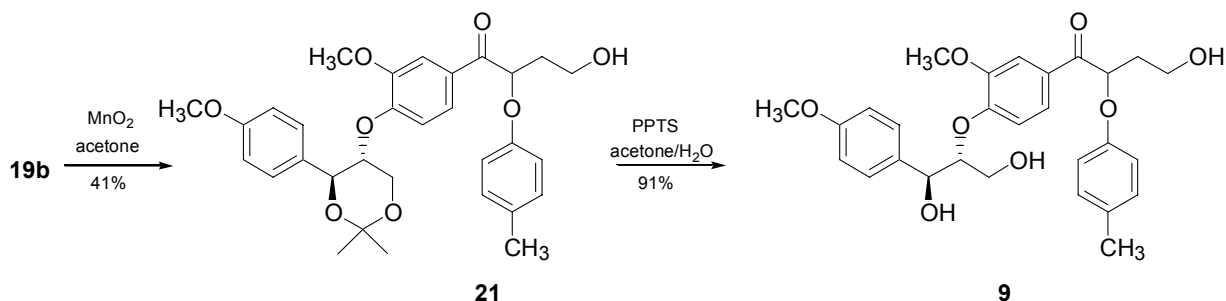
Scheme 7. Syntheses of the ketone **9**.

(2*S*,4'*R*,5'*S*),(2*S*,4'*S*,5'*R*),(2*R*,4'*R*,5'*S*),(2*R*,4'*S*,5'*R*)-1-{4-[2',2'-dimethyl-1',3'dioxan-5'-yloxy-4'-(4-methoxyphenyl)]-3-methoxyphenyl}-2-(4-methylphenoxy)-3-hydroxypropan-1-one (21)

MnO_2 (1.14 g, 13.1 mmol) was added at room temperature to a solution of 19b (0.14 mg, 0.27 mmol) in acetone (30 mL). After 7 h at room temperature under stirring the mixture was filtered over celite. The solvent was evaporated under reduced pressure to give the crude product which was purified by preparative TLC (eluent light petroleum:AcOEt 1:1). 57 mg, 0.11 mmol of 21 were obtained (yield 41%).

^{1}H NMR δ: 1.52 (s, 3H), 1.63 (s, 3H), 2.24 (s, 3H), 3.75 (s, 3H), 3.79 (s, 3H), 3.94-4.23 (m, 4H), 4.25-4.39 (m, 1H), 4.89-4.93 (m, 1H), 5.37-5.42 (m, 1H), 6.53 (d, J = 8.3, 1H), 6.72-6.84 (m, 4H), 7.02 (d, J = 8.2, 2H), 7.37 (d, J = 8.2, 2H), 7.47-7.51 (m, 2H).

(2*S*,1'*R*,2'*S*),(2*S*,1'*S*,2'*R*),(2*R*,1'*R*,2'*S*),(2*R*,1'*S*,2'*R*)-1-{4-[1',3'dihydroxypropyl-3'-(4-methoxyphenyl)]-2'-methoxyphenoxy}-2-(4-methylphenoxy)-3-hydroxypropan-1-one (9)

PPTS (13.5 mg, 53.7 μmol) was added to a solution of **21** (57 mg, 0.11 mmol) in acetone:H_2O 3:2 (4 mL). The mixture was heated at reflux for 24 h, then acetone was distilled off. Saturated aqueous $NaHCO_3$ (1 mL) was then added and the solution was extracted with AcOEt. The combined organic extracts were washed with brine, dried over Na_2SO_4, filtered and the solvent was evaporated to give **9** (48 mg, 0.1 μmol, yield 91%).

^{1}H NMR δ: 2.25 (s, 3H), 3.80 (s, 3H), 3.86 (s, 3H), 3.89-4.17 (m, 4H), 4.37 (dd, J = 8.9 and 5.0, 1H), 5.00 (m, 1H), 5.43 (d, J = 5.5, 1H) 6.74-6.81 (m, 2H), 6.84-6.94 (m, 3H), 7.01-7.06 (m, 2H), 7.32-7.35 (m, 2H), 7.57-7.68 (m, 2H).

5.5 Enzymatic Oxidation

The substrate **1** or **2** (125 μL of a solution 0.038 M in acetonitrile) and LiP (0.4 units, 0.9 nmol) were added to 2 mL of sodium tartrate buffer solution 50 mM at pH 3.5 previously degassed with argon for 15 min, under magnetic stirring in a Schlenk tube at 25ºC. H_2O_2 (4.7 μmol) in 0.8 ml of H_2O was added gradually over a period of 90 min by an infusion pump. At the end 10 μL of a 0.1 M solution of the internal standard, 4-methoxyacetophenone, in acetonitrile were added. The reaction was quenched with methanol and analysed by HPLC and LC-MS or extracted with dichloromethane, dried over anhydrous Na_2SO_4 and after evaporation of the solvent analysed by ^{1}H NMR analysis. No products were observed in experiments carried out without the presence of enzyme. The reaction of **1** led to 3,4-dimethoxybenzaldehyde (**5**) and the dimeric aldehyde (**7**), which were recognized by

comparison with authentic specimens. Moreover, the LC-MS spectrum of the mixture showed the presence of a compound with M = 482 (M + Na$^+$ = 505), which was assigned to the ketone **6** also on the basis of the presence in the ^{1}H NMR spectrum of signals at 7.4-7.5 δ attributable to the protons *ortho* to the carbonyl group in the dimethoxylated ring. For the quantitative determination (HPLC), the response factor of **6** was taken equal to that of the ketone **9**. The reaction of **2** led to the dimeric aldehyde **8**, the ketone **9** and 4-methoxybenzaldehyde **10**, which were recognised by comparison with authentic specimens.

5.6 Chemical Oxidation

The substrate **1** or **2** (125 µL of a solution 0.038 M in acetonitrile) and Co(III)W (31 mg, 9.4 µmol) were added to 2 mL of sodium tartrate buffer solution 50 mM at pH 3.5 previously degassed with argon for 15 min under magnetic stirring in a Schlenk tube. The mixture was heated at 60ºC in argon atmosphere for 48 h. At the end 10 µL of a 0.1 M solution of the internal standard, 4-methoxyacetophenone, in acetonitrile were added. The solution was extracted with dichloromethane, dried over anhydrous Na_2SO_4 and the solvent was evaporated. The products were analysed by ^{1}H NMR, HPLC and LC-MS.

5.7 Enzymatic Kinetics

The kinetics were performed in 1 ml cuvette containing 800 µL of tartrate buffer 50 mM, pH 3.5 at 25 °C. For each measure 50 µL of a solution of LiP 4.6 µM in tartrate buffer 50 mM at pH 4 were added to the buffer followed by the solution of substrates in acetonitrile (final concentration 10%). The concentration of the substrates varied from 0.18 mM to 1.4 mM for **3**, from 0.11 mM to 0.56 mM for **4** and from 0.10 mM to 0.52 mM for **2**. The reaction started by addition of 50 µL of a solution 0.012 M of H_2O_2. The k_{cat} and K_M values, were determined at 310 nm following the formation of products containing a carbonyl group in α position with respect to dialkoxylated aromatic ring, that is 3,4-dimethoxybenzaldehyde (oxidation of **3**), 3,4-dimethoxybenzaldehyde and 1-(3,4-dimethoxyphenyl)-2-phenoxy-1-ethanone (oxidation of **4**),[69] aldehyde **8** and ketone **9** (oxidation of **2**). Since two products are formed in the oxidation of **2** and **4** the rate of the process was calculated according to the following equation $v = dA/dt \times 1/(\varepsilon_A + \varepsilon_B C_B/C_A)$, where dA/dt is the change of absorbance measured at 310 nm, ε_A and ε_B are the molar extinction coefficient of reaction products A and B at 310 nm, C_A and C_B are the molar concentrations of products A and B. Kinetic parameters were not determined for the enzymatic oxidation of the trimer **1** because it was not possible to isolate the trimeric ketone **6** from the reaction mixture in a state of purity sufficient for the determination of its extinction coefficient.

5.8 Kinetics with Co(III)W

A solution of **2**, **3** or **4** (3 µmol) and AcOK (0.6 mmol) in AcOH/H_2O (70/30) was thoroughly purged with argon in a 3 ml cuvette and placed in a thermostated compartment (25 °C) of the UV-vis spectrophotometer. The reaction was started by rapid addition of 0.1 ml of a Co(III)W solution in AcOH/H_2O (70/30) (6 mM). The rate of disappearance of cobalt(III) was followed spectrophotometrically by measuring the absorbance of Co(III)W at 390 nm (ε = 1207).[57] First-order rate constants were obtained from the plot of log $(A_t-A_{inf})/(A_0-A_{inf})$ against time: $(9.9 \pm 0.5) \times 10^{-4}$ s^{-1} for **2**, $(8.0 \pm 0.4) \times 10^{-4}$ s^{-1} for **3**, and $(7.6 \pm 0.6) \times 10^{-4}$ s^{-1} for **4**.

References and Notes

1. T. K. Kirk, R. L. Farrell, *Annu. Rev. Microbiol.,* **1987,** *41,* 465-505.
2. M. Akhtar, R. A. Blanchette, T. K. Kirk, *Fungal Delignification and Biomechanical Pulping of Wood* in: -E. L. Eriksson (Ed.), Biotechnology in the Pulp and Paper Industry (Vol.57 in Advances in Biochemical Engineering Biotechnology), Springer Verlag, Berlin Heidelberg, **1997,** pp. 159-195.
3. E. de Jong, J. A. Field, J. A. M. de Bont, *FEMS Microbiol. Rev.,* **1994,** *13,* 153-188.
4. D. C. Ulmer, M. S. A. Leisola, J. Puhakka, A Fiechter, *Eur. J. Appl. Microbiol. Biotechnol.,* **1983,** *18,* 153-157.
5. J. D. Reid*, Appl. Environ. Microbiol.,* **1983,** *45,* 830.
6. D. C. Ulmer, M. S. A. Leisola, B. H. Schmidt, A Fiechter, *Appl. Environ. Microbiol.,* **1983,** *45,* 1795-1801.
7. G. F. Leatham, *Appl. Microbiol. Biotechnol.,* **1986,** *24,* 51-58.
8. J. K. Glenn, M. A. Morgan , M. B. Mayfield, M. Kuwahara, M. H. Gold, *Biochem. Biophys. Res. Comm.,* **1983,** *114,* 1077-1083.
9. M. Tien, T. K. Kirk, *Science,* **1983,** *221,* 661.
10. A. L. Andersson, V. Renganathan, A. A. Chiu, T. M. Loehr, M. H. Gold, *J. Biol. Chem.,* **1985,** *260,* 6080-6087.
11. D. Kuila, M. Tien, J. A. Fee, M. R. Ondrias, *Biochemistry,* **1985,** *24,* 3394-3397.
12. T. Umezawa, T. Higuchi, F. Nakatsubo, *Agric. Biol. Chem.,* **1983,** *47,* 2945-2948.
13. M. Tien, T. K. Kirk, *Proc. Natl. Acad. Sci. USA,* **1984,** *81,* 2280-2284.
14. M. Kuwahara, J. K. Glenn, M. A. Morgan, M. H. Gold, *FEBS Lett.,* **1984,** *169,* 247-250.
15. P. J. Harvey, H. E. Schoemaker, R. M. Bowen, J. M. Palmer, *FEBS Lett.,* **1985,** *183,* 13-16.
16. V. Renganathan, K. Miki, M. H. Gold, *Arch. Biochem. Biophys.,* **1986,** *246,* 155-161.
17. M. Tien, C. P. D. Tu, *Nature,* **1987,** *326,* 520-523.
18. M. Tien, C. P. D. Tu, *Nature,* **1987,** *328,* 742.
19. H. A. de Boer, Y. Z. Zhang, C. Collins, C. A. Reddy, *Gene,* **1987,** *60,* 93-102.
20. T. G. Jr. Ritch, V. J. Nipper, L. Akileswaran, A. Smith, D. Pribnow, M. H. Gold, *Gene,* **1991,** *107,* 119-126.
21. M. H. Gold, M. Alic, *Microbiol. Rev.,* **1993,** *57,* 605-622.
22. T. Kamaya, T. Higuchi, *FEMS Microbiol. Lett.,* **1984,** *22,* 89-92.
23. P. J. Kersten, M. Tien, B. Kalyanaraman, T. K. Kirk, *J. Biol. Chem.,* **1985,** *260,* 2609-2612.
24. K. E. Hammel, B. Kalyanaraman, T. K. Kirk, *J. Biol. Chem.,* **1986,** *261,* 16948-16952.
25. P. J. Kersten, B. Kalyanaraman, K. E. Hammel, B. Reinhammer, T. K. Kirk, *Biochem. J.,* **1990,** *268,* 475-480.
26. V. Renganathan, K. Miki, M. H. Gold, *Arch. Biochem. Biophys.,* **1985,** *241,* 304-314.
27. M. Tien, T. K. Kirk, C. Bull, J. A. Fee, *J. Biol. Chem.,* **1986,** *261,* 1687-1693.
28. A. Andrawis, K. A. Johnson, M. Tien, *J. Biol. Chem.,* **1988,** *263,* 1195-1198.
29. V. Renganathan, K. Miki, M. H. Gold, *Biochemistry,* **1987,** *26,* 5127-5132.
30. H. Wariishi, J. Huang, H. B. Dunford, M. H. Gold, *J. Biol. Chem.,* **1991,** *266,* 20694-20699.
31. T. Glumoff, P. J. Harvey, S. Molinari, M. Goble, G. Frank, J. M. Palmer, J. D. G. Smit, M. S. A. Leisola, *Eur. J. Biochem.,* **1990,** *187,* 515-520.
32. M. Tien, T. K. Kirk, *Methods in Enzymology,* **1988,** *161,* 238.
33. T. Choinowski, W. Blodig, K. H. Winterhalter, K. Piontek, *J. Mol. Biol.,* **1999,** *286,* 809-827.
34. K. Piontek, T. Glumoff, K. Winterhalter, *FEBS Lett.,* **1993,** *315,* 119-124.
35. T. L. Poulos, S. L. Edwards, H. Wariishi, M. H. Gold, *J. Biol. Chem.,* **1993,** *268,* 4429-4440.

36. L. Banci, I. Bertini, P. Turano, M. Tien, T. K. Kirk, *Proc. Natl. Acad. Sci. USA,* **1991,** *88,* 6956-6960.
37. G. Labat, B. Meunier, *Bull. Soc. Chim. Fr.,* **1990,** *127,* 553-564.
38. L. Marquez, H. Wariishi, B. H. Dunford, M. H. Gold, *J. Biol. Chem.,* **1988,** *263,* 10549-10552.
39. P. J. Harvey, J. M. Palmer, H. E. Schoemaker, H. L. Dekker, R. Wever, *Biochem. Biophys. Acta*, **1989,** *99,* 59-63.
40. R. Nakajima, I. Yamazaki, *J. Biol. Chem.,* **1978,** *262,* 2576-2581.
41. S. D. Hammerli, M. S. A. Leisola, D. Sanglard, A. Fiechter, *J. Biol. Chem.,* **1985,** *261,* 6900-6903.
42. D. Cai, M. Tien, *J. Biol. Chem.,* **1992,** *267,* 11149-11155.
43. G. D. DePillis, H. Wariishi, M. H. Gold, P. R. Ortiz de Montellano, *Arch. Biochem. Biophys.* **1990,** *280,* 217-223.
44. P. R. Ortiz de Montellano, D. E. Kerr, *J. Biol. Chem.,* **1989,** *258,* 10558-10563.
45. P.J. Harvey, H.E. Shoemaker, J.M. Palmer, *FEBS Lett.,* **1986,** *195,* 242-246.
46. P.J. Harvey, R. Floris, T. Lundell, J.M. Palmer, H.E. Shoemaker, R. Wever, *Biochem. Soc. Trans.,* **1992,** *20,* 345-349.
47. K. Lundquist, T.K. Kirk, *Phytochem.,* **1978,** *17,* 1676.
48. D.C. Goodwin, S.D. Aust, T.A. Grover, *Biochemistry,* **1995,** *34,* 5060.
49. G. Gilardi, P.J. Harvey, A.E.G. Cass, J.M. Palmer, *Biochim, Biophys. Acta,* **1990,** 1041*,* 129-132.
50. E. Baciocchi, M. Bietti, O. Lanzalunga, *Acc. Chem., Res.,* **2000,** *33,* 243-251.
51. T. K. Kirk, M. Tien, P. J. Kersten, M. D. Mozuch, B. Kalyanaraman, *Biochem. J.* **1986,** *236,* 279-287.
52. The oxidation potential of 4-methoxybenzylalcohol[53] is 0.54 V higher than that of 3,4-dimethoxybenzylalcohol[54].
53. O. R. Brown, S. Chandra, J. A. Harrison, *J. Electroanal. Chem.,* **1972,** *38,* 185-190.
54. M. Bietti, E. Baciocchi, S. Steenken, *J. Phys Chem.,* **1998,** *102,* 7337.
55. C. von Sonntag, H. P. Schuchmann, *Meth. Enzymol.* **1994,** *233,* 3-20.
56. L. Eberson, *J. Am. Chem. Soc.* **1983,** *105,* 3192-3199.
57. E. Baciocchi, M. Crescenzi, E. Fasella, M. Mattioli, *J. Org. Chem.* **1992,** *57,* 4684.
58. A related study has been carried out using phenolic lignin model compounds.[59]
59. L. Banci, S. Ciofi-Baffoni, M. Tien, *Biochemistry* **1999,** *38,* 3205-3210.
60. Similar results have been obtained using $Br_2^{\bullet-}$ which is a more selective oxidant (1.63 V vs NHE)[59] than Tl^{2+} (2.2 V vs NHE).[60]
61. H. Mohan, J. P. Mittal, *J. Phys. Chem. A,* **1997,** *101,* 10012.
62. H. A. Schwarz, R. W. Dodson, *J. Phys. Chem.* **1984,** *88,* 3643.
63. E. Janata, R. H. Schuler, *J. Phys. Chem.* **1982,** *86,* 2078.
64. P. O'Neill, S. Steenken, D. Shulte-Frohlinde, *J. Phys. Chem.* **1975,** *79,* 2773.
65. E. Baciocchi, M. Bietti, S. Stenkeen, *Chem. Eur. J.* **1999,** *5,* 1785.
66. M. Bietti, O. Lanzalunga, *J. Org. Chem.* **2002,** *67,* 2632.
67. R. Rathore, S. V. Lindeman, J. K. Kochi, *J. Am. Chem. Soc.* **1997,** *119,* 9393.
68. B. Badger, B. Brocklehurst, *Trans. Faraday Soc.* **1969,** *65,* 2582-2587.
69. E. Baciocchi, M. Bietti, M. F. Gerini, O. Lanzalunga, S. Mancinelli, *J. Chem. Soc. Perkin Trans. 2,* **2001,** 1506-1511.
70. R. S. Koduri, M. Tien, *J. Biol. Chem.* **1995,** *270,* 22254.
71. H. E. Schoemaker, *Recl. Trav. Chim. Pays-Bas*, **1990,** *109,* 255-272.
72. E. Baciocchi, M. F. Gerini, O. Lanzalunga, S. Mancinelli, *Tetrahedron* **2002,** *58,* 8087.
73. Similar conclusions were established in the oxidation of phenolic lignin oligomers.[59]
74. W. Blodig, W. A. Doyle, A. T. Smith, K. Winterhalter, T. Choinowski, K. Piontek, *Biochemistry* **1998,** *37,* 8832-8838.

75. W. A. Doyle, W. Bloding, N. C. Veitch, K. Piontek, A. T. Smith, *Biochemistry* **1998,** *37,* 15097-15105.

76. Flascka, H. A.; Barnard, A. J.; Stwrock, P.E. *Quantitative Analytical Chemistry;* Harper & Row: New York, **1969,** *2,* 149.

77. Tien, M.; Kirk, T.K. *Meth. Enzymol.* **1998,** *161,* 238.

78. Tien, M.; Kirk, T.K.; Bull, C.; Fee, J. A. *J. Biol. Chem.* **1986,** *261,* 1687.

79. Ciofi-Baffoni, S.; Banci. L.; Brandi, A. *J. Chem. Soc. Perkin Trans. 1* **1998,** 3207.

80. Rychnovsky, S. D.; Gogers, B.; Yang, G. *J.Org. Chem.* **1993,** *58,* 3511.

81. Formation of hydrated forms have also been reported in the synthesis of oligomeric β-O-4 phenolic lignin model compounds.[80]

Iron Tetraaryl Porphyrins-Catalysed Oxidation of α-Alkyl Substituted Benzyl Alcohols

1. Introduction

Metalloporphyrins are synthetic analogues of the prosthetic group of heme enzymes which catalyse the oxidation of several processes.[1] Typical biological oxidations catalysed by heme enzymes are: oxygenation by cytochrome P-450,[2-5] oxidation by peroxidases,[6,7] oxidative halogenation by chloroperoxidases[8,9] and hydrogen peroxide dismutation by catalase.[10,11] The control of the catalytic activity of the heme enzymes, in terms of substrate specificity, chemoselectivity, oxidant activation and oxidation rate, is due to the proximal ligand, the distal amino acid residues and the protein itself. In the biomimetic system it is possible to control the catalytic activity by using different metals and ligands.[1]

In order to prevent the easy oxidation of the *meso*-positions of the porphyrin ring, four phenyl groups are introduced in these positions as in the tetraphenylporphyrin iron (III) (FeTPP) showed in Figure 1.[12]
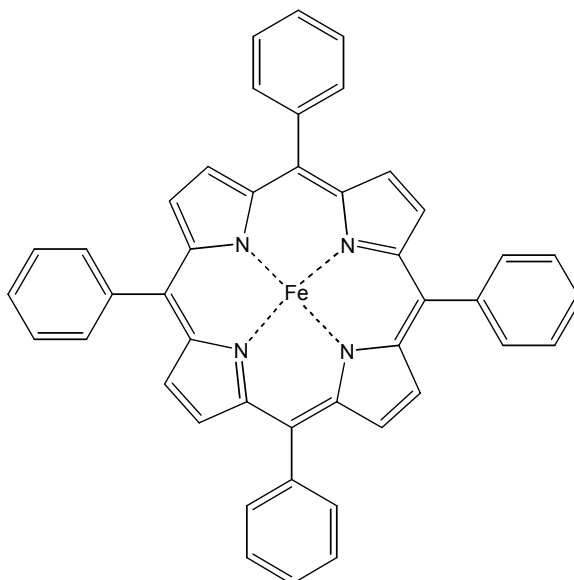
Figure 1. *Meso*-tetraphenylporphyrin iron(III) (FeTPP).

This substitution also reduce the irreversible formation of catalytically inactive μ-oxo complexes (Figure 2).[13]
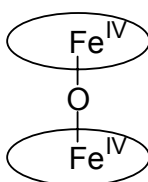
Figure 2. Schematic representation of the μ-oxo complex.

The different metal derivatives of the *meso*-tetraphenyl porphyrin constitute the first generation of metalloporphyrin catalysts. The second generation is represented by structures where alkyl or halogen substituents have been introduced in the *ortho, meta* or *para* positions of the phenyl groups, such as *meso*-tetrakis(pentafluorophenyl)porphyrin, H$_2$TPFPP,[14] *meso*-

tetramesitylporphyrin, H$_2$TMP[15,16] and *meso*-tetrakis(2,6-chlorophenyl)porphyrin, H$_2$TDCPP.[17,18] The third generation is an extension of the previous idea by having bromine, chlorine, or fluorine atoms at the β-positions of pyrroles.[19-21]

The introduction of hydrophilic substituents on the phenyl rings allowed the synthesis of water-soluble tetraarylporphyrin. These systems can better mimic the behaviour of water-soluble heme-enzymes. Either cationic or anionic groups have been introduced as in *meso*-tetrakis(4-*N*-methylpiridinium)porphyrin iron (III) chloride (FeTMPyPCl, Figure 3)[22,23] and *meso*-tetrakis(4-sulfonatophenyl)porphyrin iron (III) chloride (FeTSPPCl, Figure 4).[24]

In biomimetic systems the active oxidant is formed by reaction of the metalloporphyrin with different oxygen donors,[25] the most important being hydrogen peroxide, *t*-butyl hydroperoxide, sodium hypochlorite, *m*-chloroperbenzoic acid, iodosylbenzene, magnesium monoperoxyphtalate, potassium monopersulfate and oxygen plus reducing agent. The choice of the oxygen donor depends on the substrate structure, the catalyst and the reaction medium.
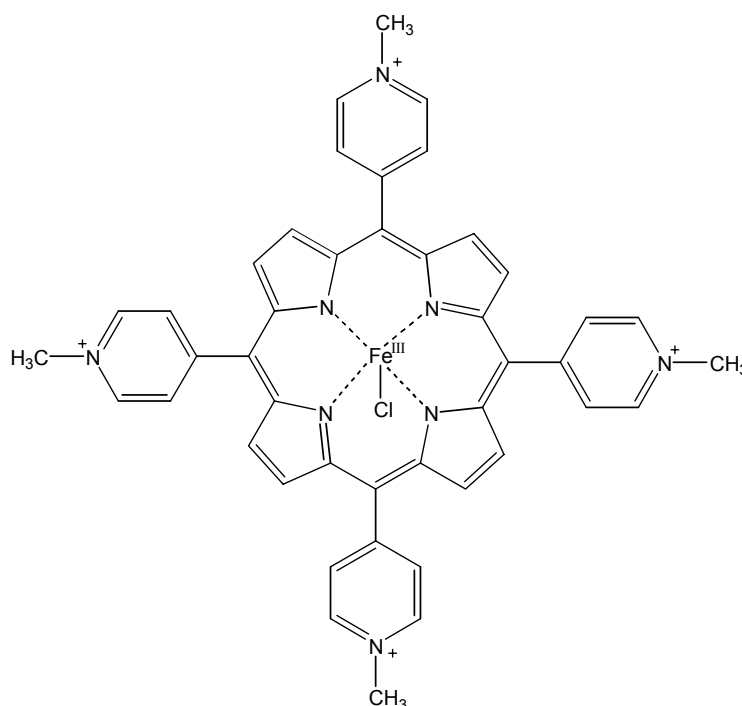
Figure 3. *Meso*-tetrakis(4-*N*-methylpiridinium)porphyrin iron (III) chloride (FeTMPyPCl).
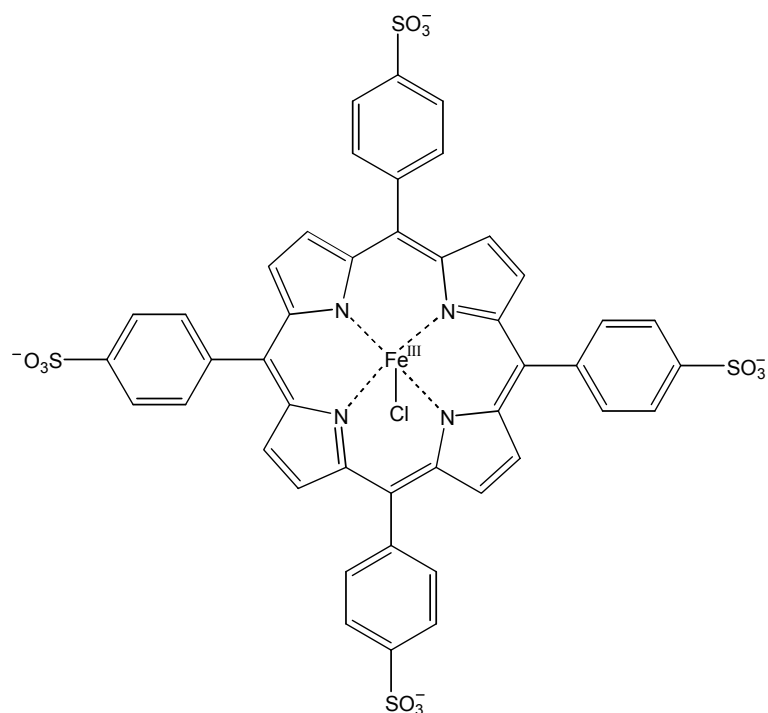
Figure 4. *Meso*-tetrakis(4-sulfonatophenyl)porphyrin iron (III) chloride (FeTSPPCl).

Reaction of the oxygen donor (DO) with the metalloporphyrin leads to the formation of the active oxidant which is an iron-oxo-complex radical cation structurally very close to that involved in the enzymatic reactions (Scheme 1).[1,25-28]

$$Por\text{-}Fe(III) + DO \longrightarrow \overset{\bullet+}{Por}\text{-}Fe(IV)=O + D$$
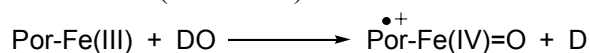
Scheme 1. Formation of the active oxidant.

The active species is able to promote several oxidation processes; the most important are reported in Scheme 2.
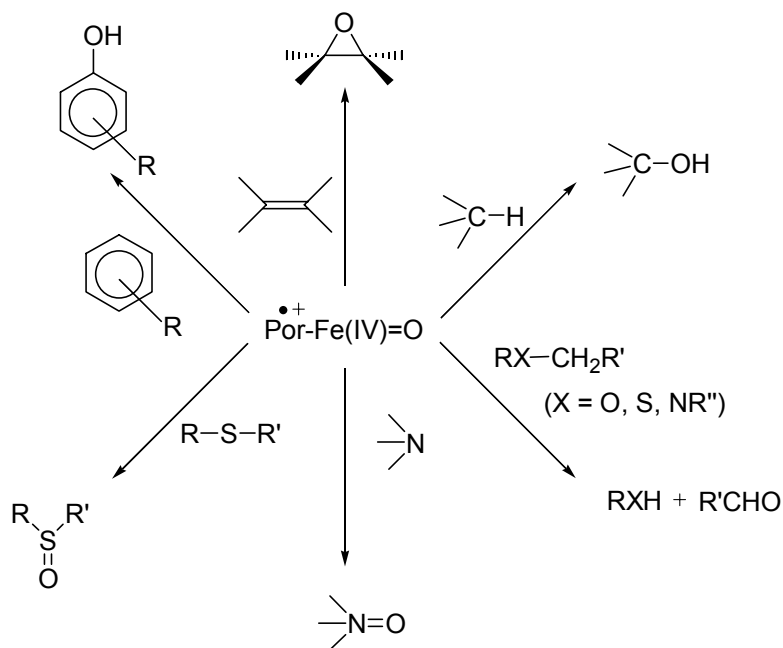
Scheme 2. Reactions catalysed by metalloporphyrins.

In recent years a particular attention has been given to the catalysis of oxidation reactions involved in degradation of lignin. Accordingly iron porphyrins are also good model systems of the two important delignifying enzymes LiP and MnP. For mechanistic studies and for the evaluation of the possible catalytic activity of metalloporphyrins low molecular LMCs have been used as substrates.[25] Among the metalloporphyrins, the sulfonated ones were found to be the most suitable in the modelling of LiP.[29] Sodium hypochlorite was used as oxygen atom donor although this oxidant cannot be developed on industrial scale because of risky and nondesired aromatic chlorination at pH < 9. Hydrogen peroxide would be the cleaner oxidant but its ability to activate the catalyst is rather low.[30] Potassium monopersulfate or *m*-chloroperbenzoic acid[31] are better oxidants. For example the KHSO$_5$ / sulfonated metalloporphyrin system has been tested with good results in the oxidative cleavage of the C$_\alpha$-C$_\beta$ bonds in propane diol derivatives.[31,32] Although several papers[33-37] appeared in the literature on this topic, further studies are needed in order to have a complete mechanistic description of the metalloporphyrin catalysed oxidation of LMCs.

To this purpose I have investigated the iron tetraarylporphyrin catalysed oxidation of a series of LMCs represented by α-alkyl substituted mono and dimethoxylated benzyl alcohols **1-8** (Figure 5).

1, X = OCH$_3$, Y = H, R = CH$_3$ **5**, X,Y = OCH$_3$, R = CH$_3$
2, X = OCH$_3$, Y = H, R = CH$_2$CH$_3$ **6**, X,Y = OCH$_3$, R = CH$_2$CH$_3$
3, X = OCH$_3$, Y = H, R = CH(CH$_3$)$_2$ **7**, X,Y = OCH$_3$, R = CH(CH$_3$)$_2$
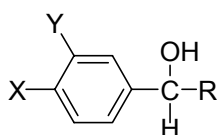**4**, X = OCH$_3$, Y = H, R = C(CH)$_3$ **8**, X,Y = OCH$_3$, R = C(CH)$_3$

Figure 5. Structure of substrates **1-8.**

In the reaction of the active specie [Por$^{+\bullet}$Fe(IV)=O] with these substrates two different mechanisms can be envisaged: hydrogen atom transfer (HAT, Scheme 3) or electron transfer (ET, Scheme 4).

In the HAT mechanism the initial step is the abstraction of the benzylic hydrogen atom from the substrate by the iron-oxo complex radical cation leading to a α-hydroxybenzylic radical and the iron-hydroxo complex [Por-Fe(IV)-OH] (Scheme 3, path **a**). The α-hydroxybenzylic radical then undergoes a fast oxygen rebound process by the iron-hydroxo complex leading to the starting catalyst and the gemdiol (Scheme 3, path **b**), precursor of the ketone (Scheme 3, path **c**).
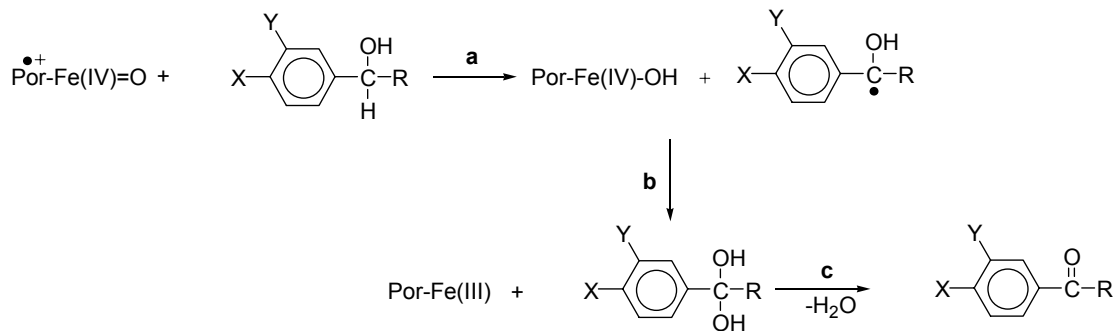
Scheme 3. The HAT mechanism.

In the ET mechanism the iron-oxo complex radical cation abstracts one electron from the substrate leading to the radical cation of the substrate and the reduced form of the iron-oxo complex [PorFe(IV)=O] (Scheme 4, path **a**). Once formed, the radical cation can undergo either the C_α-H bond cleavage (Scheme 4, path **b**) leading to α-hydroxybenzylic radical, which is oxidised to the corresponding ketone (Scheme 4, path **c**), or the C_α-C_β bond cleavage (Scheme 4, path **d**) leading to the corresponding benzaldehyde and the radical R$^\bullet$. Thus, in the ET mechanism the formation of aromatic ketones can be accompanied by that of aromatic adehydes. The ratio between the two products will depend on the structure of the alkyl group R.
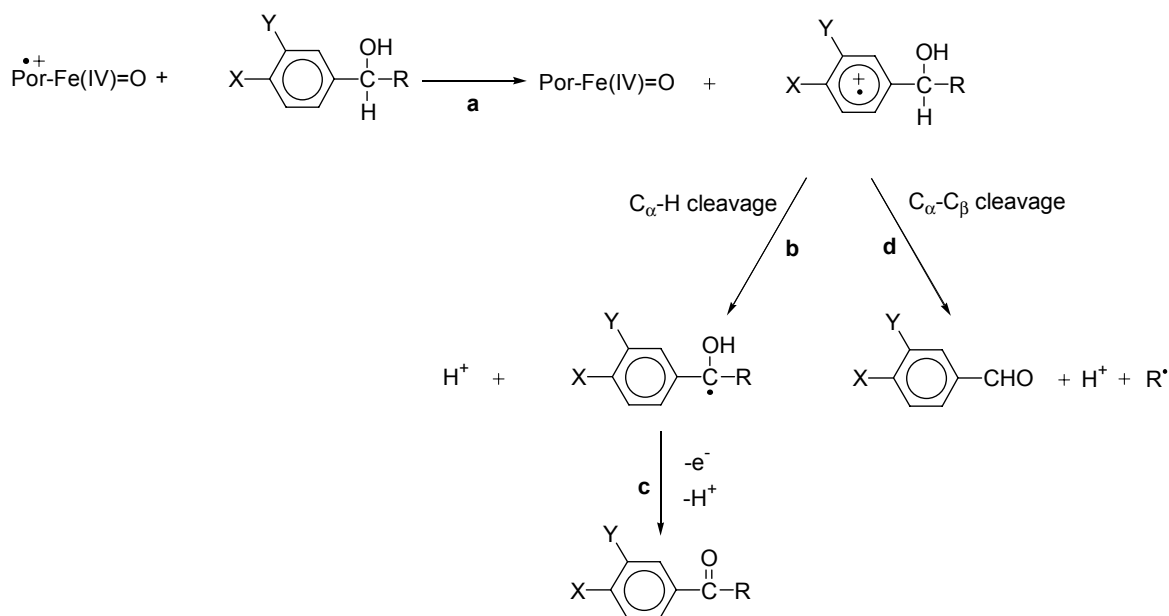
Scheme 4. The ET mechanism.

In order to determine the possible influence of the solvent on the reaction mechanism I carried out the oxidation of the alcohols **1-8** both in dichloromethane and in aqueous solution. The system iodosylbenzene / *meso*-tetrakis(pentafluorophenyl)porphyrin iron (III) chloride (FeTPFPPCl, Figure 6) was used in dichloromethane.[38] In aqueous solutions the possible effect of the porphyrin ligand was investigated by using both *meso*-tetrakis(4-*N*-methylpiridynium)porphyrin iron (III) chloride (FeTMPyPCl) and *meso*-tetrakis(4-sulfonatophenyl)porphyrin iron (III) chloride (FeTSPPCl) in combination with KHSO$_5$ as oxygen atom donor.
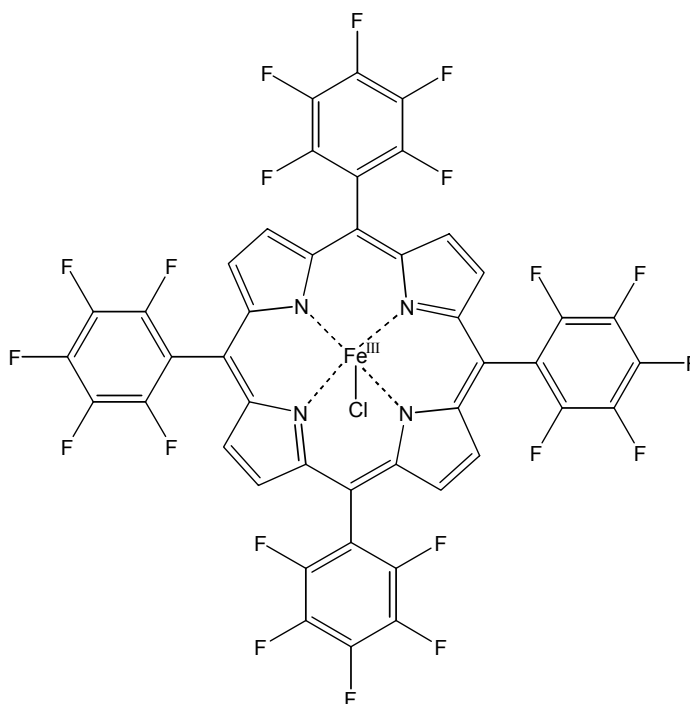
Figure 6. *Meso*-tetrakis(pentafluorophenyl)porphyrin iron (III) chloride (FeTPFPPCl).

To comparison purpose the results of the metalloporphyrin catalysed oxidations of the substrates **1-8** have been compared with those obtained in the reaction of the same substrates with the genuine one-electron oxidant Co(III)W.

2. Results

2.1 Oxidation of Compounds **1-4** *by FeTMPyPCl / KHSO$_5$*

The oxidations of substrates **1-4** with KHSO$_5$ catalysed by FeTMPyPCl were carried out in 0.1 M aqueous potassium phosphate buffer, pH 3, at 25ºC and under an argon atmosphere. KHSO$_5$ was added gradually over 60 min using a syringe pump. The substrate / oxidant / catalyst ratio was 100:300:1. After extraction with dichloromethane and addition of an internal standard, reaction products were analysed by GC, GC-MS and ^{1}H NMR. The results are reported in Table 1. The mass balance is satisfactory accounting for more than 80% of the starting material.

Table 1. Products and yields for the oxidation of compounds **1-4** with the FeTMPyPCl / KHSO$_5$ system in buffered aqueous solution.

Substrates		Reaction Products (Yields %)[a]	
$H_3CO-\bigcirc-\overset{OH}{\underset{H}{C}}-R$		$H_3CO-\bigcirc-\overset{O}{C}-R$	$H_3CO-\bigcirc-\overset{O}{C}-H$
1	R = CH$_3$	4	-
2	R = CH$_2$CH$_3$	2	-
3	R = CH(CH$_3$)$_2$	1	-
4	R = C(CH$_3$)$_3$	-	3

[a] Yields are referred to the initial amount of the substrate. The average error is ± 10%.

39

In the oxidation of **1, 2** and **3** the only reaction products, formed in very low yields, are respectively 4-methoxyacetophenone, 4-methoxypropiophenone and 2-methyl-1-(4-methoxyphenyl)-1-propanone. The only product, formed in low yield, in the oxidation of **4** is 4-methoxybenzaldehyde.

2.2 Oxidation of Compounds **5-8** by FeTMPyPCl / KHSO₅

The oxidations of alcohols **5-8** with $KHSO_5$ catalysed by FeTMPyPCl were carried out in 0.1 M aqueous potassium phosphate buffer, pH 3, at 25ºC and under an argon atmosphere. $KHSO_5$ was added gradually over 10 min using a syringe pump. The substrate / oxidant / catalyst ratio was 100:100:1. After extraction with dichloromethane and addition of an internal standard, reaction products were analysed by GC, GC-MS and ^1H NMR. The mass balance is satisfactory accounting for more than 80% of the starting material. The results are reported in Table 2.

Table 2. Products and yields for the oxidation of compounds **5-8** with the FeTMPyPCl / KHSO₅ system in buffered aqueous solution.

Substrates	Reaction Products (Yields %)[a]			
H₃CO / H₃CO—C(H)(OH)—R	H₃CO / H₃CO—C(=O)—R	H₃CO / H₃CO—C(=O)—H	2-methoxy-quinone C(OH)(H)—R	R—C(OH)(H)— / COOCH₃ COOCH₃
5 R = CH₃	37	-	25	< 0.5
6 R = CH₂CH₃	33	-	15	3
7 R = CH(CH₃)₂	31	2	23	2
8 R = C(CH₃)₃	-	49	12	3

[a] Yields are referred to the initial amount of the substrate. The average error is ± 10%.

In the oxidation of **5** the formation of the major product, 1-(3,4-dimethoxyphenyl)-1-ethanone is accompanied by the formation of 2-methoxy-5-(hydroxyethyl)-2,5-cicloexadiene-1,4-dione and of dimethyl 3-(1-hydroxyethyl)muconate. Similar results have been obtained in the oxidation of **6** which leads to 1-(3,4-dimethoxyphenyl)-1-propanone as the major product accompanied by minor amount of 2-methoxy-5-(hydroxypropyl)-2,5-cicloexadiene-1,4-dione and of dimethyl 3-(1-hydroxypropyl)muconate. In the oxidations of **5** and **6** no formation of 3,4-dimethoxybenzaldehyde has been observed. The oxidation of **7** leads to the formation of 1-(3,4-dimethoxyphenyl)-2-methyl-1-propanone, 2-methoxy-5-(1-hydroxy-2-methylpropyl)-2,5-cicloexadiene-1,4-dione, dimethyl 3-(1-hydroxy-2-methylpropyl)muconate and minor amounts of 3,4-dimethoxybenzaldehyde. 3,4-dimethoxybenzaldehyde is the major product in the oxidation of **8** accompanied by minor amount of 2-methoxy-5-(1-hydroxy-2,2-dimethylpropyl)-2,5-cicloexadiene-1,4-dione and dimethyl 3-(1-hydroxy-2,2-dimethylpropyl)muconate. No formation of 1-(3,4-dimethoxyphenyl)-2,2-dimethyl-1-propanone has been observed.

2.3 Oxidation of Compounds **5-8** by FeTSPPCl / KHSO₅

The oxidations of alcohols **5-8** with $KHSO_5$ catalysed by FeTSPPCl were carried out in 0.1 M aqueous potassium phosphate buffer, pH 3, at 25ºC and under an argon atmosphere. $KHSO_5$, was added gradually over 60 min using a syringe pump. The substrate / oxidant / catalyst ratio was 100:100:1. After extraction with dichloromethane and addition of an internal standard,

reaction products were analysed by GC, GC-MS and ^{1}H NMR. The mass balance is satisfactory accounting for more than 80% of the starting material. The results are reported in Table 3.
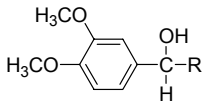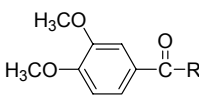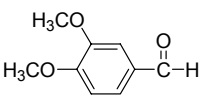
Table 3. Products and yields for the oxidation of compounds **5-8** with the FeTSPPCl / KHSO$_5$ system in buffered aqueous solution.

Substrates		Reaction Products (Yields %)[a]	
5	R = CH$_3$	11	-
6	R = CH$_2$CH$_3$	10	-
7	R = CH(CH$_3$)$_2$	6	< 0.5
8	R = C(CH$_3$)$_3$	-	6

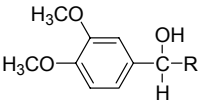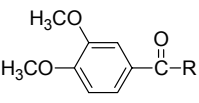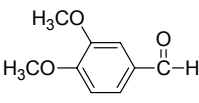[a] Yields are referred to the initial amount of the substrate. The average error is ± 10%.

In the oxidation of **5** and **6** the only reaction products are respectively 1-(3,4-dimethoxyphenyl)-1-ethanone and 1-(3,4-dimethoxyphenyl)-1-propanone. In the oxidation of **7** the formation of the major product, 1-(3,4-dimethoxyphenyl)-2-methyl-1-propanone, is accompanied by traces of 3,4-dimethoxybenzaldehyde. The latter product is the only one observed in the oxidation of **4**.

*2.4 Oxidation of Compounds **5**-**8** by FeTPFPPCl / PhIO*
The oxidations of alcohols **5-8** with PhIO catalysed by FeTPFPPCl were carried out in dry dichloromethane at 25ºC and under an argon atmosphere. The substrate / oxidant / catalyst ratio was 100:50:1. After 3 h, 1mL of Na$_2$S$_2$O$_5$ (1 M) and the internal standard were added. The organic layer was separated and dried over Na$_2$SO$_4$ anhydrous. Reaction products were analysed by GC, GC-MS and ^{1}H NMR. The mass balance is satisfactory accounting for more than 90% of the starting material. The yields referred to the oxidant are reported in Table 4.

Table 4. Products and yields for the oxidation of compounds **5-8** with the FeTPFPPCl / PhIO system in dry dichloromethane.

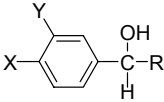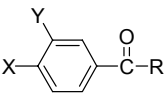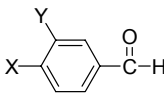| Substrates		Reaction Products (Yields %)[a]	
5	R = CH$_3$	6	-
6	R = CH$_2$CH$_3$	6	8
7	R = CH(CH$_3$)$_2$	6	22
8	R = C(CH$_3$)$_3$	3	30

[a] Yields are referred to the amount of the oxidant. The average error is ± 10%.

41

The oxidation of **5** with PhIO catalysed by FeTPFPPCl leads to the formation of 1-(3,4-dimethoxyphenyl)-1-ethanone as the only product. In the oxidations of **6,7** and **8** the formation of the major product, 3,4-dimethoxybenzaldehyde, is accompanied by minor amounts of 1-(3,4-dimethoxyphenyl)-1-propanone, 1-(3,4-dimethoxyphenyl)-2-methyl-1-propanone and 1-(3,4-dimethoxyphenyl)-2,2-dimethyl-1-propanone, respectively.

2.5 Oxidation of Compounds **5-8** *with Co(III)W*

The oxidations of substrates **5-8** with Co(III)W were carried out in 0.1 M aqueous potassium phosphate buffer, pH 3, at 25°C and under an argon atmosphere. Equimolar amount of the substrate and the oxidant have been used. After extraction with dichloromethane and addition of an internal standard, reaction products were analysed by GC, GC-MS and ^{1}H NMR. The results are reported in Table 5 where are also included the results for compounds **1-4** which were available from the literature.[40] The mass balance was always satisfactory accounting for more than 90% of the starting material.

Table 5. Products and yields for the oxidation of compounds **5-8** with Co(III)W in buffered aqueous solution.

Substrates		Reaction Products (Yields %)[a]	
		(C=O, C–R)	(C=O, C–H)
1	R = CH$_3$, X = OCH$_3$, Y = H	60[b]	
2	R = CH$_2$CH$_3$, X = OCH$_3$, Y = H	57[b]	10[b]
3	R = CH(CH$_3$)$_2$, X = OCH$_3$, Y = H	44[b]	28[b]
4	R = C(CH$_3$)$_3$, X = OCH$_3$, Y = H	-	90[b]
5	R = CH$_3$, X,Y = OCH$_3$	26	-
6	R = CH$_2$CH$_3$, X,Y = OCH$_3$	27	-
7	R = CH(CH$_3$)$_2$, X,Y = OCH$_3$	35	1
8	R = C(CH$_3$)$_3$, X,Y = OCH$_3$	-	33

[a] Yields are referred to the initial amount of the substrate. The average error is ± 10%.
[b] Ref. 40, reactions were carried out with equimolar amounts of the substrate and the oxidant (0.05 M), in AcOH / H$_2$O (55:45 w/w) at 50°C in the presence of AcOK (0.30 M).

In the oxidation of **5** and **6** the only reaction products are 1-(3,4-dimethoxyphenyl)-1-ethanone and 1-(3,4-dimethoxyphenyl)-1-propanone, respectively. In the oxidation of **7** the formation of the major product, 1-(3,4-dimethoxyphenyl)-2-methyl-1-propanone is accompanied by small amounts of 3,4-dimethoxybenzaldehyde. The oxidation of **8** leads to 3,4-dimethoxybenzaldheyde as the only product.

3. Discussion

The results of the oxidations of alcohols **1-8** by Co(III)W (Table 5) provide a good basis for the mechanistic interpretation of the results of the oxidation catalysed by metalloporphyrin, since this reaction certainly proceeds through the formation of the radical cation intermediate $ArCH(OH)R^{+\bullet}$. This species, as already described in Scheme 4, undergoes the C_α-H bond cleavage or the C_α-R bond cleavage. Thus, in the oxidation of **5** (R = Me) the radical cation undergoes exclusively the C_α-H bond cleavage (Scheme 4, path **b**). The α-hydroxybenzylic radical is then further oxidised by a second molecule of Co(III)W and after proton loss 3,4-dimethoxyacetophenone is formed (Scheme 4, path **c**). In a similar way in the oxidation of **6** (R = Et) the only product, 1-(3,4-dimethoxyphenyl)-1-propanone, is produced by C_α-H bond cleavage in **6**$^{+\bullet}$. Differently, in the oxidation of **7**, 1-(3,4-dimethoxyphenyl)-2-methyl-1-propanone, formed by C_α-H bond cleavage in **7**$^{+\bullet}$, is accompanied by small amounts (1%) of 3,4-dimethoxybenzaldehyde. This product is formed by C_α-C_β bond cleavage (Scheme 4, path **d**). Thus, when R = *i*-Pr, a competition between C_α-H and C_α-C_β bond cleavage is observed. In the oxidation of **8** (R = *t*-Bu) the only product is 3,4-dimethoxybenzaldehyde indicating that **8**$^{+\bullet}$ undergoes exclusively the C_α-C_β bond cleavage.

The observed trend for the competition between C_α-H and C_α-C_β bond cleavage in the radical cations **5**$^{+\bullet}$-**8**$^{+\bullet}$ can be rationalised on the basis of the different stability of the radical $R^\bullet$ formed in the C_α-C_β bond cleavage process. Accordingly, the aldehyde / ketone ratio increases from **5** to **8**, that is increasing the stability of the alkyl radical $R^\bullet$ in the order $CH_3^\bullet <$ $CH_2CH_3^\bullet < CH(CH_3)_2^\bullet < C(CH_3)_3^\bullet$. When these results have been compared with those reported for the oxidation of substrates **1-4**,[40] it can be noted that in monomethoxylated aromatic radical cations the C_α-C_β bond cleavage seems to be more favoured over the C_α-H bond cleavage as compared to the dimethoxylated aromatic radical cations. In fact in the oxidation of **2** significant amounts of 4-methoxybenzaldeyde are formed while in the oxidation of **6** the only product observed is 1-(3,4-dimethoxyphenyl)-1-propanone, moreover 4-methoxybenzaldehyde is the major product in the oxidation of **3** while only small amounts of 3,4-dimethoxybenzaldehyde are formed in the oxidation of **7.**

This observation is in accordance with the results obtained in the oxidation of the trimeric lignin model compounds catalysed by the LiP / H_2O_2 system (see PART I): competition between C_α-H and C_α-C_β bond cleavage was observed in the β fragmentation of dimethoxylated aromatic radical cations whereas monomethoxylated aromatic radical cations undergo only C_α-C_β bond cleavage.

On the basis of the results obtained in the oxidation by Co(III)W, the formation of 4-methoxybenzaldehyde in the oxidation of **4** promoted by the FeTMPyPCl / KHSO$_5$ system[41] and 3,4-dimethoxybenzaldehyde in the oxidation of **7** and **8** promoted by the FeTMPyPCl / KHSO$_5$ and FeTSPPCl / KHSO$_5$ systems indicates clearly that an ET mechanism is operating also in these cases.[42] A HAT mechanism (Scheme 3) can be excluded since it would have lead to the formation of the corresponding ketones as exclusive reaction products. The much lower reactivity exhibited by substrates **1-4** in the oxidation promoted by the FeTMPyPCl / KHSO$_5$ system (Table 1) as compared with that of substrates **5-8** with the same system (Table 2) also supports the hypothesis of an ET process since monomethoxylated aromatic ring are more difficult to oxidise that dimethoxylated ones due to their higher redox potential.[43] In case of a HAT process the introduction of an additional methoxy substituent in the 3-position of the aromatic ring should not effect significantly the rate of oxidation, since the benzylic C-H bond dissociation energy should not be very different for the mono and dimethoxylated systems.

The distribution of the side-chain oxidation products for the reactions of substrates **5-8** with the FeTMPyPCl / KHSO$_5$ and FeTSPPCl / KHSO$_5$ systems (Tables 2 and 3) can be compared with those obtained in the oxidation of the same substrates with Co(III)W (Table 5). In all cases a similar trend of the competition between C_α-H and C_α-C_β bond cleavage is observed.

In fact in the oxidation of substrates **5** and **6** promoted by both the biomimetic systems the only products are those due to the C_α-H bond cleavage: 3,4-dimethoxyacetophenone and 1-(3,4-dimethoxyphenyl)-1-propanone respectively. In the oxidation of substrate **7** small amount of 3,4-dimethoxybenzaldehyde are formed together with the formation of the major product 1-(3,4-dimethoxyphenyl)-2-methyl-1-propanone. Again, in the oxidation of **8,** the only process observed is the C-C bond cleavage leading to the formation of 3,4-dimethoxybenzaldehyde as the only product.

It is interesting to note that in the reactions of substrates **5-8** with the FeTMPyPCl / KHSO$_5$ system (Table 2), the formation of the side-chain oxidation products is accompanied by the formation of products of oxidation of the aromatic ring: 2-methoxy-5-hydroxyalkyl-2,5-cyclohexadiene-1,5-diones and dimethyl 3-(1-hydroxyalkyl)muconates. Formation of nuclear oxidation products have been observed in the oxidation of dimethoxylated aromatic compounds catalysed by iron (III) porphyrins and has been rationalised on the basis of an ET mechanism.[37] Once formed, the radical cation undergoes the attack of the aromatic nucleus by the reduced iron-oxo complex [Por-Fe(IV)=O] (Scheme 5, path **a**).
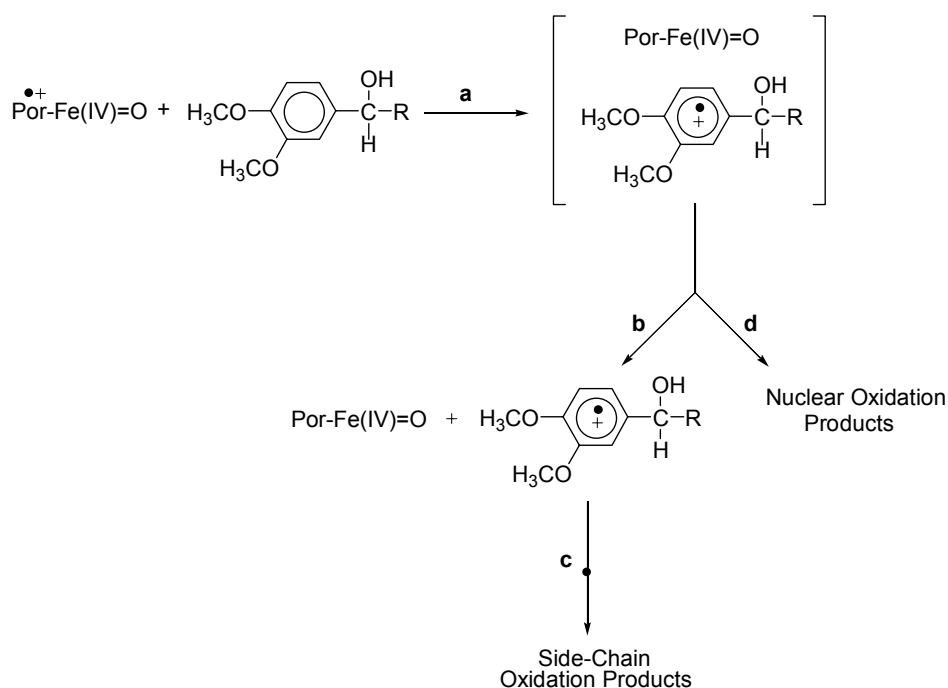

Scheme 5. Competition between side-chain and nuclear oxidation products in the reactions of **5-8** with the FeTMPyPCl / KHSO$_5$ system.

Following the suggestion by Artaud *et al.*,[37] this attack likely occurs in the solvent cage (Scheme 5, path **d**) before the separation of the free reduced iron-oxo complex and radical cation species (Scheme 5, path **b**) from which the side-chain oxidation products are formed (Scheme 5, path **c**).

According to the mechanisms proposed[37] 2-methoxy-5-hydroxyalkyl-2,5-cyclohexadiene-1,5-diones should be formed by attack of the reduced iron-oxo complex to the *ortho* position (Scheme 6), whereas dimethyl 3-(1-hydroxyalkyl)muconates should be formed by attack of the reduced iron-oxo complex to the *meta* position (Scheme 7).
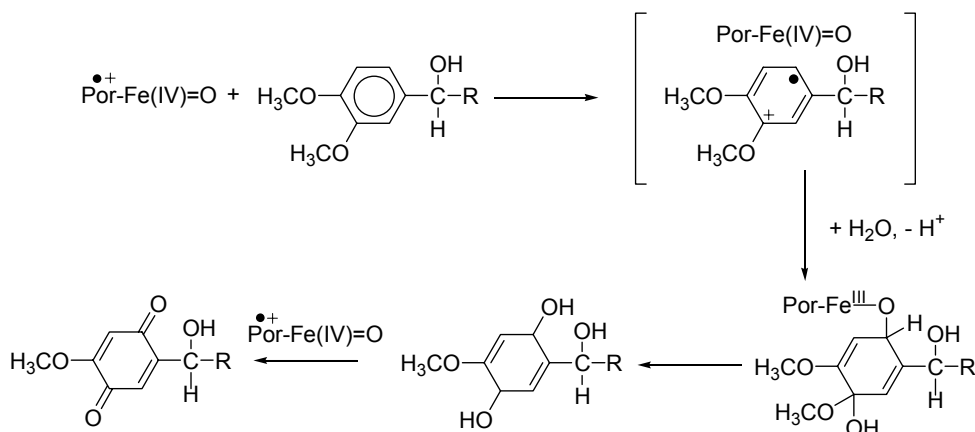
Scheme 6. Reaction mechanism for the formations of 2-methoxy-5-hydroxyalkyl-2,5-cyclohexadiene-1,5-diones.
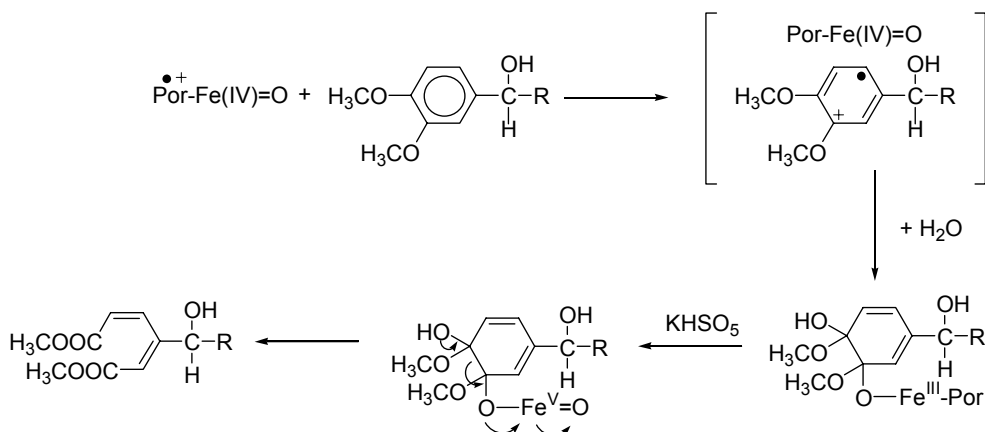

Scheme 7. Reaction mechanism for the formations of dimethyl 3-(1-hydroxyalkyl)-muconates.

Higher yields of oxidation products are observed in the reactions of **5-8** promoted by the FeTMPyPCl / KHSO$_5$ system as compared to those obtained with the FeTSPPCl / KHSO$_5$ system. The higher reactivity of FeTMPyPCl compared to that of FeTSPPCl is likely due to the presence of stronger electron withdrawing substituents on the porphyrin ligand that not only increase the stability of the iron-oxo complex in the oxidative reaction conditions but also increase the redox potential of the catalyst.[14,46-48]

The observation that nuclear oxidation products are observed only in the oxidations catalysed by FeTMPyPCl and not in those catalysed by FeTSPPCl is also in accordance with the greater reactivity of the former catalyst. The ratio between nuclear to side-chain oxidation products should depend on the ability of the reduced iron-oxo complex [Por-Fe(IV)=O] to attack the radical cation in the solvent cage before it escapes (Scheme 6). Thus, in the oxidations of **5-8** catalysed by FeTMPyPCl the reduced iron-oxo complex is highly reactive and attacks the aromatic nucleus in the solvent cage whereas in the oxidations of the same substrates catalysed by FeTSPPCl the reduced iron-oxo complex is less reactive and the radical cation can escape from the solvent cage leading exclusively to side-chain oxidation products. The

45

absence of nuclear oxidation products in the oxidation of substrates **1-4** catalysed by FeTMPyPCl can be rationalised on the basis of the insufficient activation of the aromatic ring when only one methoxy group is present.

The results obtained in the oxidation of substrates **5-8** in organic solvent (Table 4) are significantly different from those obtained in aqueous solution. In the oxidation of **5** with the FeTPFPPCl / PhIO system the only product formed is again 3,4-dimethoxyacetophenone, however the oxidation of substrates **6,7** and **8** leads to both 3,4-dimethoxybenzaldehyde and the aromatic ketones with the aldehyde / ketone ratios which increase by increasing the stability of R$^\bullet$. The presence of 3,4-dimethoxybenzaldehyde among the products cannot be explained by a HAT mechanism. The occurrence of an ET mechanism is also unlikely since it has been found that under the same conditions monomethoxylated and unsubstituted benzyl alcohols display a similar reactivity.[39] In line with the previous suggestions[39] it is possible to rationalise the observed aldehyde / ketone ratios in the oxidation of substrates **5-8** with a competition between the HAT mechanism, from which the aromatic ketones are produced (Scheme 9, path **a**), and the formation of an intermediate complex between the alcohol and the iron-oxo complex radical cation (Scheme 9, path **b**) which decomposes to give the product of C_α-C_β bond cleavage.[49] The fragmentation of this complex leads to 3,4-dimethoxybenzaldehyde and the alkyl radical R$^\bullet$ (Scheme 9, path **c**). Again the C_α-C_β bond cleavage is influenced by the relative stability of the alkyl radical R$^\bullet$ in accordance with the trend observed in Table 4. It is interesting to note that the aldehyde / ketone ratios are always higher in dimethoxylated substrates **5-8** as compared to monomethoxylated ones **1-4**, thus suggesting that a more stable intermediate complex is formed when the aromatic ring of the benzyl alcohols is substituted with two methoxy groups.
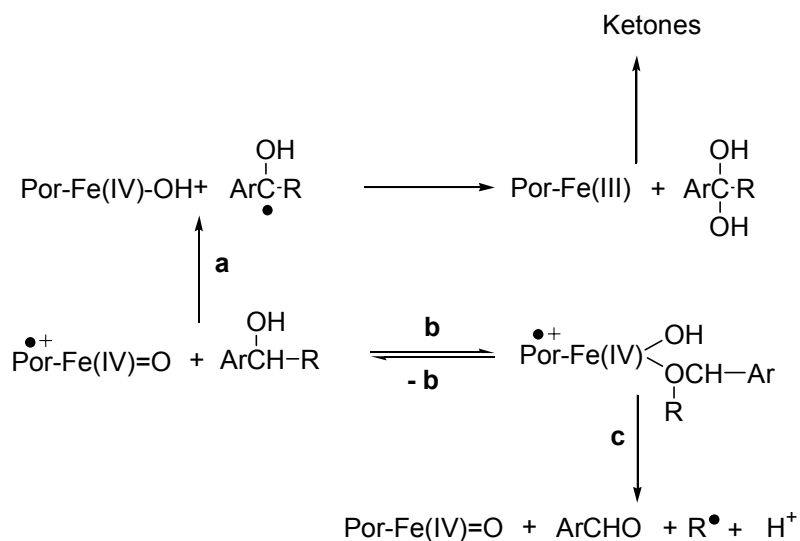
Scheme 9. Proposed mechanism for the oxidations of substrates **5-8** with the FeTPFPPCl / PhIO system.

4. Conclusions

On the basis of the data previously discussed it would seem that the mechanism of the oxidations of LMCs catalysed by biomimetic systems depends on solvent polarity. In the high polar aqueous medium an electron transfer mechanism for the oxidations of substrates **1-8** is very likely, whereas in a low polar solvent, like dichloromethane, the data are better interpreted by two competing mechanism: HAT and formation of a complex between the iron-oxo porphyrin and the substrate.

46

The presence of stronger electron withdrawing substituents on FeTMPyPCl makes this catalyst more efficient than FeTSPPCl. With the former system the formation of side-chain oxidation products is accompanied by nuclear oxidation products. The absence of nuclear oxidation products with FeTSPPCl indicates that this catalyst is more suitable to mimic the behaviour of lignin peroxidase since in the enzymatic system the restricted access to the heme active site makes the attack of the iron-oxo complex to the aromatic ring unlikely.

5. Experimental Section

5.1 Instrumentation

^{1}H-NMR spectra were recorded on a Bruker AC300P spectrometer in CDCl$_3$. GC-MS analyses were performed on a HP5890 GC (OV1 capillary column, 12 m x 0.2 mm) coupled with a HP5970 MSD. GLC analyses were performed on a Varian CP-3800 gas chromatograph (CP SIL 5CB capillary column, 30 m x 0.25 mm).

5.2 Materials

All the reagents and solvents were of the highest commercial quality available and used without further purification (unless otherwise specified). Milli-Q-filtered water was used for all solutions. Iodosylbenzene was prepared by hydrolysis of iodosylbenzene diacetate.[49] Mp: 210-211°C (Lit. 210-212°C). Co(III)W was prepared using the literature procedure[50] with some modifications.[51]

5.3 Substrates

Substrates **1-4** were available from a previous work.[40] Substrates **5-8** were synthesised according to previously described procedures:[40] 1-(3,4-dimethoxyphenyl)-1-ethanol (**5**) was prepared by reduction of 3,4-dimethoxyacetophenone with NaBH$_4$; 1-(3,4-dimethoxyphenyl)-1-propanol (**6**) was prepared by reaction of ethylmagnesium bromide with 3,4-dimethoxybenzaldehyde; 1-(3,4-dimethoxyphenyl)-2-methyl propanol (**7**) and 1-(3,4-dimethoxyphenyl)-2,2-dimethyl propanol (**8**) were prepared by reaction of 3,4-dimethoxyphenylmagnesium bromide with the appropriate acid chloride (isobutyryl chloride and trimethylacetyl chloride, respectively) followed by reduction with NaBH$_4$.

5.4 Products

4-Methoxybenzaldehyde, 3,4-dimethoxybenzaldehyde, 4-methoxyacetophenone, 3,4-dimethoxyacetophenone and 4-methoxypropiophenone are commercially available. 1-(3,4-dimethoxyphenyl)-1-propanone was prepared from 1-(3,4-methoxyphenyl)-1-propanol by oxidation with MnO$_2$ according to a literature procedure.[52] 2-Methyl-1-(4-methoxyphenyl)-1-propanone, 1-(3,4-methoxyphenyl)-2-methyl-1-propanone and 1-(3,4-methoxyphenyl)-2,2-dimethyl-1-propanone have been prepared as precursors of compounds **3,7** and **8**.

5.5 Oxidation of Compounds **1-4** by FeTMPyPCl / KHSO$_5$ in 0.1 M Potassium Phosphate Buffer (pH 3)

The substrates **1-4** (20 μmol, 500 μl of a solution 0.04 M in CH$_3$CN) and FeTMPyPCl (0.2 μmol, 500 μl of a solution 4 mM in 0.1 M potassium phosphate buffer, pH 3) were added to 1 mL of 0.1 M potassium phosphate buffer, pH 3. The solutions were degassed with argon for 15 min, under magnetic stirring in a Schlenk tube at 25ºC. KHSO$_5$ (60 μmol) in 0.8 ml of 0.1 M potassium phosphate buffer at pH 3 was added gradually over a period of 60 min by an infusion pump. At the end 40 μL, of a 0.1 M solution of the internal standard, 4-methylbenzophenone, in acetonitrile were added. The reactions were extracted with dichloromethane, dried over anhydrous Na$_2$SO$_4$ and after evaporation of the solvent analysed by ^{1}H NMR, GC-MS and GCL. The reactions products were identified by comparison with

authentic specimens. No products were observed in experiments carried out in the absence of either the catalyst or the oxidant.

5.6 Oxidation of Compounds 5-8 by FeTMPyPCl / KHSO₅ in 0.1 M Potassium Phosphate Buffer (pH 3)

The substrates **5-8** (20 µmol, 500 µl of a solution 0.04 M in CH_3CN) and FeTMPyPCl (0.2 µmol, 500 µl of a solution 4 mM in 0.1 M potassium phosphate buffer, pH 3) were added to 1 mL of 0.1 M potassium phosphate buffer, pH 3. The solutions were degassed with argon for 15 min, under magnetic stirring in a Schlenk tube at 25ºC. $KHSO_5$ (20 µmol) in 0.5 ml of 0.1 M potassium phosphate buffer at pH 3 was added gradually over a period of 10 min by an infusion pump. At the end 40 µL of a 0.1 M solution of the internal standard, 4-methylbenzophenone, in acetonitrile were added. The reactions were extracted with dichloromethane, dried over anhydrous Na_2SO_4 and after evaporation of the solvent analysed by ¹H NMR, GC-MS and GCL. 3,4-Dimethoxybenzaldehyde, 3,4-dimethoxyacetophenone, 1-(3,4-dimethoxyphenyl)-1-propanone and 1-(3,4-dimethoxyphenyl)-2-methyl-1-propanone were identified by comparison with authentic specimens. 2-Methoxy-5-hydroxyalkyl-2,5-cicloexadiene-1,4-diones and dimethyl 3-(1-hydroxyalkyl)muconates were identified by comparison of the ¹H NMR and GC-MS spectra with those reported in the literature.[53] No products were observed in experiments carried out in the absence of either the catalyst or the oxidant.

5.7 Oxidation of Compounds 5-8 by FeTSPPCl / KHSO₅ in 0.1 M Potassium Phosphate Buffer (pH 3)

The substrates **5-8** (20 µmol, 500 µl of a solution 0.04 M in CH_3CN) and FeTMPyPCl (0.2 µmol, 500 µl of a solution 4 mM in 0.1 M potassium fosfate buffer, pH 3) were added to 1 mL of 0.1 M potassium fosfate buffer, pH 3. The solutions were degassed with argon for 15 min, under magnetic stirring in a Schlenk tube at 25ºC. $KHSO_5$ (20 µmol) in 0.5 ml of 0.1 M potassium phosphate buffer at pH 3 was added gradually over a period of 60 min by an infusion pump. At the end 40 µL of a 0.1 M solution of the internal standard, 4-methylbenzophenone, in acetonitrile were added. The reactions were extracted with dichloromethane, dried over anhydrous Na_2SO_4 and after evaporation of the solvent analysed by ¹H NMR, GC-MS and GCL. The reactions products were identified by comparison with authentic specimens. No products were observed in experiments carried out in the absence of either the catalyst or the oxidant.

5.8 Oxidation of Compounds 5-8 by FeTPFPPCl / PhIO in Dichloromethane

The substrates **5-8** (125 µmol) in 1 mL of dry dichloromethane were reacted with FeTPFPPCl (1.25 µmol, 25 µl of a solution 50 mM in dry dichloromethane) and PhIO (13.7 mg, 62.5 µmol) under an argon atmosphere for 3 h. At the end 1mL of $Na_2S_2O_5$ (1 M) and 200 ml of a 0.1 M solution of the internal standard, 4-methylbenzophenone, in acetonitrile were added. The organic layer was separated and dried over Na_2SO_4 anhydrous. After evaporation of the solvent the reactions were analysed by ¹H NMR, GC-MS and GCL. All the reactions products were identified by comparison with authentic specimens with the exception of 1-(3,4-dimethoxyphenyl)-2,2-dimethyl-1-propanone which was identified on the basis of the ¹H NMR signals at 0.9 δ attributable to the protons of the methyl groups. No products were observed in experiments carried out in the absence of either the catalyst or the oxidant.

5.9 Oxidation of Compounds 5-8 promoted by Co(III)W in 0.1 M Potassium Phosphate Buffer (pH 3)

The substrates **5-8** (20 µmol, 500 µl of a solution 0.04 M in CH_3CN) and Co(III)W (66 mg, 20 µmol) were added to 1.5 mL of potassium phosphate buffer solution 0.1 M at pH 3

previously degassed with argon for 15 min under magnetic stirring in a Schlenk tube. The mixture was kept at 25ºC in argon atmosphere for 12 h. At the end 40 µL of a 0.1 M solution of the internal standard, 4-methylbenzophenone, in acetonitrile were added. The reactions were extracted with dichloromethane, dried over anhydrous Na_2SO_4 and after evaporation of the solvent analysed by ^{1}H NMR, GC-MS and GCL. The reactions products were identified by comparison with authentic specimens.

References and Notes

1. B. Meunier, *Chem. Rev.,* **1992,** *92,* 1411-1456.
2. P. R. Ortiz de Montellano, *Cytochrome P450*; *Structure, Mechanism and Biochemistry*, Plenum Press (Ed.), New York, **1985.**
3. V. Ullrich, *Top. Curr. Chem.,* **1979,** *83,* 67-104.
4. T. D. Porter, M. J. Coon, *J. Biol. Chem.,* **1991,** *266,* 13469-13472.
5. J. T. Grooves, G. A. McClusky, *J. Am. Chem. Soc,* **1976,** *98,* 859-861.
6. H. B. Dunford, *Peroxidase in Chemistry and Biology,* J. Everse, K. E. Everse, M. B. Grischam (Eds.), CRC Press, Boca Raton, **1991,** *Vol. II.*
7. H. P. Dunford, *Adv. Inorg. Biochem.,* **1982,** *4,* 41-68.
8. L. P. Hager, D.R. Morris, F. S, Brown, H. Eberwein, *J. Biol. Chem,* **1966,** *241,* 1769-1777.
9. S. R. Blanke, L. P. Hager, *J. Biol. Chem,* **1988,** *263,* 18739-18743.
10. J. E. Frew, P. Jones, *Adv. Inorg. Bioinorg. Mech.,* **1984,** *3,* 175-212.
11. I. Fita, M. G. Rossmann, *J.Mol. Biol.,* **1985,** *185,* 21-37.
12. T. C. Bruice, *Aldrich. Acta,* **1988,** *21,* 87-94.
13. R. A. Sheldon, Metalloporphyrin in Catalytic Oxidations, Marcel Dekker (Ed.), 1994.
14. C. K. Chang, F. Ebina, *J. Chem. Soc., Chem. Commun.,* **1981,** 778-779.
15. J. T. Groves, T. E. Nemo, *J. Am. Chem. Soc.,* **1983,** *105,* 5786-5791.
16. O. Bortolini, B. Meunier, *J. Chem. Soc., Chem. Commun.,* **1983,** 1364-1366.
17. P. S. Traylor, D. Dolphin, T. G. Traylor, *J. Chem. Soc., Chem. Commun.,* **1984,** 279-280.
18. B. De Poorter, B. Meunier, *Tetrahedron Lett.,* **1984,** *25,* 1895-1896.
19. T. G. Traylor, S. Tsuchiya, *Inorg. Chem.,* **1987,** *26,* 1338-1339.
20. T. Wijesekera, A. Matsumoto, D. Dolphin, D. Lexa, *Angew. Chem., Int. Ed. Engl.,* **1990,** *29,* 1028-1030.
21. P. Hoffmann, G. Labat, A. Robert, B. Meunier, *Tetrahedron Lett.,* **1990,** *31,* 1991-1994.
22. P. Hambright, Adeyeme, A. Shaimim, S. Levielle, *Inorg. Chem.,* **1985,** *23,* 55.
23. D. R. Leonard, J. R. Lindsay Smith, *J. Chem, Soc. Perk. Trans. II*, **1990,** 1917-1923.
24. E. B. Fleisher, J. M. Palmer, T. S. Srivastava, A. Chatterjce, *J. Am. Chem. Soc.,* **1971,** *93,* 3162-3167
25. B. Meunier, A. Robert, G. Pratviel, J. Bernadou, *Metalloporphyrins in Catalytic Oxidation and Oxidative DNA Cleavage,* K. M. Kadish, K. M. Smith, R. Guilard (Eds.), in The Porphyrin Handbook, Academic Press, New York, **2000.**
26. J. T. Groves, R. C. Haushalter, M. Nakamura, T. E. Nemo, B. J. Evans, *J. Am. Chem. Soc.,* **1981,** *103,* 2884-2886.
27. J. R. Lindsay Smith, D. N. Mortimer, *J. Chem. Soc., Chem. Commun.,* **1985,** 64-65.
28. J. R. Lindsay Smith, D. N. Mortimer, *J. Chem, Soc. Perk. Trans. II*, **1986,** 1743-1749.
29. D Dolphin, T. Nakano, T. E. Maione, T. K. Kirk, R. Farrel *Lignin Enzymic and Microbial Degradation,* INRA (Ed.), Paris, **1987,** pp. 157-162.
30. G. L. Labat, B. Meunier, *J. Org. Chem.,* **1989,** *54,* 5008-5011.
31. F. Cui, D. Dolphin, *Can. J. Chem,* **1992,** *70,* 2314-2318.
32. G. Labat, B. Meunier, *New J. Chem.,* **1989,** *13,* 801-804.
33. G. Labat, B. Meunier, *J. Org. Chem.,* **1989,** *54,* 5008-5011.
34. R. Dicosimo, H. –C., Szabo, *Biocatal. Biomimetics,* **1989,** *392,* 123-140.
35. C. Crestini, R. Saladino, P. Tagliatesta, T. Boschi, *Bioorg. Med. Chem.,* **1999,** *7,* 1897-1905.
36. K. Wiezetzerbin, B. Meunier, J. Bernadou, *Chem Comm.,* **1997,** 2321-2322.
37. I. Artaud, K. Ben-Aziza, D. Mansuy, *J. Org. Chem,* **1993,** *58,* 3373-3380.
38. The results of the oxidations of substrates **1-4** with the FeTPFPPCl / PhIO system are reported in the literature.[39]

39. E. Baciocchi, S. Belvedere, M. Bietti, *Tetrahedron Lett.,* **1998,** *39,* 4711-4714.
40. E. Baciocchi, S. Belvedere, M. Bietti, O. Lanzalunga, *Eur. J. Org. Chem.,* **1998,** *2,* 299-302.
41. No products have been observed in the reaction of substrates **1-4** with the FeTPPSCl / KHSO$_5$ system.
42. It is likely that 4-methoxybenzaldehyde is also formed as minor product in the oxidation of **3** by the FeTMPyPCl / KHSO$_5$ system, however the substrate conversion was too low to reveal traces of this product.
43. The oxidation potential of 4-methoxybenzylalcohol[44] is 0.54 V higher than that of 3,4-dimethoxybenzylalcohol[45].
44. O. R. Brown, S. Chandra, J. A. Harrison, *J. Electroanal. Chem.,* **1972,** *38,* 185-190.
45. M. Bietti, E. Baciocchi, S. Steenken, *J. Phys Chem.,* **1998,** *102,* 7337.
46. W. Nam, H. J. Ham, S. −Y. Oh, Y. J. Lee, M. −H. Choi, S. −Y. H., Kim, S. K. Woo, W. Shin, *J. Am. Chem. Soc.,* **2000,** *122,* 8677-8684.
47. H. Fujii, *J. Am. Chem. Soc.,* **1993,** *115,* 4641-4648.
48. J. F. Bartoli, O. Brigand, P. Battioni, D. Mansuy, *J. Chem. Soc., Chem. Commun.,* **1990,** 440-442.
49. H. Saltzman, J. G. Sharefkin, *Org. Synthesis Coll., Vol V,* 658.
50. L. Eberson, *J. Am. Chem. Soc.* **1983,** *105,* 3192-3199.
51. E. Baciocchi, M. Crescenzi, E. Fasella, M. Mattioli, *J. Org. Chem.* **1992,** *57,* 4684.
52. Vogel, Text Book of Pratical Organic Chemistry, **1989,** 445.
53. H. W. H. Schmidt, S. H. Haemmerli, H. S. Schoemaker, M. S. A. Leisola, *Biochemistry,* **1989,** *28,* 1776-1783.

The Role of Ketyl Radicals in Photoyellowing of Lignin Containing Pulps and Paper

1. Introduction

Lignin containing pulps and papers undergo rapid colour reversion when exposed to light (photoyellowing), a behaviour which has limited their utilisation.[1] It has been demonstrated that this process proceeds through a photooxidative discolouration of lignin in the fibre wall and becomes more important in the case of high yield pulps.[2] Lignin, which absorbs at longer wavelengths than cellulose, is the component of pulps and papers primarily responsible for photoyellowing. This behaviour is associated to the presence of lignin functional groups that interact with the UV portion of sunlight in the region between 300 and 400 nm producing chromophores that absorb visible light.[1]

Due to the industrial and environmental relevance of the processes involving in lignin degradation and discolouration, a considerable effort has been made towards the understanding of their mechanistic aspects.[1] Several photochemical studies[2-4] have been carried out aiming to determine the chromophores mainly responsible of the interaction with light and to detect changes occurring during the exposure to light that lead to the formation of coloured products. The knowledge of the mechanism of photoyellowing is of fundamental importance in order to prevent or reduce this process by chemical modification of lignin functional groups or by use of additives such as antioxidants, reducing agents and UV screens.[5-14]

Three main chemical changes have been observed during the light-induced yellowing of lignin: increase in phenolic hydroxyl content, increase in aromatic carbonyl groups and decrease of β-O-4 linkages.[2] These chemical changes have been attributed to the concomitant operation of three main processes:
1) Formation of phenoxyl radicals *(phenol pathway)*,
2) β-Cleavage of α-aryloxy substituted aromatic ketones *(phenacyl pathway)*,
3) Cleavage of ketyl radicals with formation of phenoxyl radicals and enols which tautomerise to give aromatic ketones *(ketyl pathway)*.
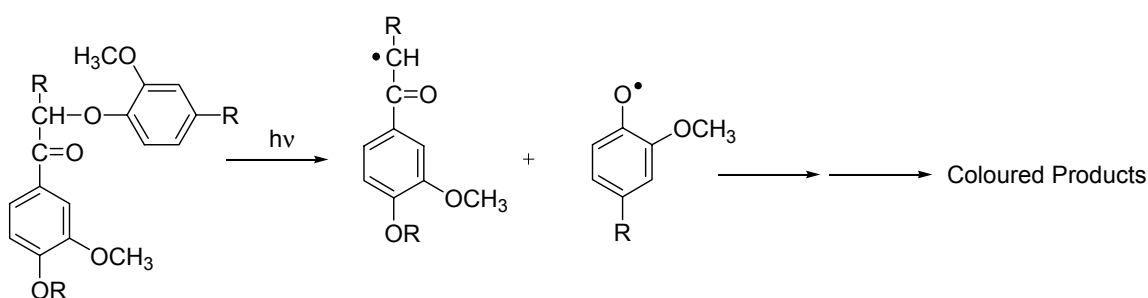
1) Phenol Pathway

Scheme 1. The phenol pathway.
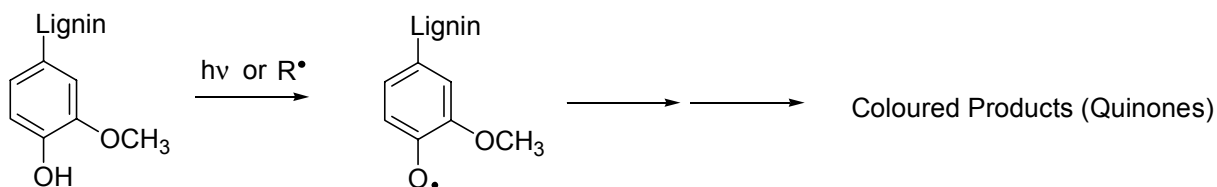
In the *phenol pathway*[4,15-18] a phenoxyl radical is formed by direct excitation of phenols or by hydrogen atom transfer reactions of phenolic groups. Phenoxyl radicals are further oxidised to coloured products, mainly quinones. Although the mechanism for formation of phenoxyl radicals and the structure of some of the coloured chromophores are known, the mechanism by which these radicals are transformed into coloured products is still largely unknown. Reactive oxygen species (ROS) such as the hydroxyl radical ($HO^\bullet$), superoxide anion and hydroperoxide radical ($O_2^{\bullet-}$ / $HO_2^\bullet$) and singlet oxygen ($^1O_2$) certainly play a key role in these processes.[15,19,20] In particular both $HO^\bullet$ and $HO_2^\bullet$ radicals can attack the aromatic rings of the

phenoxyl radicals, leading to the formation of dihydroxylated aromatic rings, which are then transformed into the quinones.[17]

Many attempts have been made to reduce the photoyellowing with the suppression of the *phenol pathway* by chemical modification (e.g. alkylation or acetylation) of the phenolic OH, nevertheless none of these attempts has been fully successful. By these studies it was estimated that the *phenol pathways* accounts for less than a third of the observed photoyellowing.[4]

2) Phenacyl Pathway

Although the content of α-carbonyl groups in lignin is relatively low, they may play a role in the mechanism of photoyellowing of bleached high yield pulps.[21] This is due to the *phenacyl pathway*[22-28] in which the β-cleavage of α-aryloxy substituted aromatic ketones leads to a pair of phenacyl and phenoxyl radicals (Scheme 2). The phenoxyl radicals produced are then oxidised to quinones whereas aromatic ketones with lower molecular weights are produced from phenacyl radicals.


Scheme 2. The phenacyl pathway.

3) Ketyl Pathway

In the *ketyl pathway*[4,27,29-31] the cleavage of ketyl radicals leads to a phenoxyl radical and an enol (Scheme 3, path **c**), which tautomerises to the corresponding ketone (Scheme 3, path **d**). Ketyl radicals can be formed by photoreduction of aromatic ketones (Scheme 3, path **a**). Excitation of the α-carbonyl chromophore followed by intersystem crossing leads to the carbonyl triplet state which then can abstract an hydrogen atom e.g. from a phenolic group leading to a pair of phenoxyl and ketyl radicals.[21] Ketyl radicals can also be formed by hydrogen abstraction from arylglycerol β-aryl ethers (Scheme 3, path **b**). These structures are relatively stable when directly irradiated however they are consumed in the presence of compounds which may produce hydrogen atom abstracting species (e.g. ROS).[28]
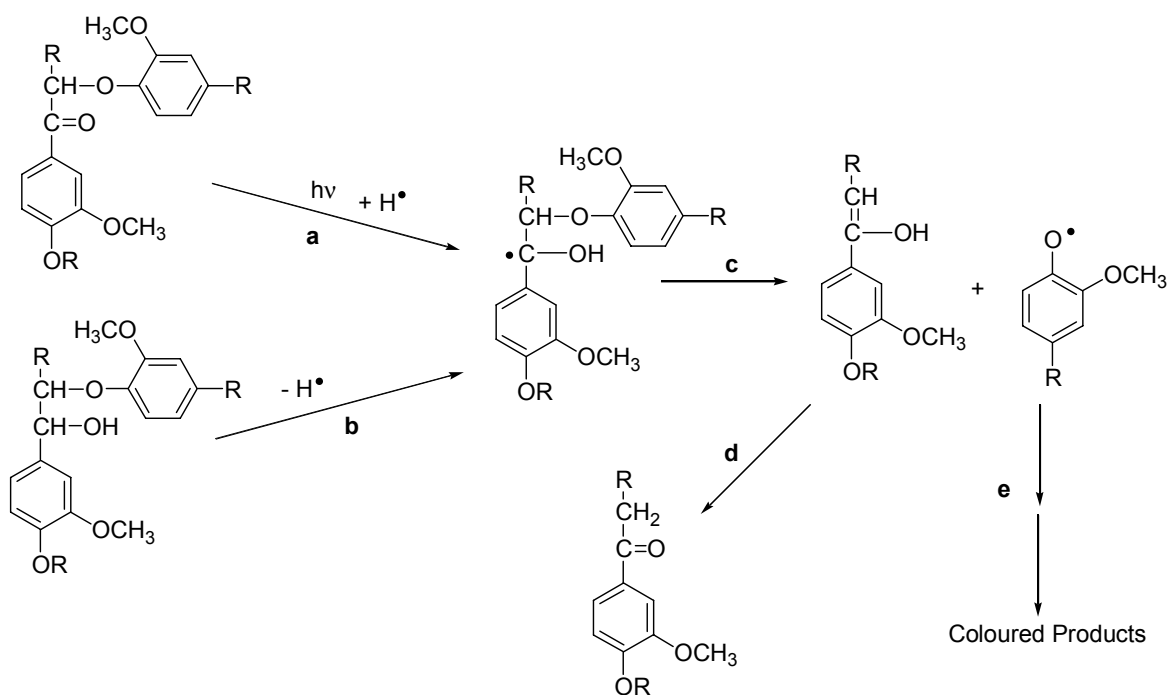
Scheme 3. The ketyl pathway.

Due to the great abundance of arylglycerol β-aryl ethers structures in lignin (accounting for about 50% of the phenylpropane units)[32] the *ketyl pathway* could represent the most important mechanism of photoyellowing.[4] Thus, a number of studies have been carried out to assess the role of this pathway in the light induced yellowing of lignin.[27,29,30,33] In this context it is of fundamental importance to determine the rate of fragmentation of ketyl radicals since the ketyl pathway would play a significant role only if the fragmentation process is relatively fast. On the other side, if the lifetime of the ketyl radical is long enough then alternative pathways become available to compete with the β−fragmentation such as reaction with molecular oxygen leading to α-carbonyl-β-aryl ether structures (Scheme 4) and then to a greater fraction of photoyellowing occurring via *phenacyl pathway*.
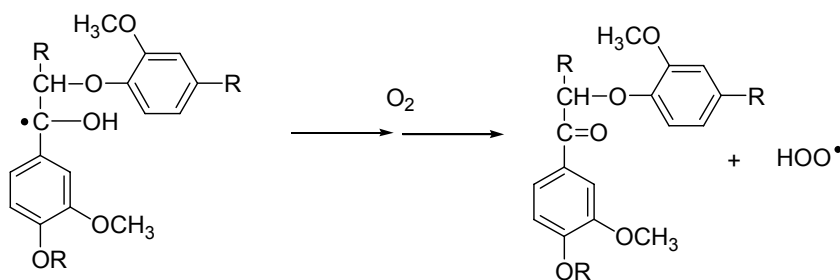
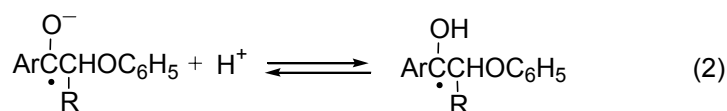**Scheme 4.** Reaction of the ketyl radical with oxygen.

In an early study, the ketyl radical generated by hydrogen atom transfer from 1-phenyl-2-phenoxyethanol to the *tert*-butoxyl radical was reported to fragmentate with a high rate constant ($k > 2 \times 10^6$ s^{-1}).[29] An even higher rate constant (in excess of 5×10^7 s^{-1}) was estimated for the fragmentation of the ketyl radical of α-(*p*-methoxyphenoxy)-*p*-methoxyacetophenone.[27] Moreover, product studies of the reaction of *tert*-butoxyl radical with 1-phenyl-2-phenoxyethanol revealed the presence of the products of photofragmentation: phenol and acetophenone.[29] However, in a more recent study, the involvement of the ketyl

pathway in the photoyellowing process was questioned since it was observed that α-phenoxyacetophenone was the primary photoproduct formed by reaction of the ketyl radical of 1-phenyl-2-phenoxyethanol with oxygen (Scheme 4), acetophenone and phenol being formed as secondary photoproducts.[33] Moreover, a much lower rate constant, around 10 s^{-1}, was estimated for the fragmentation of the ketyl radical 1-phenyl-2-phenoxyethanol-1-yl radical.[33] The relatively long lifetime of this ketyl radical was confirmed by kinetic studies of the hydrogen atom abstraction from thiophenol and Arrhenius expression for the β-scission.[34]

To better assess the role of the ketyl pathway in the photoyellowing of lignin containing pulps and paper I carried out both time-resolved and product studies by generating ketyl radicals with lignin related structures by means of radiation and photo-chemical techniques.

In the radiation chemical studies I produced the ketyl radicals with lignin related structures by reaction of α-carbonyl-β-aryl ether lignin models **1-5**, differing in the number and/or position of methoxy substituents, and the presence or absence of a γ methyl group, with the solvated electron produced by pulse radiolysis of an aqueous solution (eq. 1).[27] The radical anion thus produced by reduction of the ketone in neutral or acidic conditions can be rapidly protonated by the solvent to form the ketyl radical (eq. 2).
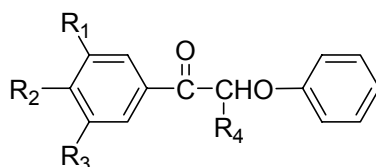

1, $R_1, R_2, R_3, R_4 = H$
2, $R_1, R_3, R_4 = H$, $R_2 = OCH_3$
3, $R_1, R_2 = OCH_3$, $R_3, R_4 = H$
4, $R_1, R_2, R_3 = OCH_3$, $R_4 = H$
5, $R_1, R_2, R_3 = H$, $R_4 = CH_3$

Figure 1. Structure of substrates **1-5.**

$$ArCCHOC_6H_5 + e_{aq}^- \longrightarrow ArCCHOC_6H_5 \qquad (1)$$

$$ArCCHOC_6H_5 + H^+ \rightleftharpoons ArCCHOC_6H_5 \qquad (2)$$
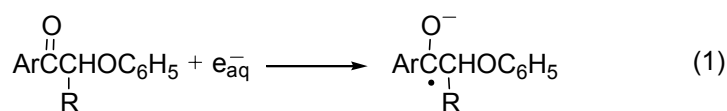
In the photochemical studies I have generated the ketyl radicals by photoactivation of suitable electron donor-acceptor (EDA) complexes. These complexes are formed by interaction of electron deficient species (electron acceptors) and electron rich species (electron donors).[35] In particular I have used charge-transfer (CT) ion pairs which are EDA complexes formed by a negatively-charged donor (the carboxylated donors **6-8**)[36] and a positively-charged acceptor (methylviologen, MV^{2+}).[36] Their photoactivation promote a very fast electron transfer from the anionic donor to the cationic acceptor.
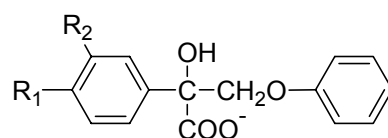
6, R$_1$, R$_2$ = H
7, R$_1$ = OCH$_3$, R$_2$ = H
8, R$_1$, R$_2$ = OCH$_3$

Figure 2. Structure of substrates **6-8.**

Photoexcitation of the [MV^{2+} / **6-8**] ion pairs leads to the instantaneous formation of the reduced acceptor (methyl viologen radical cation, MV$^{+\bullet}$) and an acyloxy radical [ArC(COO$^{\bullet}$)(OH)CH$_2$(OC$_6$H$_5$)] (eq. 4) which undergoes a fast decarboxylation[37] with formation of the ketyl radicals (eq. 5).

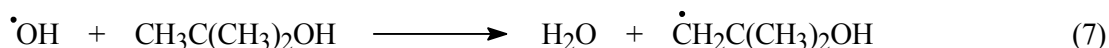$$ (3) $$

$$ (4) $$

$$ (5) $$
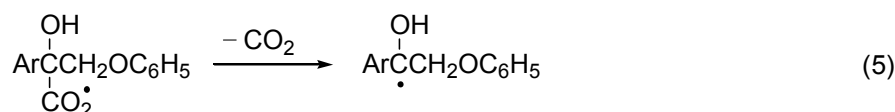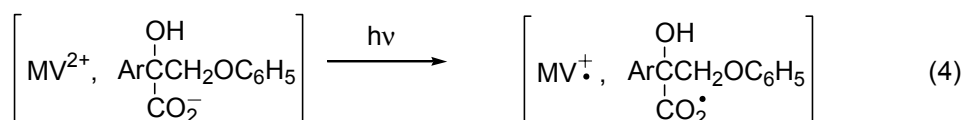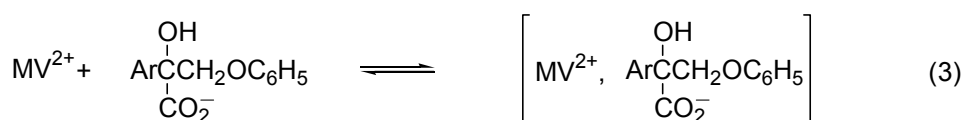
2. Results

2.1 Pulse Radiolysis Study

Ketyl radicals were generated in aqueous solution, containing 10% of 2-methyl-2-propanol, by reaction of α-carbonyl-β-aryl ether lignin models **1-5** with the solvated electrons (eqs. 1-2). 2-Methyl-2-propanol was added in order to scavenge the hydroxyl radical $^{\bullet}$OH (eq. 8, $k = 6 \times 10^8$ M^{-1}s^{-1})[39] and to increase the solubility of the ketone.

$$ H_2O \rightsquigarrow H^+, {}^{\bullet}OH, e^-_{aq} \qquad (6) $$

$$ {}^{\bullet}OH + CH_3C(CH_3)_2OH \longrightarrow H_2O + {}^{\bullet}CH_2C(CH_3)_2OH \qquad (7) $$

The hydrated electron (e$_{aq}^-$) reacts with the ketone leading to the ketyl radical anion (eq. 1), with diffusion-controlled rates.[40]

Experiments were carried out in neutral (pH = 6.0) and basic (pH = 11.0) conditions under argon, air or N$_2$/O$_2$ 9:1 (v/v). As an example, in Figure 3 are displayed the time-resolved absorption spectra observed in the reaction of e$_{aq}^-$ with **2** in argon saturated aqueous solutions at pH = 6.0 and pH = 11.0, recorded 18 μs after the electron pulse.

At pH 6.0 (filled circles) the spectrum shows three absorption bands centred around 330 nm, 430 nm and 560 nm. This spectrum can be reasonably assigned to the ketyl radical **2H$^{\bullet}$** and is similar to the spectrum of the ketyl radical produced in the same way by pulse radiolysis of 4-

methoxyacetophenone, which displayed three absorption bands centred at 310, 410 and 520 nm.[41] The three absorption bands are all quenched by oxygen as expected for a carbon centred radical.
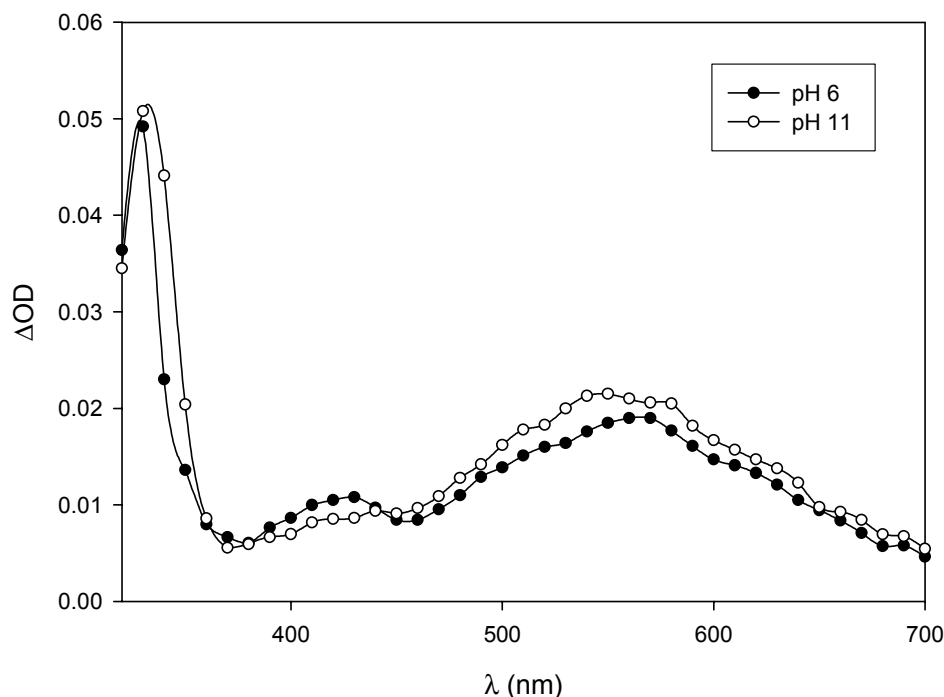
Figure 3. Absorption spectra observed on reaction of e_{aq}^- with **2** (0.2 mM) at T = 25°C, recorded after pulse radiolysis of an Ar-saturated aqueous solution (pH = 6.0 and pH = 11), containing 1 M 2-methyl-2-propanol at 18 μs after 1 μs, 10-MeV electron pulse (dose ~ 2.9 nC).

An analogous behavior was observed also with the other α-carbonyl-β-aryl ether lignin models **1, 3, 4** and **5**. However, the position of the absorption bands was found to be influenced by the nature of the ring substituents (Table 1).

Table 1. Spectral data for the ketyl radicals and radical anions of the ketones **1-5**, generated by pulse radiolysis in aqueous solution at pH ≈ 6.0 and at pH ≈ 11.0.

Ketone	λ_{max} / nm	
	pH 6.0	**pH 11.0**
1	380, 440	330, 390, 460
2	330, 430, 560	330, 540
3	340, 490, 590	340, 600
4	350, 450, 560	350, 460, 540
5	330, 490, 580	330, 460

When the spectrum was recorded in alkaline solution (Figure 3, empty circles) the shape and position of the absorption bands slightly changed. The bands should be now assigned to the ketyl radical anion $2^{-\bullet}$ on the basis of a pKa $\approx$ 9-10 that can be estimated for the ketyl radical $2H^{\bullet}$.[42]

The spectral data for the ketyl radicals and radical anions of **1-5** are collected in Table 1.

In neutral solution, the rate of decay of the ketyl radicals $1H^{\bullet}$-$5H^{\bullet}$ was measured spectrophotometrically by following the change in optical density at the wavelengths corresponding to the UV and visible absorption maxima (see Table 1). Under these conditions the ketyl radicals were found to decay by a second-order reaction and the same values of the decay rates were determined for all the absorption bands, fully supporting their assignment to the same transient species. The rate of decay was found to be highly dose-dependant and at the lowest doses (ca. 0.35 nC), which allowed a reliable measurement of the decay rates, the decay better fitted first-order kinetics. In Figure 4 the decays of $4H^{\bullet}$ at different doses in argon-saturated solutions at pH 6 are reported as an example. The decay rates of the ketyl radicals $1H^{\bullet}$-$5H^{\bullet}$ at low doses under argon are reported in the second column of Table 2.

Table 2. Rate constants for the decay of $1H^{\bullet}$-$5H^{\bullet}$ generated by pulse radiolysis under argon or O_2 (10% (v/v) in N_2) saturated aqueous solution (pH 6), measured at T = 25 °C (doses 3.5 G/pulse).

Ketyl Radical	Argon $k\,(s^{-1})$	O_2 10% in N_2 $k_2\,(M^{-1}s^{-1})$
$1H^{\bullet}$	1.7×10^3	2.7×10^9
$2H^{\bullet}$	2.5×10^3	2.5×10^9
$3H^{\bullet}$	2.7×10^3	1.9×10^9
$4H^{\bullet}$	2.5×10^3	1.8×10^9
$5H^{\bullet}$	1.7×10^3	2.3×10^9

Figure 4. The dose dependent decays of the absorption at 450 nm observed after pulse radiolysis of an aqueous solution of **4** (0.2 mM) at T = 25°C, argon saturated at pH = 6.0, containing 1 M 2-methyl-2-propanol after 1 μs, 10-MeV electron pulse.

When the solutions are air saturated a very fast decay of the ketyl radical bands is observed. Under these conditions it was not possible to measure the rate of reaction of ketyl radicals with molecular oxygen. To this purpose the solutions were saturated with O_2 (10% v/v in N_2). In Figure 5 the decays of the absorption at 450 nm observed after pulse radiolysis of an aqueous solution of **4** in both Ar saturated and O_2 (10% v/v in N_2) saturated at pH = 6.0 are reported.
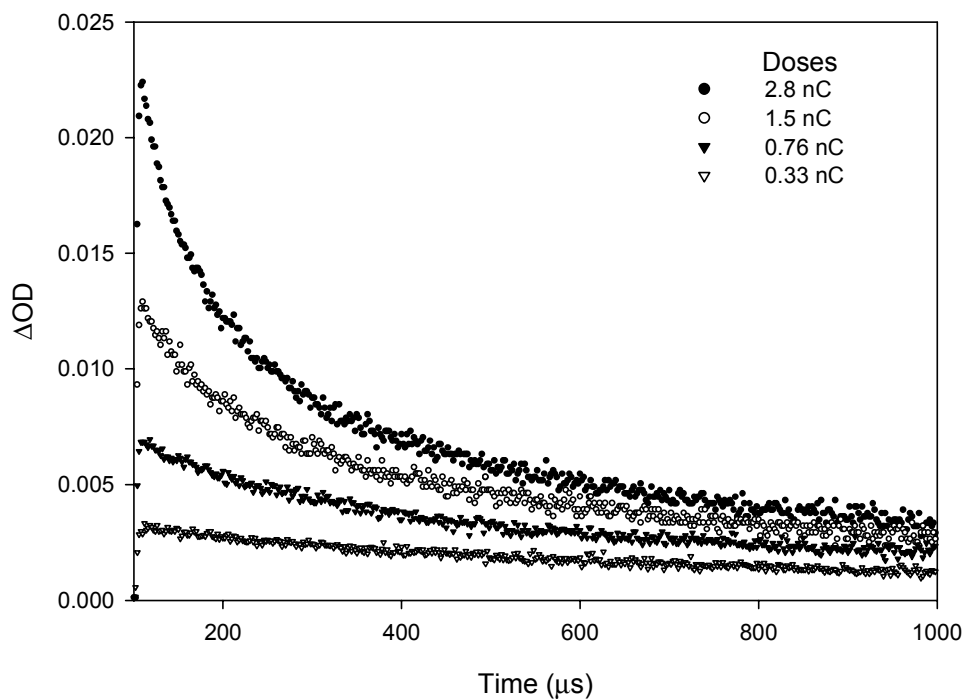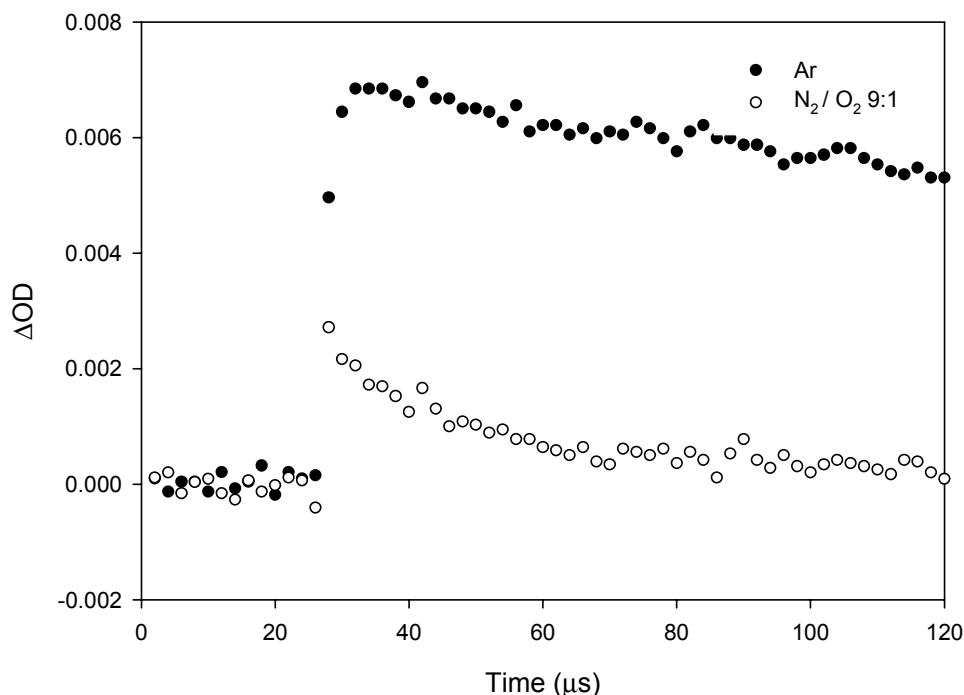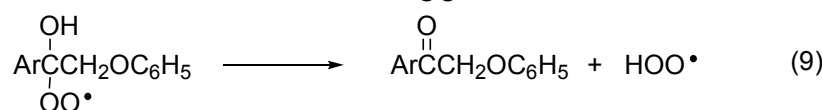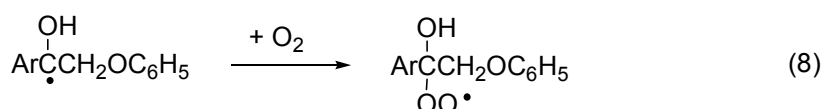
Figure 5. Decays of the absorption at 450 nm observed after pulse radiolysis of an aqueous solution of **4** (0.2 mM) at T = 25°C, in Ar saturated (black circles) and saturated 9:1 N_2/O_2 mixture (white circles) at pH = 6.0, containing 1 M 2-methyl-2-propanol after 1 µs, 10-MeV electron pulse (dose ~ 0.33 nC).

The rate of the reaction of the ketyl radicals **1H$^•$-5H$^•$** with oxygen was measured spectrophotometrically by following the change in optical density at the wavelengths corresponding to the UV and visible absorption maxima reported in Table 2. The second-order rate constants have been calculated by dividing the pseudo first-order rate constants k_{obs} for the concentration of oxygen (0.15 mM)[44] and are reported in the third column of Table 2. The reaction rates are very similar and a slight decrease is observed by increasing the number of methoxy substituents in the aromatic ring or in the presence of a γ-methyl substituent.

The decay of the ketyl radicals **3H$^•$** and **4H$^•$** is accompanied by the formation of stable products, likely the starting ketones **3** and **4**, which absorb around 350 nm.

In Figure 6 it can be noted that the build-up of the ketone **4** (ca. 5.8×10^3 s^{-1}) is slower than the decay of the ketyl radical **4H$^•$** (ca. 2.7×10^5 s^{-1}) and is somewhat delayed. This is due to the fact that the reaction of the ketyl radicals **3H$^•$** and **4H$^•$** with O_2 leads to the formation of the α-hydroxyperoxyl radicals (eq. 8) from which the ketones are formed by release of hydroperoxyl radical HOO$^•$ (eq. 9).[45]

$$\underset{\overset{|}{\underset{•}{C}}}{\overset{OH}{Ar}}CH_2OC_6H_5 \xrightarrow{+\ O_2} \underset{\underset{OO^•}{\overset{|}{C}}}{\overset{OH}{Ar}}CH_2OC_6H_5 \qquad (8)$$

$$\underset{\underset{OO^•}{\overset{|}{C}}}{\overset{OH}{Ar}}CH_2OC_6H_5 \longrightarrow \underset{\overset{\|}{C}}{\overset{O}{Ar}}CH_2OC_6H_5\ +\ HOO^• \qquad (9)$$
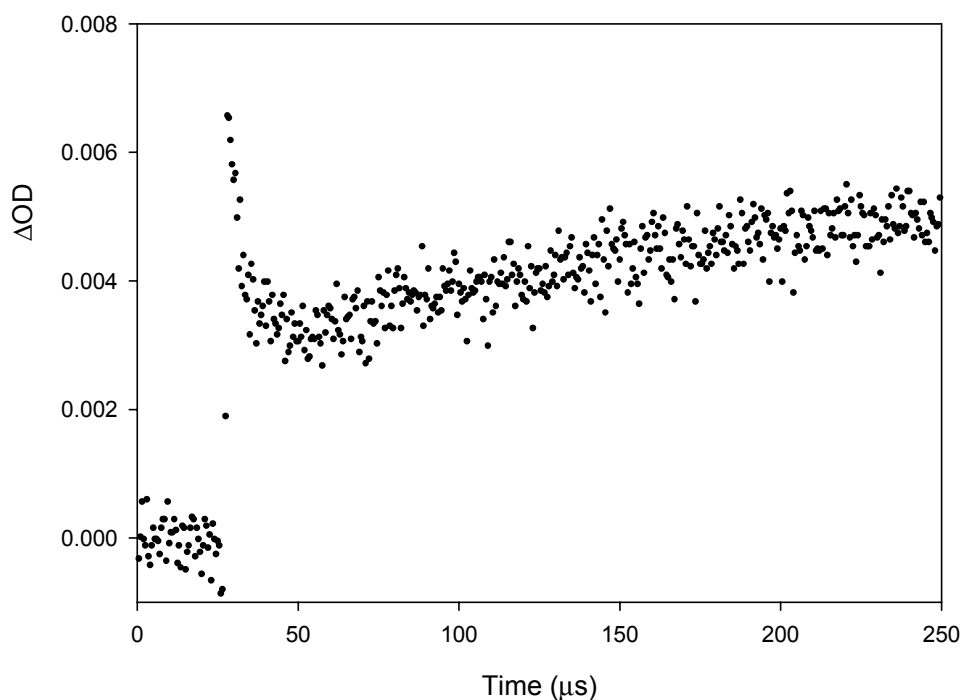
Figure 6. Decay and following build-up of the absorption at 350 nm observed after pulse radiolysis of an aqueous solution of **4** (0.2 mM) at T = 25°C, saturated 9:1 N_2/O_2 mixture at pH = 6.0, containing 1 M 2-methyl-2-propanol after the 1 μs, 10-MeV electron pulse (dose ~ 1.5 nC).

2.2 Steady-State Photoirradiation

Methylviologen triflate [MV(OTf)$_2$] was added to aqueous solutions of the sodium salt of the carboxylate anions **6-8** (generated in situ by dissolution of the free carboxylic acid in aqueous sodium bicarbonate). A light yellow colour, which can be attributed to the formation of the CT ion pair,[46] developed immediately. Formation of the charge-transfer ion pairs between the carboxylates **6-8** and MV^{2+} was revealed by the presence of the characteristic charge-transfer bands in the UV spectra between 320 nm and 420 nm.[36] In Figure 7 is reported, as an example, the UV spectra of the [MV^{2+}/**6**] ion pair and to a comparison purpose that of the carboxylate anion **6**.
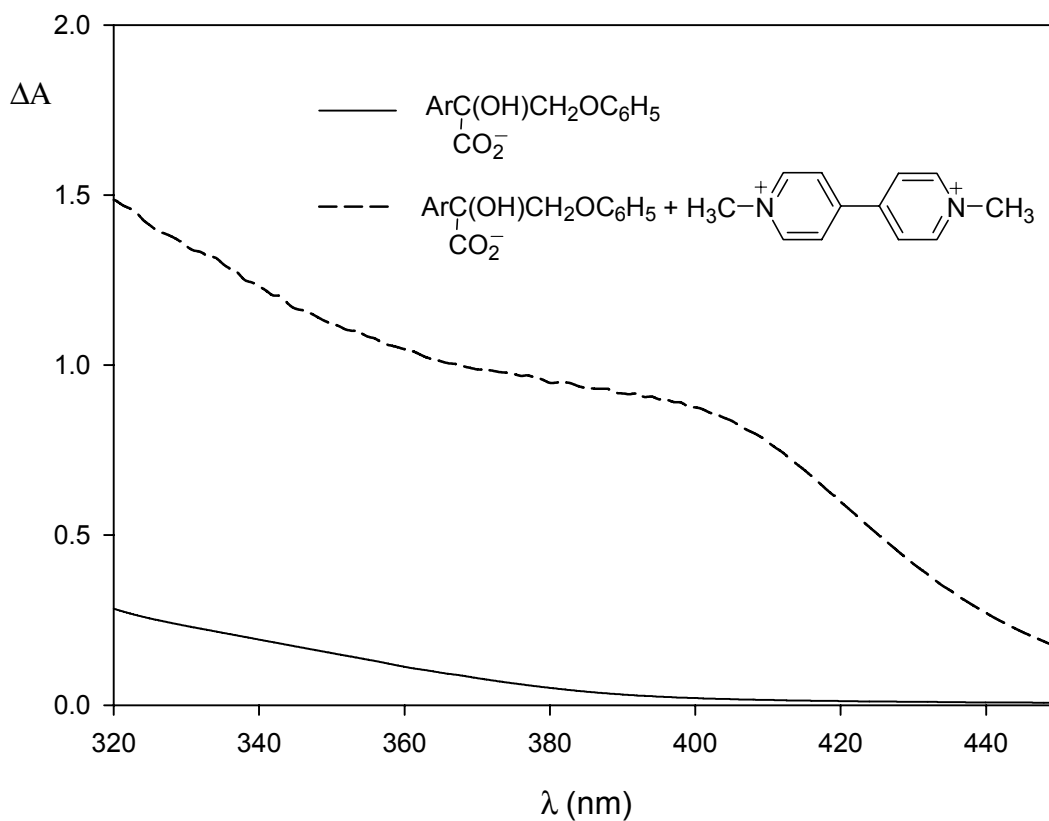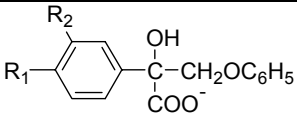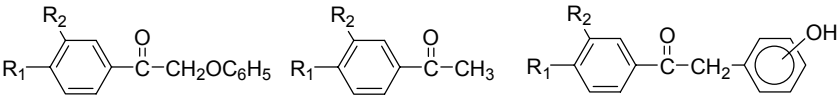
Figure 7. UV spectra of the carboxylate of **6** (solid line) and of [MV^{2+}/**6**] ion pair (dashed line).

The solutions of the CT ion pairs were saturated with argon or with oxygen and then irradiated for 1 h in a photoreactor equipped with 10 x 14 W black phosphorous lamps with emission at λ_{MAX} 360 nm. A deep blue coloration of the solution characteristic of MV$^{+\bullet}$ developed in the steady-state photoirradiation under argon.[47,48] After extraction with chloroform and addition of an internal standard, reaction products were analysed by ^{1}H NMR. The results are reported in Table 3. The mass balance was always satisfactory, accounting for more than 85% of the starting material.

Table 3. Products and yields in the photoirradiation of $MV^{2+}/6\text{-}8$ ion pairs.

Substrates	Reaction Products		
R_2-substituted $R_1\text{-}C_6H_3\text{-}C(OH)(CH_2OC_6H_5)COO^-$	$R_1\text{-}C_6H_3(R_2)\text{-}C(=O)\text{-}CH_2OC_6H_5$	$R_1\text{-}C_6H_3(R_2)\text{-}C(=O)\text{-}CH_3$	$R_1\text{-}C_6H_3(R_2)\text{-}C(=O)\text{-}CH_2\text{-}C_6H_4\text{-}OH$
6 (R_1, R_2 = H) Ar 60'	15	<1	
O$_2$ 60'	25	<1	
O$_2$ 15'	12	-	
7 (R_1 = OCH$_3$, R_2 = H) Ar 60'	20	1	<1
O$_2$ 60'	52	4	2
O$_2$ 15'	24	<1	<1
8 (R_1, R_2 = OCH$_3$) Ar 60'	11	2	7
O$_2$ 60'	22	3	19
O$_2$ 15'	10	1	4

[a] Yields are referred to the initial amount of the substrate. Average of three determinations, error $\pm$ 5%.

The photoirradiation [$MV^{2+}/6$] under argon leads to the formation of 2-phenoxy-1-phenylethanone (**1**) as the major photoproduct. Acetophenone was formed in very small amounts (< 1 % referred to the starting material). Higher yields of **1** were observed when the solution was saturated with oxygen. In the photoirradiation of [$MV^{2+}/7$] again the major product is 1-(4-methoxyphenyl)-2-phenoxy ethanone (**2**), accompanied by small amounts of 4-methoxyacetophenone, 2-(2-hydroxyphenyl)-4-methoxyacetophenone and 2-(4-hydroxyphenyl)-4-methoxyacetophenone. Also in this case a significant increase of the reaction yields was observed under oxygen. When the reaction time was reduced to 15 min, only traces of 4-methoxyacetophenone were observed. Photoirradiation of [$MV^{2+}/8$] again leads to 1-(3,4-dimethoxyphenyl)-2-phenoxy ethanone (**3**) as the major photoproduct accompanied by minor amounts of 2-(2-hydroxyphenyl)-3,4-dimethoxyacetophenone, 2-(4-hydroxyphenyl)-3,4-dimethoxyacetophenone and of 3,4-dimethoxyacetophenone. As in the photoirradiation of the [$MV^{2+}/7$] ion pair, higher yields of products were observed when the solution was saturated with oxygen; moreover the relative amounts of minor photoproducts is reduced with an irradiation time of 15 min. In a control experiment (photoirradiation of 1-(3,4-dimethoxyphenyl)-2-phenoxy ethanone in H$_2$O/CH$_3$CN 3:2, under the same experimental conditions used for the irradiation of [$MV^{2+}/8$]) it was checked that minor photoproducts 3,4-dimethoxyacetophenone, 2-(2-hydroxyphenyl)-3,4-dimethoxyacetophenone and 2-(4-hydroxyphenyl)-3,4-dimethoxyacetophenone are formed by further photolysis of the primary photoproduct **3**.

2.3 Laser Flash Photolysis Study

Time resolved laser flash photolysis studies have been carried out only with the carboxylate **7** which gave the higher yields of photoproducts. The ketyl radical obtained from **7** (**2H**$^\bullet$) was generated by laser flash photolysis (355 nm) of an argon saturated aqueous solution of MV(OTf)$_2$ (20mM) and **7** (20mM). In Figure 8 (filled square) is shown the transient spectrum observed 200 ns after the laser pulse. The spectrum exhibited two main absorptions: a strong, sharp band with λ_{MAX} = 390 nm and a broad absorption band in the visible region. These bands can be attributed to the reduced form of methylviologen (MV$^{+\bullet}$), the absorption spectrum of which has two maxima (390 and 605 nm) in aqueous solution.[47] It is likely that the broad band in the visible region results from the overlapping of the 605 nm absorption of MV$^{+\bullet}$ with another low intensity band in the 400-550 nm region which could be attributed to the ketyl radical **2H**$^\bullet$ on the basis of the absorption spectrum recorded for this species by pulse radiolysis (Figure 3). This assignment is further justified by the fact that the bands at 390 and 600 nm increase slightly in intensity in the former 2 μs (Figure 8, insets a and c), while, on the same time-scale, the absorption in the 400-550 nm region decreases in intensity (Figure 8, inset b). Two isosbestic points can be identified at λ=410 and λ=540 nm.

The decay of the ketyl radical **2H**$^\bullet$ is likely due to the fast oxidation by MV^{2+} (eq. 10).[36,49] Ketyl radical **2H**$^\bullet$ is characterised by a very low oxidation potential[50] and should be easily oxidised by MV^{2+}.[52]

$$\text{H}_3\text{CO}-\underset{\text{OH}}{\overset{\bullet}{\text{C}}}-\text{CH}_2\text{O}- \quad + \text{ MV}^{2+} \longrightarrow \text{H}_3\text{CO}-\underset{\text{O}}{\overset{\|}{\text{C}}}-\text{CH}_2\text{O}- \quad + \text{ H}^+ + \text{ MV}^{\overset{+}{\bullet}} \qquad (10)$$
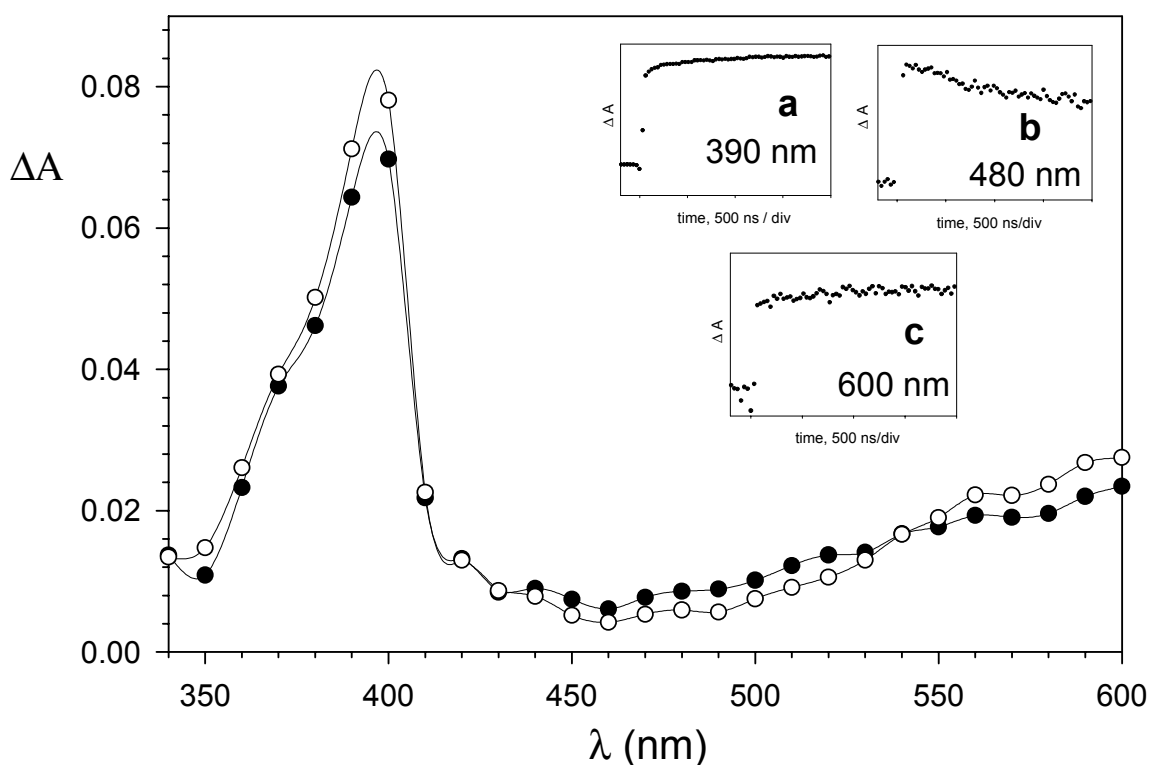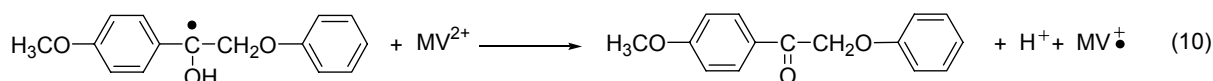

Figure 8. Time-resolved absorption spectra recorded 200 ns (filled circles) and 2 μs (empty circles) following the 8-ns laser excitation (355 nm) of an Ar-saturated aqueous solution of the [MV^{2+}/**7**] ion pair. Insets: (a) Build-up of the absorption at 390 nm. (b) Decay of the absorption at 480 nm. (c) Build-up of the absorption at 600 nm.

3. Discussion

Reaction of α-carbonyl-β-aryl ether lignin models **1-5** with the solvated electrons produced by pulse radiolysis of water solutions allowed the spectral characterisation of ketyl radicals **1H$^\bullet$-5H$^\bullet$**. The assignment of the absorption spectra observed after the pulse to the ketyl radicals is supported by the fact that a similar spectrum is produced in the same way by pulse radiolysis of 4-methoxyacetophenone. Moreover, the assignment of the absorption bands to a carbon centred radical is in agreement with the fact that these bands are quenched by oxygen. Finally, when the spectra were recorded in alkaline solution, the shape and position of the absorption bands slightly changed in line with the formation of ketyl radical anions.

It is interesting to note that the observation of the transient absorption spectra of ketyl radicals **1H$^\bullet$-5H$^\bullet$** differs from the results of Scaiano and co-workers that were unable to observe the ketyl radical of α-(*p*-methoxyphenoxy)-*p*-methoxyacetophenone.[27] The only transient observed after the pulse was the 4-methoxyphenoxyl radical and this result was interpreted with a β-fragmentation process of the ketyl radical too fast to be followed spectrophotometrically ($k > 5 \times 10^7$ s^{-1}). The decay rates of the ketyl radicals **1H$^\bullet$-5H$^\bullet$**, which I have measured spectrophotometrically under acidic conditions following the change in optical density at the wavelengths corresponding to the UV and visible absorption maxima (290-300 nm, 420-450 nm and 600-1000 nm), are indeed more than four orders of magnitude lower than 5×10^7 s^{-1}. Ketyl radicals were found to decay by a second-order reaction and the rate of decay was found to be highly dose-dependant. At the lowest doses that allowed a reliable determination of the rate constants (ca. 0.35 nC) the decay rates for the ketyl radicals **1H$^\bullet$-5H$^\bullet$** were found to obey a first-order process. The values, reported in Table 2, are very similar and comprised in the range 1.7×10^3 s^{-1} - 2.7×10^3 s^{-1}, thus the decay of the ketyl radicals does not change significantly by increasing the number of aryl methoxy substituents or in the presence of a γ-methyl substituent.[54] Since the rate of decay of the ketyl radicals that I determined should be considered an upper limit for the rate of β fragmentation, the results obtained are more in accordance with the low fragmentation rate determined by Mulder and co-workers for the fragmentation of the 1-phenyl-2-phenoxyethanol-1-yl radical.[33]

Analysis of the time-resolved absorption spectra of **3H$^\bullet$** and **4H$^\bullet$** under oxygen showed that the decay of the ketyl radicals is accompanied by the formation of stable products, i. e. the starting ketones **3** and **4**. It was also observed that the build-up of the ketones was slower than the decay of the ketyl radicals and somewhat delayed. Thus, in this timescale, it was possible to follow the reaction of the ketyl radicals **3H$^\bullet$** and **4H$^\bullet$** with O$_2$ leading to the formation of the α-hydroxyperoxyl radicals (eq. 8) and the subsequent formation of ketones **3** and **4** by release of the hydroperoxyl radical HOO$^\bullet$ (eq. 9).[45] Determination of the rate of reaction of ketyl radicals with molecular oxygen (eq. 8) is an important result of this study, which has a bearing in the context of the photoyellowing process. The second-order rate constants, reported in the third column of Table 2, have been calculated by dividing the pseudo first-order rate constants k_{obs} for the concentration of oxygen (ca. 0.15 mM).[44] Reaction rates are typical for reactions of carbon-centred radicals with oxygen[55] and are very close together, only a slight decrease is observed by increasing the number of methoxy substituents in the aromatic ring or in the presence of a γ-methyl substituent.

The high reactivity of ketyl radicals with lignin-related structures with oxygen coupled with the low rates of β-fragmentation of the same species suggest that α-aryloxy substituted aromatic ketones should be formed preferentially with respect to the products of fragmentation (aromatic ketones and phenoxyl radicals) by interaction of lignin with sunlight. The results of the steady state photoirradiation and laser flash photolysis experiments can be rationalised on the basis of reactions 3-5 and 10. The formation of MV$^{+\bullet}$ is clearly visible by the deep blue coloration which developed in the steady-state photoirradiation under argon and, in the LFP experiment with the [MV^{2+}/**7**] ion pair, by the observation of the two

absorption bands of $MV^{+\bullet}$ centred at 390 nm and 605 nm. Formation of $MV^{+\bullet}$ should be accompanied by that of the ketyl radical, in fact a low intensity broad absorption appears in the 400-550 nm region overlapping with the 605 nm band of $MV^{+\bullet}$. Analysis of the spectral evolution in the former 2 μs indicate that an additional amount of $MV^{+\bullet}$ is formed after the laser pulse by oxidation of the ketyl radical $2H^{\bullet}$ induced by MV^{2+} (eq. 10). The occurrence of reaction 10 is confirmed by the formation of 1-(4-methoxyphenyl)-2-phenoxyethanone, the product of oxidation of $2H^{\bullet}$, in the steady-state photoirradiation of the CT ion pairs $[MV^{2+}/7]$. The analysis of the results of steady-state photoirradiation of the CT ion pairs $[MV^{2+}/6-8]$ clearly indicates that 1-aryl-2-phenoxyethanones **1-3** are formed as primary photoproducts. The small amounts of acetophenones are likely formed by further photolysis of 1-aryl-2-phenoxyethanones and not by β-fragmentation of the ketyl radicals. Accordingly, under oxygen atmosphere, it was observed that the yields of acetophenones relative to those of 1-aryl-2-phenoxyethanones decreased significantly by reducing the irradiation time from 60 to 15 min. This hypothesis is further confirmed by the observation of the two α-carbonyl β-1 products 2-(2-hydroxyphenyl)-3,4-dimethoxyacetophenone and 2-(4-hydroxyphenyl)-3,4-dimethoxy-acetophenone) in the steady-state irradiation of the $[MV^{2+}/7]$ and $[MV^{2+}/8]$ ion pairs. These products are formed according to the mechanistic pathways already described in the photoirradiation of 3,4-dimethoxy-α-(2'-methoxyphenoxy)acetophenone (guaiacylacetoveratrone) in ethanol/water mixture.[56] When excited, 1-aryl-2-phenoxyetanones **1-3** undergo an intramolecular β-cleavage leading to a phenoxyl and a phenacyl radical pair (Scheme 5, path **a**). Hydrogen atom abstractions by the phenoxyl and phenacyl radicals form phenol and acetophenones (Scheme 5, path **b**). Phenol is not observed among the photoproducts since it is readily oxidised to water-soluble species under the reaction conditions. In cage recombination the radical pair leads to a cyclohexadienone coupling product (Scheme 5, path **c**) which, via a prototropic rearrangement, is converted into the α-carbonyl β-1 compounds (Scheme 5, path **d**).[1,22,23,58] The amount of secondary photoproducts increase by increasing the number of aryl methoxy substituents, in the order **8** > **7** > **6**, in accordance with the fact that the absorption of light emitted from the lamps of the by products 1-aryl-2-phenoxyetanones increases in the order **3** > **2** > **1**.
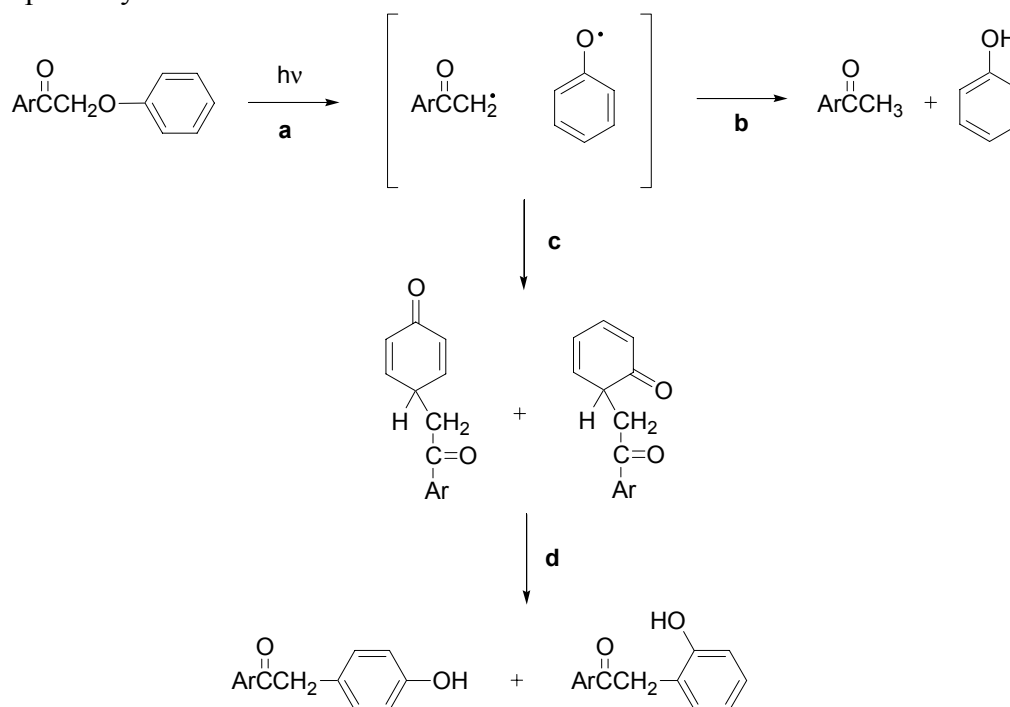
Scheme 5. Formation of secondary photoproducts in the photoirradiation of 1-aryl-2-phenoxyethanones **1-3**.

Significantly higher yields of photoproducts were observed when the solutions of the $[MV^{2+}/\textbf{6-8}]$ ion pairs were saturated with oxygen. In argon degassed solutions, photogenerated $MV^{+\bullet}$ absorbs the light emitted by the lamps and an "inner filter" effect results which prevents efficient photolysis.[36] In the presence of oxygen, $MV^{+\bullet}$ does not accumulate since it is rapidly oxidised to MV^{2+} (eq. 11) and the solutions did not develop the characteristic blue coloration of the reduced viologen.[59,60]

$$MV^{+\bullet} \; + \; O_2 \; \rightarrow \; MV^{2+} \; + \; O_2^{-\bullet} \qquad\qquad (11)$$
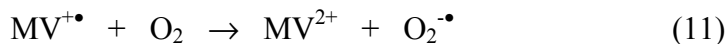
4. Conclusions

By using time-resolved techniques I was able to detect and characterise spectrophotometrically for the first time ketyl radicals with lignin related structures. By combining all the information obtained with the different precursors and methods of generation of the ketyl radicals, I was able to elucidate some of the unsolved mechanistic aspects associated with the photoyellowing of lignin containing pulps and papers. Low fragmentation rates of ketyl radicals appear to be a rather general process in ketyl radicals with lignin-related structures. The implication for the lignin photochemistry is that ketyl radicals of this type will not cleave to produce aromatic ketones and phenoxyl radicals fast and efficiently so that other reactions, i.e. with molecular oxygen, likely occur. Thus, only a minor role is played by the *ketyl pathway* in the photoyellowing process. A major role would instead be played by the β-cleavage of α-aryloxy substituted aromatic ketones *(phenacyl pathway)* that are formed by the reaction of ketyl radicals with O_2.

5. Experimental Section

5.1 Instrumentation
^{1}H-NMR and ^{13}C-NMR spectra were recorded on a Bruker AC300P spectrometer in $CDCl_3$. GC-MS analyses were performed on a HP5890 GC (OV1 capillary column, 12 m x 0.2 mm) coupled with a HP5970 MSD. UV-vis measurement was performed on a HP 8453 spectrophotometer. Pulse radiolysis experiments were performed by using a 10 MeV electron linear accelerator (Daresbury Laboratory, Warrington). Laser Flash Photolysis experiments were carried out with an Applied Photophysics LK-50 laser kinetic spectrometer using the third armonic (355 nm) of a Quantel Brilliant-B Q-switched Nd:YAG laser. The laser energy was adjusted to ≈ 10 mJ at 355 nm by the use of the appropriate filter.

5.2 Materials
All the reagents and solvents were of the highest commercial quality available and used without further purification (unless otherwise specified). Milli-Q-filtered water was used for all solutions. Methyl viologen ditriflate was prepared accordingly to a procedure reported in literature.[36]

5.3 Substrates
Substrates **1-5** were synthesised by reaction of α-bromoacetophenones with phenol in dry acetone and anhydrous K_2CO_3 according to the literature[60] and were recrystallised from methanol. α-bromoacetophenone, α-bromo-4-methoxyacetophenone, α-bromopropiophenone are commercially available. α-Bromo-3,4-dimethoxyacetophenone and α-bromo-3,4,5-trimethoxyacetophenone were synthesized by bromination of the corresponding acetophenones with bromine in chloroform as described in the literature.[61]
2-phenoxy-1-phenyletanone (1). From 2-bromoacetophenone. Yield 20%. Mp: 72-74°C (Lit. 74°C).[62] ^{1}H NMR δ: 5.28 (s, 2H), 6.92-7.03 (m, 3H), 7.26-7.34 (m, 2H), 7.46-7.67 (m, 3H),

7.99-8.04 (m, 2H); GC-MS m/z (%) M$^+$ 212 (20), 106 (8), 105 (100), 91 (6), 77 (55), 65 (7), 51 (18).

1-(4-methoxyphenyl)-2-phenoxyetanone (2). From 2-bromo-4'-methoxyacetophenone. Yield 51%. Mp: 64-65°C (Lit. 63-64°C).[63] ^{1}H NMR (CDCl$_3$) δ: 3.88 (s, 3H), 5.21 (s, 2H), 6.93-7.00 (m, 5H), 7.25-7.31 (m, 2H), 7.98-8.03 (m, 2H); GC-MS m/z (%) M$^+$ 242 (8), 136 (9), 135 (100), 121 (5), 92 (7), 77 (16).

2-bromo-3',4'-dimethoxyacetophenone. Yield 93%. ^{1}H NMR (CDCl$_3$) δ: 3.95 (s, 3H), 3.97 (s, 3H), 4.41 (s, 2H), 6.91 (d, $J = 8.4$, 1H), 7.55 (d, $J = 2.2$, 1H), 7.62 (dd, $J = 8.4$ and 2.2, 1H); GC-MS m/z (%) M$^+$ 260 (13) and 258 (13), 166 (10), 165 (100), 151 (10), 107 (6), 79 (10), 77 (6), 51 (6).

1-(3,4-dimethoxyphenyl)-2-phenoxyetanone (3). From 2-bromo-3',4'-dimethoxyacetophenone. Yield 38%. Mp: 93-95°C (Lit. 95-96°C).[64] ^{1}H NMR (CDCl$_3$) δ: 3.94 (s, 3H), 3.97 (s, 3H), 5.24 (s, 2H), 6.90-6.99 (m, 4H), 7.27-7.29 (m, 2H), 7.57-7.69 (m, 2H); GC-MS m/z (%) M$^+$ 272 (8), 166 (10), 165 (100), 151 (6), 77 (11).

2-bromo-3',4'5'-trimethoxyacetophenone. Yield 53%. ^{1}H NMR (CDCl$_3$) δ: 3.93 (s, 6H), 3.94 (s, 3H), 4.42 (s, 2H), 7.26 (d, $J = 2.2$, 2H); GC-MS m/z (%) M$^+$ 290 (15) and 288 (14), 196 (11), 195 (100) 181 (8), 137 (6), 66 (7).

1-(3,4,5-trimethoxyphenyl)-2-phenoxy etanone (4). From 2-bromo-3',4',5'-trimethoxyacetophenone. Yield 59 %. Mp: 98-100°C. ^{1}H NMR (CDCl$_3$) δ: 3.92 (s, 6H), 3.93 (s, 3H), 5.23 (s, 2H), 6.92-7.03 (m, 3H), 7.25-7.35 (m, 4H); GC-MS m/z (%) M$^+$ 302 (10), 196 (11), 195 (100), 77 (12).

2-phenoxy-1-phenylpropanone (5). From 2-bromopropiophenone. Yield 35 %. Mp: 76-78°C (Lit. 78-79°C).[65] ^{1}H NMR (CDCl$_3$) δ: 1.71 (d, $J = 6.8$, 3H), 5.48 (q, $J = 6.8$, 1H), 6.83-6.97 (m, 3H), 7.18-7.28 (m, 2H), 7.43-7.63 (m, 3H), 8.06-8.12 (m, 2H); GC-MS m/z (%) M$^+$ 226 (16), 122 (9), 121 (100), 105 (42), 93, (10), 77 (66), 51 (17).

Substrates **6-8** have been synthesized following the synthetic sequence reported in Scheme 6.
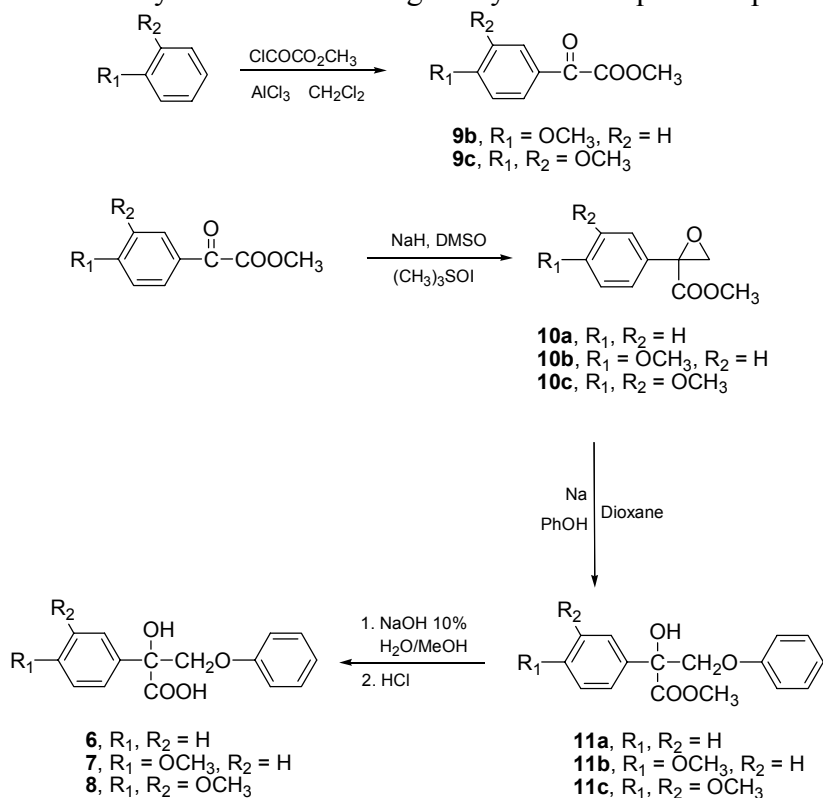
Scheme 6. Synthesis of compounds **6-8.**

68

Methyl benzoylformate is commercially available. Methyl 4-methoxybenzoylformate **(9b)** and methyl 3,4-dimethoxybenzoylformate **(9c)** were prepared by a Friedel-Crafts acylation of anisole and veratrole, respectively, with methyl chlorooxoacetate according to a literature procedure.[66]

Methyl 4-methoxybenzoylformate (9b). Yield 86%: ^{1}H NMR δ: 3.90 (s, 3H, OCH$_3$), 3.97 (s, 3H, OCH$_3$), 6.98 (d, J = 8.8, 2H, ArH), 8.02 (d, J = 8.8, 2H, ArH); GC-MS m/z (%) M$^+$ 194 (3), 136 (9), 135 (100), 107 (7), 92 (12), 77 (15), 64 (6).

Methyl 3,4-dimethoxybenzoylformate (9c). Yield 46%: ^{1}H NMR (CDCl$_3$, 300 MHz) δ 3.95 (s, 3H, OCH$_3$), 3.97 (s, 3H, OCH$_3$), 3.98 (s, 3H, OCH$_3$), 6.92 (d, J = 8.5, 1H, ArH), 7.58 (d, J = 2.0, 1H, ArH), 7.66 (dd, J = 8.5 and 2.0, 1H, ArH); GC-MS m/z (%) M$^+$ 224 (11), 166 (10), 165 (100), 79 (10), 77 (7), 51 (6).

Methyl 2,3-epoxy-2-phenylpropanoate (10a)[67]

1.2 g, 0.03 mol of sodium hydride (60% mineral oil dispersion) was placed in a three-necked, round-bottomed flask and washed three times with light petroleum ether, by stirring and decanting the liquid portion, in order to remove the mineral oil. The system was evacuated until the last traces of petroleum ether were removed from the sodium hydride and filled with argon. Trimethyloxosulfonium iodide (6.6 g, 0.03 mol) was added, then DMSO (40 mL) was added dropwise and hydrogen evolution was observed. When hydrogen evolution ceased (15-20 min) methyl benzoyl formate, solved in DMSO (10 mL), was added dropwise and the mixture was stirred at 30°C for 16 h and at 50°C for 1 h. After cooling, water was added to the reaction mixture which was then extracted with diethyl ether. The collected organic extracts were dried over anhydrous Na$_2$SO$_4$ and the solvent was evaporated. The residue obtained (1.52 g) contained the methyl 2,3-epoxy-2-phenylpropanoate which was not isolated but directly used in the next step.

^{1}H NMR (CDCl$_3$, 300 MHz) δ 2.98 (d, J = 6.5, 1H), 3.43 (d, J = 6.5, 1H), 3.79 (s, 3H), 7.35-7.39 (m, 3H), 7.48-7.53 (m, 2H).

Methyl 2-hydroxy-3-phenoxy-2-phenylpropanoate (11a)[68]

To a solution of phenol (545 mg, 5.8 mmol) in dry dioxane (4 mL) Na (133 mg, 5.8 mmol) was added and the mixture was heated at reflux until all sodium was consumed. After cooling, methyl 2-phenyl-2,3-epoxypropionate (1.03 g, 5.8 mmol) in dry dioxane (0.5 mL) was added dropwise and the mixture was heated at reflux for 3 h. The reaction mixture was cooled and 50 mL of a solution of NH$_4$OH 2 N was added. The mixture was then extracted with diethyl ether and the collected organic extracts were washed three times with 10% NaOH aqueous solution and once with water. The organic phase was dried over anhydrous Na$_2$SO$_4$ and the solvent was evaporated under reduced pressure. The crude product (0.82 g) was purified by flash chromatography on silica gel (gradient of elution light petroleum-AcOEt 8:1-6:1). 464 mg, 1.8 mmol of the pure product were obtained (yield 31%).

^{1}H NMR δ 3.82 (s, 3H), 4.16 (d, J = 9.1, 1H), 4.66 (d, J = 9.1, 1H), 6.90-7.01 (m, 1H), 7.24-7.46 (m, 5H), 7.67-7.72 (m, 2H).

^{13}C NMR δ 53.2, 73.7, 78.3, 114.9, 121.4, 128.3, 129.4, 129.4, 137.5, 158.4, 173.2.

2-Hydroxy-3-phenoxy-2-phenylpropanoic acid (6)

A mixture of 464 g, 1.8 mmol of methyl 2-hydroxy-3-phenoxy-2-phenylpropanoate, 15 mL of 10% NaOH aqueous solution and 7.5 mL of methanol was heated at reflux for 5 h. After cooling methanol was evaporated and concentrated hydrochloric acid was added, the formation of a precipitate was observed. The mixture was extracted three times with AcOEt. The collected organic extracts were washed once with water, dried over anhydrous Na$_2$SO$_4$ and the solvent was evaporated under reduced pressure. 420 mg, 1.6 mmol of the pure product (yield 89%) were obtained.

^{1}H NMR δ: 4.15 (d, J = 9.3, 1H), 4.73 (d, J = 9.3, 1H), 6.91-7.03 (m, 3H), 7.25-7.43 (m, 5H), 7.70-7.75 (m, 2H).

^{13}C NMR δ: 73.4, 78.3, 115.0, 121.9, 125.6, 128.7, 129.0, 129.6, 136.5, 158.1, 175.7.

Compounds **2** and **3** were prepared from **9b** and **9c** according to the procedure described for compound **1**.

Methyl 2,3-epoxy-2-(4-methoxyphenyl)propanoate (10b).[67] ^{1}H NMR (CDCl$_3$, 300 MHz) δ 2.97 (d, J = 6.3, 1H), 3.39 (d, J = 6.3, 1H), 3.78 (s, 3H), 3.81 (s, 3H), 6.90 (d, J = 8.9, 2H), 7.42 (d, J = 8.9, 2H).

Methyl 2-hydroxy-2-(4-methoxyphenyl)-3-phenoxypropanoate (11b).[68] Yield 18%: ^{1}H NMR δ 3.80 (s, 3H), 3.81 (s, 3H), 4.13 (d, J = 9.4, 1H), 4.62 (d, J = 9.4, 1H), 6.88-7.01 (m, 5H), 7.24-7.32 (m, 2H), 7.60 (d, J = 9.0, 2H). ^{13}C NMR δ 53.4, 55.3, 73.9, 78.1, 113.9, 115.0, 121.5, 127.0, 129.5, 129.6, 159.5, 159.8, 173.6.

2-Hydroxy-2-(4-methoxyphenyl)-3-phenoxypropanoic acid (7). Yield 83%: ^{1}H NMR δ 3.82 (s, 3H), 4.12 (d, J = 9.4, 1H), 4.73 (d, J = 9.4, 1H), 6.90-7.01 (m, 5H), 7.24-7.30 (m, 2H), 7.63 (d, J = 8.8, 2H). ^{13}C NMR δ 55.4, 73.4, 78.0, 114.1, 115.0, 121.8, 127.0, 128.5, 129.6, 158.1, 160.0, 176.1.

Methyl 2-(3,4-dimethoxyphenyl)-2,3-epoxypropanoate (10c).[67] ^{1}H NMR (CDCl$_3$, 300 MHz) δ 2.99 (d, J = 6.2, 1H), 3.41 (d, J = 6.2, 1H), 3.79 (s, 3H), 3.89 (s, 3H), 3.90 (s, 3H), 6.86 (d, J = 8.2, 1H), 7.02-7.10 (m, 2H).

Methyl 2-(3,4-dimethoxyphenyl)-2-hydroxy-3-phenoxypropanoate (11c).[68] Yield 15%: ^{1}H NMR δ 3.83 (s, 3H), 3.89 (s, 3H), 3.92 (s, 3H), 4.13 (d, J = 9.4, 1H), 4.63 (d, J = 9.4, 1H), 6.86-7.02 (m, 4H), 7.17-7.33 (m, 4H). ^{13}C NMR δ 53.3, 55.7, 55.9, 73.9, 78.0, 109.0, 110.8, 114.9, 118.0, 121.5, 129.4, 129.9, 148.9, 149.1, 158.4, 173.4.

2-(3,4-Dimethoxyphenyl)-2-hydroxy-3-phenoxypropanoic acid (8). Yield 70%: ^{1}H NMR δ 3.89 (s, 3H), 3.91 (s, 3H), 4.13 (d, J = 9.2, 1H), 4.68 (d, J = 9.2, 1H), 6.87-7.01 (m, 4H), 7.24-7.31 (m, 4H). ^{13}C NMR δ 56.0, 73.5, 77.9, 108.9, 110.9, 115.0, 118.1, 121.8, 129.0, 129.5, 149.0, 149.3, 158.1, 176.7.

5.4 Pulse Radiolysis

The pulse radiolysis experiments were performed using a 10 MeV electron linear accelerator which supplied 0.5 ms pulses with doses of 10 Gy. Experiments were performed at room temperature using aqueous solutions containing the substrate (0.2 mM) and 2-methyl-2-propanol (1 M). Solutions were saturated with argon, oxygen or with a 9:1 N$_2$/O$_2$ mixture. Experiments were performed at pH 6 (5 mM Na$_2$HPO$_4$ adjusted with 0.1 M HClO$_4$) and at pH 11 (5 mM Na$_2$B$_4$O$_7$ x 10 H$_2$O adjusted with 0.1 M NaOH). A flow system was employed in all the experiments. The rate constants were obtained by averaging 3 to 5 values, each consisting of the average of 3 to 10 shots, and were reproducible to within 5 %.

5.5 Steady-state photooxidation

Aqueous solutions of the sodium salt of the α-hydroxycarboxylates of substrates **1-3** were prepared by adding 50 μmol, 20 μmol or 10 μmol of the free acid and 55 μmol, 22 μmol or 11 μmol of NaHCO$_3$ respectively to 1 mL of milli-Q-filtered water. Different concentrations of the three substrates were chosen in order to have an absorbance of the charge-transfer complexes at 350 nm of ca. 1. The solutions were sonicated until complete dissolution then filtered and transferred to a Pyrex test tube. An equimolar amount of methyl viologen ditriflate with respect to the substrate was then added. The solutions were degassed with argon for 30 min or saturated with oxygen and then photoirradiated for 60 min. The solutions saturated with oxygen were also photoirradiated for 15 min. At the end, a solution of the internal standard (phenylacetic acid) was added. The solutions were acidified, extracted with chloroform, dried over anhydrous Na$_2$SO$_4$ and the solvent was evaporated. The products were analysed by ^{1}H NMR.

5.6 Laser flash photolysis

The solutions were prepared as described in the steady-state photooxidation. Laser Flash Photolysis experiments were carried out by irradiating a 3 mL Suprasil quartz cell (10 mm × 10 mm) containing an argon-saturated aqueous solution of the sodium salt of **2** (20 mM), prepared as described in the steady state photoirradiation, and of methyl viologen ditriflate (20 mM). The experiments were carried out at T = 25±0.5 °C under magnetic stirring. A flow system was employed in all the experiments. The rate constants were obtained by averaging 3 to 5 values, each consisting of the average of 5 to 10 shots, and were reproducible to within 5 %.

References and Notes

1. O. Lanzalunga, M. Bietti, *J. Photochem. Photobiol. B: Biol.,* **2000,** *56,* 85-108.
2. C. Heitner, Light-Induced Yellowing of Wood-Containing Papers, C. Heitner, J. C. Scaiano (Eds.), in The Photochemistry of Ligninocellulosic Material, ACS Symp. Series, Vol. 531, Am. Chem. Soc., Washington DC, **1993,** pp. 2-25.
3. R. S. Davidson, *J. Photochem. Photobiol. B: Biol.,* **1996,** *33,* 3-25.
4. G. J. Leary, *J. Pulp Paper Sci.,* **1994,** *20,* J154-J160.
5. R. C. Francis, C. W. Dence, T. C. Alexander, R. Agnemo, S. Omori, *Tappi J.,* **1991**, 127-133.
6. A. Castellan, C. Noutary, R. S. Davidson, *J. Photochem. Photobiol. A: Chem.,* **1994,** *84,* 311-316.
7. R. S. Davidson, L. Dunn, A. Castellan, A. Nourmamode, *J. Photochem. Photobiol. A: Chem.,* **1995,** *86,* 275-282.
8. V. Trichet, S. Grelier, A. Castellan, H. Choudhury, R. S. Davidson, *J. Photochem. Photobiol. A: Chem.,* **1996,** *95,* 181-188.
9. C. M. Cook, A. J. Ragauskas, *J. Photochem. Photobiol. A: Chem.,* **1997,** *104,* 217-224.
10. T. Q. Hu, B. R. James, Y. Wang, *J. Pulp Paper Sci.,* **1999,** *25,* 312-317.
11. P. McGarry, C. Heitner, J. Schmidt, R. Seltzer, G. Cunkle, J.-P. Wolf, *J. Pulp Paper Sci.,* **2000,** *26,* 59-66.
12. P. D. Evans, N. L. Owen, S. Schmid, R. D. Webster, *J. Polym. Degrad. Stab.,* **2002,** *76,* 291-303.
13. P. McGarry, C. Heitner, J. Schmidt, A. Rodenhiser, R. St. John Manley, G. Cunkle, T. Thompson, *J. Photochem. Photobiol. A: Chem.,* **2002,** *151,* 145-155.
14. Y. Pu, S. Anderson, L. Lucia, A. J. Ragauskas, *J. Photochem. Photobiol. A: Chem.,* **2004,** *163,* 215-221.
15. M. G. Neumann and A. E. H. Machado, *J. Photochem. Photobiol. B: Biol.,* **1989,** *3,* 473-481.
16. A. Castellan, N. Colombo, A. Nourmamode, J. H. Zhu, D. Lachenal, R. S. Davidson, L. Dunn, *J. Wood Chem. Tech.,* **1990,** *10,* 461-493.
17. I. A. Shkrob, M. C. Depew, K. S. Wan, *Res. Chem. Intermed.,* **1992,** *17,* 271-285.
18. D. Shukla, N. P. Shepp, N. Mathivanan, L. J. Johnston, *Can. J. Chem.,* **1997,** *75,* 1820-1829.
19. C. Bonini, M. D'Auria, L. D'Alessio, G. Mauriello, D. Tofani, D. Viggiano, F. Zimbardi, *J. Photochem. Photobiol. A: Chem.,* **1998,** *113,* 119-124.
20. H. Takagi, I. Forsskåhl, H. Perakyla, S. Omori, C. W. Dence, *Holzforschung,* **1990,** *44,* 217-222.
21. G. Brunow, B. Eriksson, *Acta Chem. Scand.,* **1971,** *25,* 2779-2781.
22. C. Vanucci, P. Fornier de Violet, H. Bouas-Laurent, A. Castellan, *J. Photochem. Photobiol. A: Chem.,* **1988,** *41,* 251-265.
23. A. Castellan, N. Colombo, C. Cucuphat, P. Fornier de Violet, *Holzforschung,* **1989,** *43,* 179-185.
24. J. C. Netto-Ferreira, I. G. J. Avellar; J. C. Scaiano, *J. Org. Chem.,* **1990,** *55,* 89-92.
25. J. A. Schmidt, A. B. Berinstain, F. de Rege, C. Heitner, L. J. Johnston, J. C. Scaiano, *Can. J. Chem.,* **1991,** *69,* 104-107.
26. W.-U. Palm, H. Dreeskamp, H. Bouas-Laurent, A. Castellan, *Ber. Bunsenges. Phys. Chem.,* **1992,** *96,* 50-61.
27. J. C. Scaiano, M. K. Whittlesey, A. B. Berinstain, P. R. L. Malenfant, R. H. Schuler, *Chem. Mater.,* **1994,** *6,* 836-843.
28. D. S. Argyropoulos, Y. Sun, *Photochem. Photobiol.,* **1996,** *64,* 510-517.
29. J. C. Scaiano, J. C. Netto-Ferreira, V. Wintgens, *J. Photochem. Photobiol. A: Chem.,* **1991,** *59,* 265-268.

30. J. A. Schmidt, C. Heitner, *J. Wood Chem. Tech.,* **1993,** *13,* 309-325.
31. R. Ruggiero, A. E. H. Machado, A. Castellan, S. Grelier, *J. Photochem. Photobiol. A: Chem.,* **1997,** *110,* 91-97.
32. K. V. Sarkanen, *Lignins: Occurence, Formation, Structure and Reactions,* K. V. Sarkanen, C.H. Ludwig (Eds.), Wiley-Interscience, New York, **1971,** pp. 95-195.
33. Y. Huang, D. Pagé, D. D. M. Wayner, P. Mulder, *Can. J. Chem.,* **1995,** *73,* 2079-2085.
34. P. H. Kandanarachchi, T. Autrey, J. A. Franz, *J. Org. Chem.,* **2002,** *67,* 7937-7945.
35. J. K. Kochi, *Acc. Chem. Res.,* **1992,** *25,* 39-47.
36. T. M. Bockman, S. M. Hubig, J. K. Kochi, *J. Org. Chem.,* **1997,** *62,* 2210-2221.
37. This process is too fast ($k > 10^7$ s^{-1}) to be followed in the nanosecond timescale.[36,38]
38. J. W. Hilborn, J. A. Pincock, *J. Am. Chem. Soc.,* **1991,** *113,* 2683.
39. G. V. Buxton, C. L. Greenstock, W. P. Helman, A. B. Ross, *J. Phys. Chem. Ref. Data,* **1988,** *17,* 513-886.
40. A. B. Ross, W. G. Mallard, W. P. Helman, B. H. J. Bielski, G. V. Buxton, D. A. Cabeli, C. L. Greenstock, R. E. Huie, P. Neta, *NRDL/NIST Solution Kinetics Database: Ver 1;* 1.0 ed. NIST, U.S. Department of Commerce: Gaithersburg, MD, **1992.**
41. The absorption spectrum of the ketyl radical 4-MeOC$_6$H$_4$C$^\bullet$(OH)CH$_3$ was recorded 20 µs after the pulse (3 MeV van de Graaf accelerator, 300 ns electron pulse, 5 Gy/pulse) of an argon saturated aqueous solutions (pH = 5.5) containing 4-methoxyacetophenone (0.05 mM) and 2-methyl-2-propanol (0.1 M).
42. A value of 10.1 for the *p*Ka of the ketyl radical of *s*-phenetyl alcohol is reported in the literature.[43]
43. T. Autrey, P. Kandanarachchi, J. A. Franz, *J. Phys. Chem. A* **2001,** *105,* 5948-5953.
44. S. L. Murov, I. Carmicael, G. L. Hug, "Handbook of Photochemistry" 2nd Ed., Marcel Dekker, New York, **1993.**
45. *The Chemistry of Free Radicals: Peroxyl Radicals.* Alfassi, Z. V. Ed.; John Wiley & Sons: New York, **1997.**
46. E. M. Kosower, *J. Am. Chem. Soc.,* **1956,** *80,* 3253.
47. T. Watanabe, K. Honda, *J. Phys. Chem.,* **1982,** *86,* 2617.
48. T. M. Bockman, J. K. Kochi, *J. Org. Chem.,* **1990,** *55,* 4127.
49. J. R. Barnett, A. S. Hopkins, A. Ladwith, *J. Chem. Soc., Perkin Trans. 2,* **1973,** 80.
50. An E° value of –0.51 V vs SCE in CH$_3$CN was calculated for the benzyl radical 4-CH$_3$OC$_6$H$_4$CH$^\bullet$OCH$_3$ [51] A lower value should be expected in the presence of the α-substituent CH$_2$OC$_6$H$_5$.
51. D. D. M. Wayner, V. D. Parker, *Acc. Chem. Res.,* **1993,** *26,* 287-294.
52. E$_{1/2}$ = –0.46 V vs. SCE in CH$_3$CN.[53]
53. C. R. Bock, J. A. Connor, A. R. Gutierrez, T. J. Meyer, D. G. Whitten, B. P. Sullivan, J. K. Magle, *J. Am. Chem. Soc.,* **1979,** *101,* 4815-4824.
54. While substituent effects on the phenyl ring α to the radical center should not significantly effect the rate of scission of the ketyl radical, a substitution to the 2-position may enhance the rate of β-scission.[34]
55. B. Maillard, K. U. Ingold, J. C. Scaiano, *J. Am. Chem. Soc.,* **1983,** *105,* 5095-5099.
56. In polar solvents β-cleavage should occur from both singlet and triplet states.[25,57]
57. J. K. S. Wan, M. Y. Tse, M. C. Depew, *Res. Chem. Intermed.,* **1992,** *17,* 59-75.
58. A. Castellan, J. H. Zhu, N. Colombo, A. Nourmamode, R. S. Davidson, L. Dunn, *J. Photochem. Photobiol. A: Chem.,* **1991,** *58,* 263-273.
59. M. A. J. Rodgers, *Radiat. Phys. Chem.,* **1984,** *23,* 245.
60. K. Tsukuhara, R. G. Wilkins, *J. Am. Chem. Soc.,* **1985,** *107,* 2632.
61. E. Baciocchi, M. Bietti, M. F. Gerini, O. Lanzalunga, S. Mancinelli, *J. Chem. Soc. Perkin Trans. 2,* **2001,** 1506-1511.
62. W. B. Whithney, H. R. Henze, *J. Am. Chem. Soc,* **1938,** *60,* 1148-1150.
63. J. C. Netto-Ferreira, J. C. Scaiano, *Tetrahedron Lett.,* **1989,** *30,* 443-446.

64. L. Hurrell, L. J. Johnston, N. Mathivan, D. Vong, *Can J. Chem,* **1993,** *71,* 1340-1348.
65. M. Kopp, *Bull. Soc. Chim. Fr.,* **1954,** 628-635.
66. O. Itoh, T. Nagata, I. Nomura, T. Takanaga, T. Sugita, K. Ichikawa, *Bull. Chem. Soc. Jpn.,* **1984,** *47,* 810-814.
67. E. J. Corey, M. Chaykovsky, *J. Am. Chem. Soc.,* **1965,** *87,* 1353-1364.
68. M. David, J. Sauleau, A. Sauleau, *Can. J. Chem.,* **1985,** *63,* 2449-2454.

SUMMARY

In this thesis, I have investigated three important aspects of lignin degradation involving radicals and radical ions.

1. The H_2O_2 promoted oxidation of two non-phenolic trimeric lignin model compounds catalysed by LiP were studied. According to an electron transfer mechanism the cleavage of the C-C bond β with respect to the dialkoxylated ring (where the positive charge is initially localized) is accompanied by the cleavage of the C-C bond β to a monoalkoxylated ring. Likely in the oxidative degradation of lignin C-C bonds can efficiently be broken which are not in a β position with respect to the ring where the positive charge is initially localised. Moreover by enzymatic steady state kinetic study it was showed that the size of the model substrate influences the efficiency of the oxidation catalysed by LiP. The observation of a substantial activity of the enzyme with the trimeric model, too big to enter the enzyme active site and the access channel, supports the recent suggestion of a substrate oxidation mediated by the LiP surface residue Trp 171.

2. The mechanism of the oxidations of LMCs catalysed by metalloporphyrins depends on the solvent polarity. In the high polar aqueous medium the oxidations occur by an electron transfer mechanism, whereas in a low polar solvent, like dichloromethane, the oxidations of the same substrates occur by two competing mechanism: hydrogen atom transfer and formation of a complex between the iron-oxo porphyrin and the substrate. The higher reactivity of FeTMPyPCl compared to that of FeTSPPCl is likely due to the presence of stronger electron withdrawing substituents on the porphyrin ligand that not only increase the stability of the iron-oxo complex in the oxidative reaction conditions but also increase the redox potential of the catalyst.

3. By means of photo and radiation-chemical techniques, detection and spectral characterization of ketyl radicals with lignin related structures was accomplished. The observation that fragmentation rates of ketyl radicals are rather low implicates that, in lignin photochemistry, ketyl radicals react with molecular oxygen before the cleavage occur. Thus, only a minor role is played by the ketyl pathway in the photoyellowing process. A major role would instead be played by the β-cleavage of α-aryloxy substituted aromatic ketones *(phenacyl pathway)* that are formed by the reaction of ketyl radicals with O_2.